AN INJECTABLE HYDROGEL SYSTEM WITH UNIQUE TUNABLE STIFFNESS FOR TISSUE ENGINEERING

WANG LISHAN

NATIONAL UNIVERSITY OF SINGAPORE

2012

Founded 1905

AN INJECTABLE HYDROGEL SYSTEM WITH UNIQUE TUNABLE STIFFNESS FOR TISSUE ENGINEERING

WANG LISHAN

(M.Sc.), NUS

A THESIS SUBMITTED

FOR THE DEGREE OF DOCTOR OF PHILOSOPHY

DEPARTMENT OF CHEMISTRY

NATIONAL UNIVERSITY OF SINGAPORE

2012

Acknowledgements

I would like to express my deepest gratitude to my supervisors, Dr Motoichi Kurisawa and Assoc. Prof. Eugene Khor for their precious advice, patience, encouragement and guidelines throughout my study under their supervision. I also wish to thank Prof. Ying and Ms Noreena in Institute for Bioengineering and Nanotechnology (IBN), Agency of Science, Technology and Research for their support and encouragement during my Ph.D candidature.

I would like to thank my friends and lab mates in IBN for their support, help and encouragement. I especially thank Joo Eun Chung, Peggy Chan, Fan Lee, Praveen Thoniyot, Shujun Gao, Chan Du, Majad Khan, Jerome Boulaire, Susi Tan, Tianyi Wang, Kun Liang, Keming Xu.

Special thanks to my family and friends who have supported me throughout the last few years: my husband Kah Juay and my lovely son Zi Zhuo, my parents and parents-in-law.

I finally thank National University of Singapore for granting me admission as a Ph.D candidate.

Wang Lishan

January 2012

Table of Contents

Summary

Tissue cells feel and respond to the stiffness of their substrate and consequently regulate many important physiological functions accordingly. Many approaches to study such effect by controlling the mechanical properties of substrates have been investigated. Most often, these studies dealt with polyacrylamide and poly(dimethylsiloxane) (PDMS) gels. These model substrates may not be appropriate for *in vivo* use due to inherent toxicity of such polymers and/or their crosslinkers and poor cell adhesion characteristics.

Our approach is to design an injectable hydrogel system with unique tunable stiffness to address the goal of understanding the independent effect of stiffness on various cell functions not only on two-dimensional (2D) but also in three-dimensional (3D) environment. Particularly, the full understanding of cell responses to stiffness in 3D is highly crucial to advance cell-based therapies in tissue engineering. In this study, gelatin-phenol (Gtn-Phenol) conjugates differing in the amount of conjugated phenols were successfully synthesized. The hydrogels composed of Gtn-Phenol conjugate were formed using the oxidative coupling of phenol moieties catalyzed by hydrogen peroxide (H_2O_2) and horseradish peroxidase (HRP). The independent tuning of stiffness and gelation rate was clearly demonstrated in this hydrogel system where the stiffness of the Gtn-Phenol hydrogel was readily tuned by the H_2O_2 concentration while HRP determined the gelation rate.

Human mesenchymal stem cells (hMSCs) are multipotent stem cells that can differentiate into a variety of cell types. The Gtn-Phenol hydrogels supported hMSCs attachment directly without additional coating with adhesive ligands regardless of the

hydrogel stiffness. The cells on stiffer Gtn-HPA hydrogels showed a higher proliferation rate, larger spreading area, more organized cytoskeletons, more stable focal adhesions and faster migration rate. Stimulation of neurogenesis of hMSCs by the hydrogel stiffness was evident when the storage modulus (G') of hydrogel was less than 2500 Pa. The cells on a softer hydrogel (600 Pa) expressed more neurogenic protein markers. The myogenesis of hMSCs was directed by the hydrogel stiffness when G' was greater than 8000 Pa. Stimulation of osteogenic differentiation of hMSCs was observed in the cells when they were cultured on the hydrogel with stiffness higher than 20000 Pa when a broader range of control in stiffness was made possible in an improved Gtn-HPA-Tyr hydrogel system. In 3D studies, the proliferation rate and differentiation of hMSCs was adversely affected by the increase of hydrogel stiffness. The neurogenesis of hMSC by hydrogel stiffness in 3D using Gtn-HPA hydrogels was also demonstrated.

Substrate stiffness is also a key component of regulating fibroblast phenotype during the wound healing process. Our study on human fibroblast (HFF-1) has validated the effect of hydrogel stiffness on the proliferation of HFF-1. The fibroblasts exhibited a higher proliferation rate on stiffer Gtn-HPA hydrogels in 2D. In contrast, the cells cultured inside the hydrogel (3D) remained non-proliferative for 12 days before an effect of stiffness on proliferation was observed.

With its unique control in stiffness, *in situ* forming ability, efficient gelling mechanism, the ease of formulation, biocompatibility, biodegradability and cost effectiveness, the Gtn-HPA hydrogel offers a great potential for regenerative applications of cell-based therapies *in vivo*.

List of Tables

List of Figures

Chapter I

Introduction

1. Introduction

1.1. Introduction to hydrogels for tissue engineering application

The concept of tissue engineering was proposed by Langer et al. in the early 1990s as "the application of the principles and methods of engineering and the life sciences toward the fundamental understanding of structure–function relationships in normal and pathological mammalian tissues and the development of biological substitutes that restore, maintain or improve tissue function" [1]. This strategy of tissue engineering generally involves the incorporation of the appropriate cells into a tissue-engineered scaffold, which serves as a temporary extracellular matrix (ECM) until cells produce the matrix along time and finally neo-tissue replaces the scaffold. Tissue engineering approaches mainly consist of the following key components: cells, biomaterial scaffolds and growth factors or other biological or mechanical signals. The scaffold plays an important role in regulating cell migration, proliferation, and ECM production [2]. The scaffolds should provide physical and biological properties such as sufficient mechanical strength, preventing cells from floating out of the defect, facilitating cell proliferation, cell signaling, and stimulating matrix production by cells. Therefore, engineering of such scaffolds is an essential requisite for successful tissue engineering.

Hydrogels are a class of crosslinked polymers that, due to their hydrophilic nature, can absorb large quantities of water. These materials offer uniquely moderate-to-high physical, chemical, and mechanical stability in their swollen state [3]. Hydrogels have been widely used as biomaterials for controlled drug delivery and as scaffolds in tissue

engineering due to their highly hydrated polymeric networks and many other favorable characteristics [4-6]. Their high water content renders them compatible with living tissues and proteins and their rubbery nature minimizes damage to the surrounding tissue. They possess excellent permeability for influx of nutrients and excretion of metabolites. Their mechanical properties parallel those of soft tissues, making them particularly appealing for engineering of these tissues. Also, biodegradable hydrogels allow for the replacement of the hydrogels over time by the extracellular matrix produced and the creation of the microenvironment for tissue regeneration when cells are incorporated.

1.1.1. Polymers used to form hydrogels

Recent years have witnessed a surge of interest in using synthetic hydrogels in tissue engineering approaches owing to the fact that their appealing properties such as hydrophilic-hydrophobic balance, mechanical and structural properties, degradation profile, etc. can be molecularly tailored. They have small batch-to-batch variation and ease to scale up in comparison to naturally derived polymers. Most commonly used synthetic materials include hydrolytically stable cross-linked poly(2-hydroxyethylmethacrylate) (HEMA) for ophthalmic uses [7-9], polyacrylamide gels with a wide well-controlled range in stiffness [10], injectable poly(*N*-isopropylacrylamide) (PNIPAAm) gels exhibiting temperature sensitivity due to its phase transition behavior above the lower critical solution temperature (LCST) [11-13], poly(ethylene glycol) (PEG) with proteinase sensitivity crosslinks [14-17], poly(vinyl alcohol) (PVA) hydrogels [18-20], temperature sensitive and biodegradable polyphosphazenes consisting

of a hydrophilic PEG block and hydrophobic amino acid or a peptide block [21, 22], and polypeptides gel with pH or temperature sensitivity [23].

On the other hand, naturally derived polymers are widely chosen for tissue engineering applications due to their biofunctional features, low cytotoxicity and biodegradability. These polymers have the advantage of mimicking many features of extracellular matrixes found in the native tissue and thus have the potential to regulate various cell functions, The most commonly used naturally derived polymers are polysaccharide-based such as hyaluronic acid, alginate, chitosan, dextran and agarose or protein-based, such as collagen, gelatin, and fibrin. The details will be discussed in the following section.

1.1.1.1. Polysaccharide-based naturally derived polymers

Polysaccharides are a class of biopolymers constituted by simple sugar monomers. These biological polymers can be obtained from different sources such as microbial, animal and vegetal [24]. These polysaccharidic polymers have been widely proposed as biomaterials in tissue engineering applications largely due to non-toxicity, low costs and probably the chemical similarities with heparin rendering its good hemocompatibility. Following is a short list of polysacchardes that are intensively studied as biomaterials.

Hyaluronic acid (HA), a linear high molecular mass polysaccharide, composed of the repeating disaccharide units D-glucuronic acid and N-acetyl-D-glucosamine (Figure 1-1). It is a naturally occurring non-sulfated glycosaminoglycan and a major

macromolecular component of the intercellular matrix of most connective tissues such as cartilage, vitreous of the human eye, umbilical cord and synovial fluid. It is not only a structural element, but also interacts with binding proteins, contributing to that regulation of water balance; behaving like a lubricant protecting articular cartilage surface and acting as a scavenger molecule for free radicals [25]. It also plays an important role in many other biological processes, such wound healing, inflammation, angiogenesis cell proliferation and differentiation [26]. HA can be easily modified to possess various functionalities such as hydrazide, glycidyl methacrylate, thiol and phenol derivatives [27-30]. HA and its gel have shown a great potential in tissue engineering such as artificial skin, facial intradermal implants, wound healing and soft tissue augmentation [31-34]. However, thermodynamically the hydrophilic, polyanionic surfaces of HA biomaterials do not favor cell attachment and tissue formation. Therefore, to enhance cell interactions, surface coating with ECM proteins, such as type I collagen and fibronectin, have been developed by creating physically or covalently linked functional domains [35, 36].

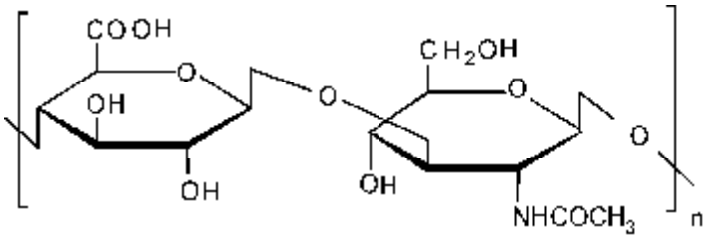

Figure 1-1. Chemical structure of hyaluronic acid (HA).

Alginates are naturally occurring polysaccharides and consist of guluronic (G) and mannuronic (M) acids organized into blocks of varying composition (G-blocks, M-blocks and MG-blocks) (Figure 1-2). It is a well-known biomaterial obtained from brown algae. The gelation occurs when divalent cations such as Ca^{2+}, Mg^{2+}, Ba^{2+} or Sr^{2+} interact with G-blocks to form ionic bridges between different polymer chains [37]. Because of their biocompatibility, low toxicity, relatively low cost, and gentle gelation conditions, hydrogel prepared from alginates are used as wound dressing, dental impression, and immobilization matrix, transplantation of chondrocytes and hepatocytes [2, 38-42]. Although the mechanical properties and swelling degree can be regulated by controlling the cross-link density (e.g. by altering the concentration of divalent cations or alginate), for hydrogel formed by ionic interaction, any changes occurring in the environment such as pH and ionic strength would disrupt the gel formation, leading to dissociation of the hydrogel. Covalent crosslinking of alginate by enzyme-mediated oxidative coupling [43] and Schiff-base formation were explored [44] to solve the problem of its instability as a physical crosslinked counterpart.

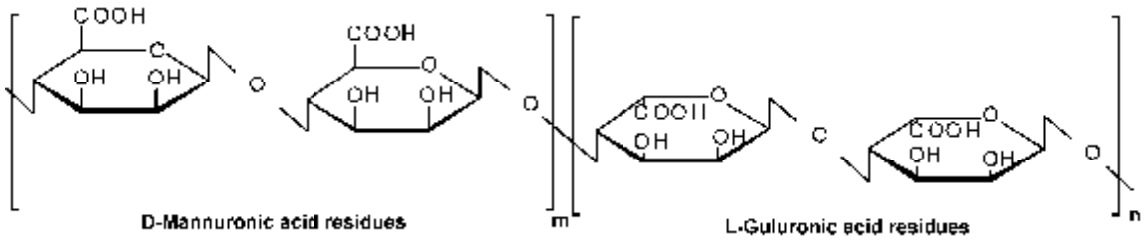

Figure 1-2. Chemical structure of alginate.

Chitosan is partially deacetylated derivative of chitin, which is found particularly in the shell of crustacean, cuticles of insects and cell walls of fungi. It usually contains less than 40 % of *N*-acetyl-D-glusosamine residues (Figure 1-3). Due to its structural similarity to natural glycosaminoglycans (GAGs), easy degradation by chitosanase and lysozyme, low toxicity and its biocompatibility, it was found in many biomedical applications in skin, bone, cartilage, liver, nerve and blood vessel [45, 46]. Chemical modifications to its amino and hydroxyl groups in chitosan molecules to improve its solubility were performed through the conjugations of varied hydrophilic moieties [47, 48]. Sugars and antigen were also attempted as conjugation moiety to chitosan to improve the recognition of cells, viruses, and bacteria for the tissue engineering application [49, 50].

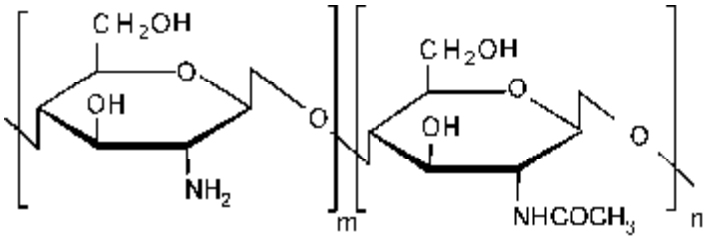

Figure 1-3. Chemical structure of chitosan.

Dextran is a glucose homopolysaccharide consisting of an α-(1→6)-linked glucan with branches attached to the O-3 of the backbone chain units (Figure 1-4). It is composed of chains of varying length from 10 to 150 kilo Daltons (kD). It has been used as an antithrombotic since the dextran binds to erythrocytes, platelets and vascular endothelium by reducing their aggregation and adhesiveness, respectively. Dextrans

typically have high molecular weight, resulting in relatively good mechanical properties. They are chemically similar to GAGs and highly hydrophilic, but they have been shown to be resistant to both protein adsorption and cell adhesion. In addition, they have abundant pendant hydroxyl groups amenable to chemical modification. Dextran derivatives with functional groups such as acrylate, thiols, phenols, maleimide, and vinyl sulfones have been synthesized and their hydrogels composed of dextran-L-Lactate-HEMA or methacrlyated dextran have been explored for the tissue engineering application [51-56].

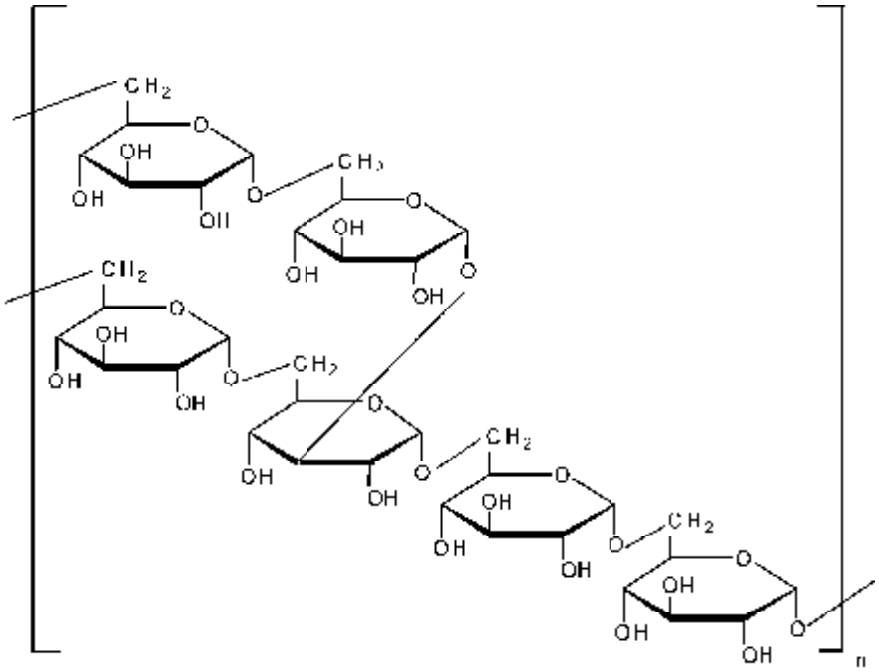

Figure 1-4. Chemical structure of dextran.

Agarose is another type of marine algal polysaccharide. It is a linear polysaccharide consisting of (1→3)-β-D-galactopyranose-(1→4)-3.6-anhydro-α-L-

galactopyranose as the basic units and contains a few ionized sulfate groups [57] (Figure 1-5). The viscoelastic properties of aqueous agarose gels depend strongly on the degree of desulfation of its native polysaccharide. The propensity to form gels increases with increasing desulfation [58]. Attempts have been made to covalently bind chitosan to agarose gels to incorporate charge to the gels leading to the enhancement of neurite growth [59].

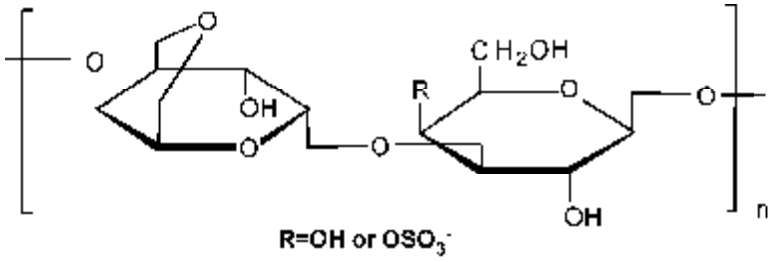

Figure 1-5. Chemical structure of agarose.

1.1.1.2. Protein-based naturally derived polymers

1.1.1.2.1. Collagen

Collagen is a biological protein, with a high content of glycine (Gly) (near 33 %) and of imino acids. Gly is present in the polypeptide chain as every third residue, forming a $(gly\text{-}X\text{-}Y)_n$ repeating pattern which adopts a left-handed helical structure (α chain). The most common tripeptide sequence found in collagen is composed of Gly, proline (Pro) and hydroxyproline (Hyp) (Gly-pro-Hyp). Three α chains wrap around one another with a right-handed twist, in a tightly packed triple helix (Figure 1-6). Among those protein-based naturally derived polymers investigated, collagen is regarded by many as an ideal

scaffold or matrix for tissue engineering as it is a major protein component of the extracellular matrix, providing support to connective tissues such as skin, tendons, bones, cartilage, blood vessels and ligaments [60, 61]. It is composed of combinations of amino acid sequence such as Arginine-Gly-Aspartic acid (RGD) that are recognized by cells for adhesion and it is readily degraded by enzymes secreted from the cells such as collagenase. Collagen sponges have been reported to promote cell and tissue attachment and growth [25] and to enhance bone formation by promoting the differentiation of osteoblast [62]. Although the collagen-based hydrogels have numerous advantages, their use as tissue-engineering scaffolds is limited due to their inherent physical weakness and high degradation rate [38]. Crosslinking is necessary in order to tailor its mechanical properties and the degradation of collagen. Chemical crosslinking of collagen using glutaraldehyde [63], diphenylphosphoryl azide [60] diepoxy compounds [64], diisocynates [65] or carbodiimides [66] was explored. A broad range of tissue engineering products based on animal-sourced collagen scaffolds have been developed and commercialized such as Apligraf® as an artificial skin product, Revitix™ as topical cosmetic product, inFUSE® collagen sponges as bone graft.

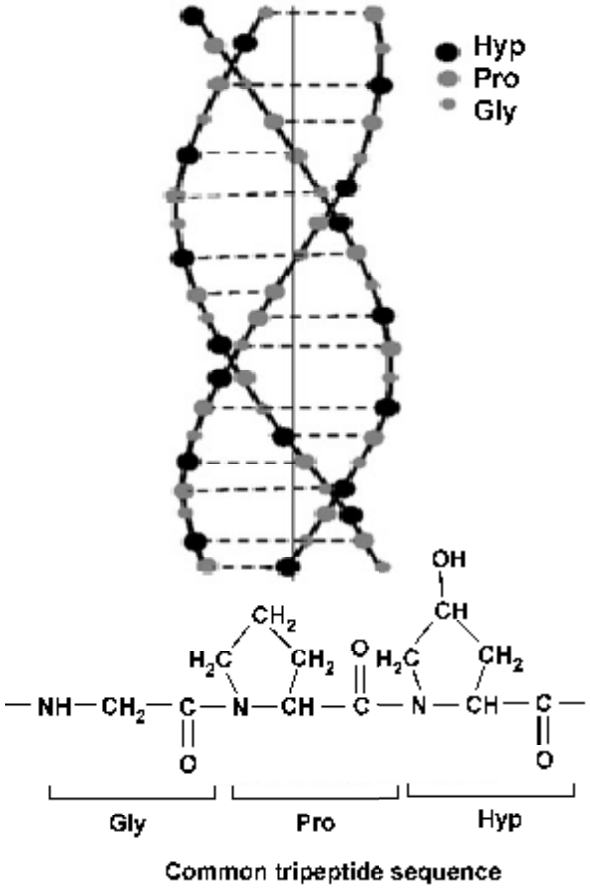

Figure 1-6. Chemical structure of collagen [25].

1.1.1.2.2. Gelatin

Gelatin is a denatured, biodegradable polypeptide derived from the controlled partial hydrolysis of collagen by either acid or alkaline processing methods. This processing affects the electrical nature of collagen, yielding gelatin with different isoelectric points (IEPs). The alkaline process, through hydrolysis of amide groups of collagen, yields gelatin with a high density of carboxyl groups, which makes the gelatin negatively changed and reduces the IEP of gelatin. In contrast, the electrostatic nature of collagen is hardly modified through the acid process because of a less invasive reaction to

amide groups of collagen. As a result, the IEP of the gelatin that is obtained remains similar to that of collagen (Figure 1-7).

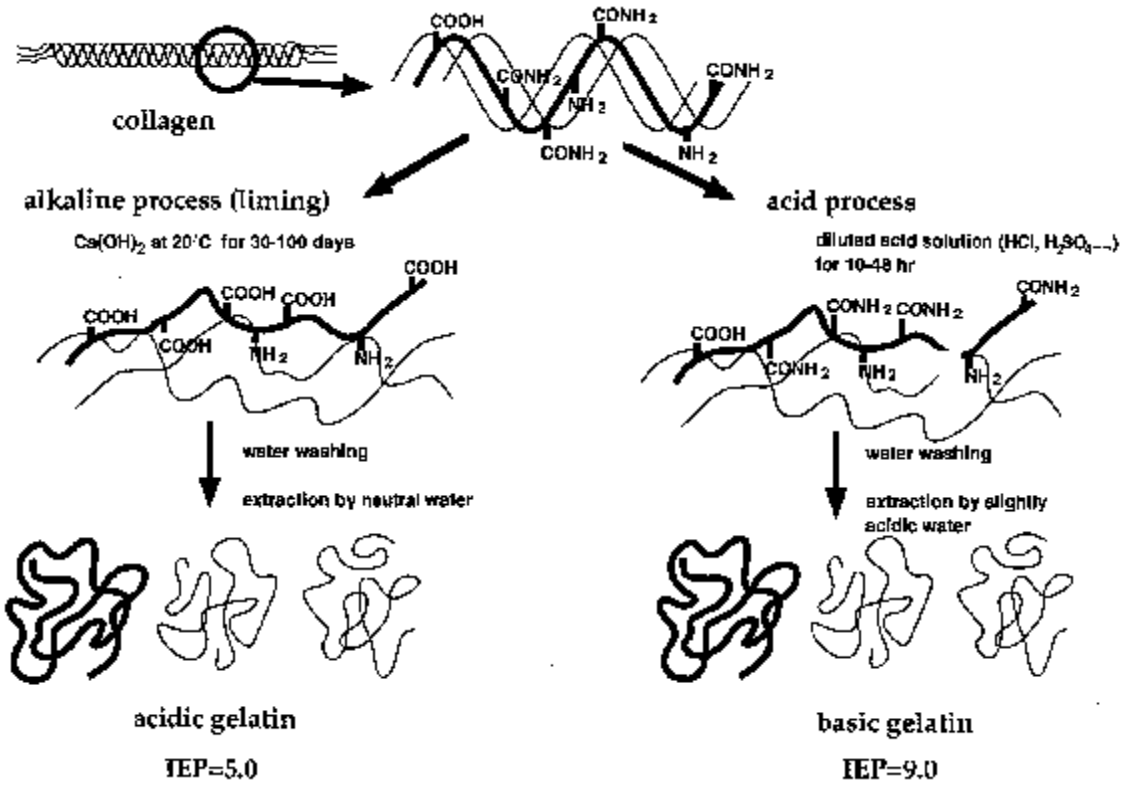

Figure 1-7. Preparative process for acidic and basic gelatins from collagen [67].

Gelatin contains a large number of Gly, Pro and Hyp. It is commonly used for biomedical applications because of its biodegradability and biocompatibility in physiological environments. It has relatively low antigenicity because of being denatured in contrast to collagen which is known to have antigenicity due to its animal origin [68]. Gelatin sponges, injectable hydrogels and gelatin microparticles embedded in hydrogels networks for encapsulation and deliver an active biomolecules to improve the temporary

cell functions have been explored for tissue engineering for bone, cartilage and skin [68-71].

1.1.1.2.3. Fibrin

Fibrin is another source of naturally derived polymer. It can be produced from the patient's own blood and used as an autologous hydrogel for tissue engineering with no toxicity and immunogenicity. The most attractive feature of fibrin-based materials are their biological activity, and many studies have investigated the possibility of using them as scaffolds for various tissue engineering applications such as cartilage, bone, cardiovascular, and chronic wound healing [69]. Fibrin gel is used as biological adhesives in surgery due to its haemostatic, chemotactic and mitogenic properties [72]. Fibrin forms gel by the enzymatic polymerization of fibrinogen in the presence of thrombin [38]. Thrombin cleaves peptide fragments from the soluble plasma protein fibrinogen, yielding insoluble fibrin peptides that aggregate for form fibrils (Figure 1-8) and its gel [73]. Both concentrations of thrombin and fibrinogen and other variables such as the local pH, ionic strength and the concentration of calcium can influence the structure and properties of a resultant fibrin gel [74]. It has been widely used as a cell carrier of many cell types, such as keratinocytes, urothelium cells, tracheal epithelial cells, murine embryonic stem cells, mesenchymal progenitor cells and chondrocytes due to its biomimetic and physical properties [69]. But rapid degradation can represent a problem for its use as a shape-specific scaffold in tissue engineering. Optimizing its composition to obtain shape stability and integrity is a means to further improve the fibrin gel system. Its degradation

can be slowed down by the addition of apronitin, a proteinase inhibitor [75] or by chemical modification such as PEGylated fibrin [76] to improve its stability.

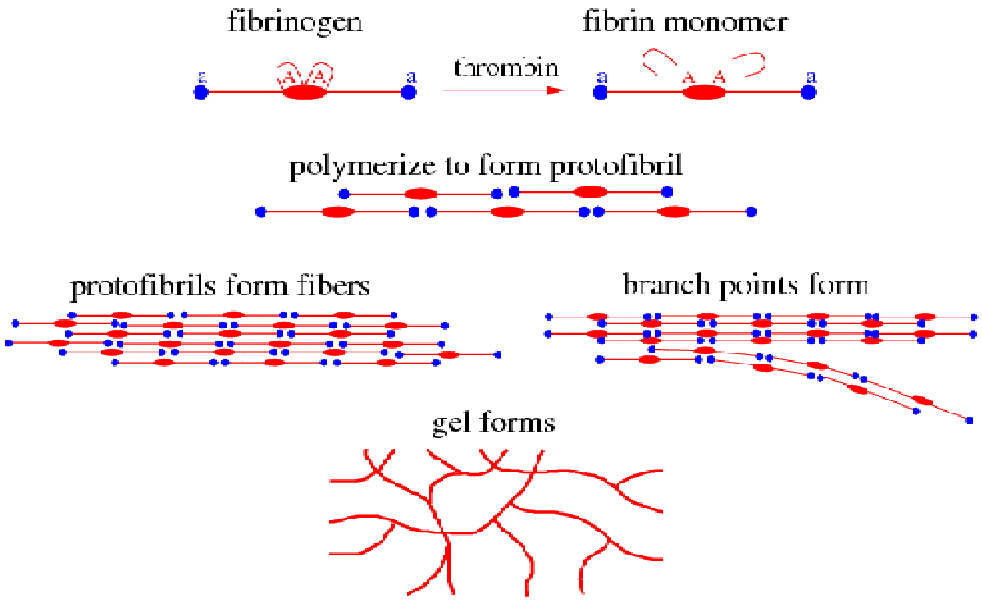

Figure 1-8. Schematic presentation of fibrin gel formation activated by thrombin [73].

1.1.2. Crosslinking methods to form hydrogels

As discussed above, a variety of synthetic and naturally derived materials have been used to form hydrogels for tissue engineering scaffolds. They were crosslinked to become hydrogels by chemical, physical method or a combination of both [77]. Stability and mechanical properties of the resultant hydrogel were closely linked to the method employed to form such hydrogel. It is generally believed that chemically crosslinked hydrogels is superior to hydrogels formed by physical methods in the respect of the stability and mechanical properties. The physical methods involve no covalent bond formation such as ionic interaction [37], stereocomplexation [78, 79], hydrophobic interaction [80, 81], self assembly [82, 83] and inclusion complexation [84]. There has

been a wide variety of strategies to prepare chemically crosslinked hydrogels. They were done through radical polymerization using redox- or photo-initiators, Michael-type addition reaction, Schiff-base formation, disulfide bond formation, reaction between thiols and acrylate or sulfones, click chemistry, aldehyde-mediated crosslinking and enzyme-mediated crosslinking [15, 28-30, 51, 85-90].

1.1.3. Strategies of hydrogels application for tissue engineering

Different strategies have been applied to use hydrogels for tissue engineering application. In one approach, a suitable hydrogel is implanted into the defect site to provide mechanical support to enhance migration of cells, which have the ability to proliferate and produce the tissue matrix, from the neighboring tissues into the defect site. In more advanced approaches, hydrogels are also used to deliver growth factors and gene delivery vectors to the defect site so as to accelerate the regeneration of tissue. Chemotactic factors diffuse into the neighboring tissue and bind to the cell receptors and accelerate their migration into the defect site. An ideal scaffold for this purpose is expected to navigate the tissue regeneration process by providing necessary cues for a desired cell function, and degrade as the tissue repair proceeds. Most often, when the defect sites are large and the cell migration from the residual surrounding tissues is minimal or impeded, a cell population which has the ability to produce the lost tissue is placed onto the defect site after encapsulating within the hydrogels for repair [91].

To achieve the implantation of such cell-loaded hydrogels, in one way, the hydrogels are preformed and processed *in vitro* prior to encapsulating the bioactive agents or cells and the subsequent *in vivo* implantation (Figure 1-9A). In the other, the

cells can be incorporated and suspended in the gels precursors prior to gelation and the gels precursors can be injected into the body as a liquid that forms gel *in situ* (Figure 1-9B). Comparing to its counterpart, the advantage of *in situ* polymerization is that the gel precursors containing cells can be injected into the defect site through small incisions and their subsequent polymerization enables a homogenous encapsulation of cells within the hydrogel. Since the fluidic precursors of the cell-hydrogel system can fill any irregular defect shapes, hydrogel-based scaffolds are highly suitable for treating defects which are not easily accessible, unless one adopts an invasive surgical procedure. They can be easily formulated with cells by simple mixing, and do not require a surgical procedure to be implanted or in the case of biodegradable ones, to be removed. The *in situ* polymerization also results in improved contact between the native tissue and hydrogel.

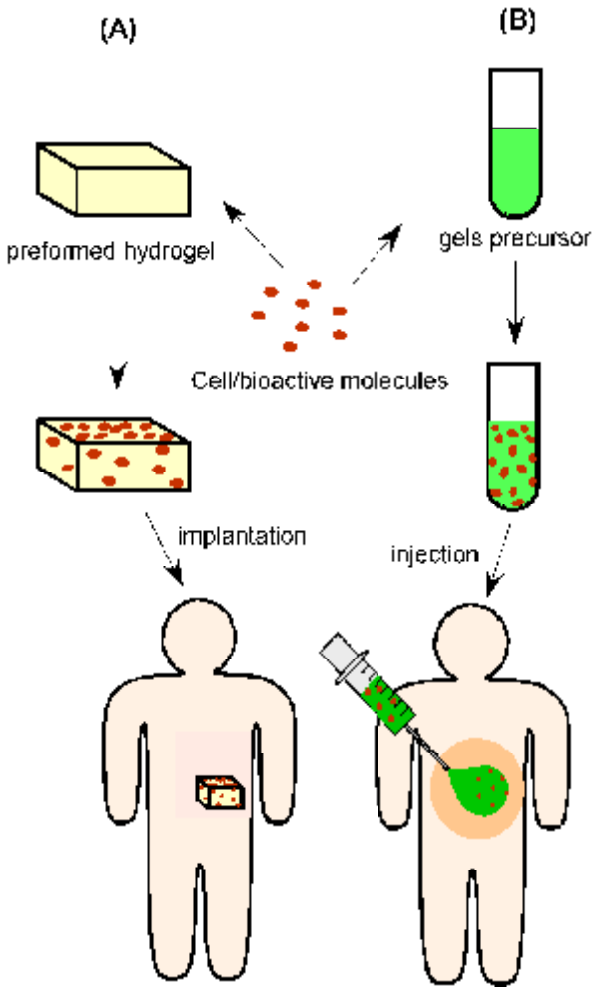

Figure 1-9. Strategies of hydrogels application in combination with cells/bioactive molecules: (A) preformed hydrogel, (B) injectable hydrogels.

Advances in polymeric materials engineering has offered new opportunities of delivery by minimally invasive surgical methods, aimed at minimizing patient trauma and speeding up recovery. To this end, various *in situ* polymerization techniques/hydrogels either by chemical or physical crosslinking methods, such as photopolymerization, stimuli responsive polymers, multi-functional polymers, self-assembling peptide-based systems, and enzyme-mediated crosslinking systems have been widely explored for

minimally invasive applications. In photopolymerization, components of the hydrogel along with viable cells are injected in a fluid state into the defect site arthroscopically, followed by subsequent polymerization within the defect site using a light source such as ultraviolet (UV) radiation [92]. The advantages are the spatial and temporal control, as well as the fast curing rate obtained under physiological conditions at room temperature. The stimuli-responsive hydrogels consists of polymer networks that can undergo a discontinuous and macroscopic phase transition between a liquid and solid state when subjected to a small change in one or more environmental stimuli such as temperature, pH, light, radiation forces, and chemical triggers [87, 93-96]. The *in situ* forming protein-based hydrogel is driven by self-assembly with respect to temperature, pH, and chemical triggers in the presence of biological fluids [97-100]. This self-assembly is generally mediated by secondary forces such as ionic interactions, hydrogen bonds, hydrophobic interactions, and van der Waals interaction [98]. In addition to their *in situ* gelation capability, these protein-based hydrogels also provide the necessary biochemical cues to support cell proliferation and tissue formation [100].

Another approach that has been employed for *in situ* hydrogel formation involves the mixing of two precursor solutions having functional groups such that they form hydrogels upon reactions between the functional groups. Schiff base reaction of amine and aldehyde groups and Michael-type addition reaction between the vinylsulfone endgroups and thiol-bearing compounds have been extensively explored for this reason [15, 44, 101, 102]. Hydrogels formed by enzyme-mediated crosslinking reaction take advantages of the high substrate specificity of enzyme to control and predict the crosslinking reaction. Transglutaminase (TG) is one of the typical enzymes that are

capable of catalyzing crosslinking reactions. It has the ability to form amide linkage between the γ-carboxamide group of glutamine residues and primary amines such as the one in lysine [103]. Horseradish peroxidase (HRP) is a single-chain β-type hemoprotein that catalyzes the coupling of phenols or aniline derivatives in the presence of hydrogen peroxide [104]. The hydrogels were formed through the oxidative coupling of phenol moiety, which was catalyzed by HRP and H_2O_2 [43, 52, 89, 105].

As mentioned earlier in section **1.1.2.**, the stability and mechanical properties of the resultant hydrogel is closely linked to the method employed to form such hydrogel. Covalent bonds are usually strong and permanent unlike physical crosslinks. Moreover, concerning the bioactive molecules or cells in the injectable hydrogels, the gel forming conditions of these hydrogels should be mild, physiologically stable and easily integrated into clinical procedures so that their activity and functions are not compromised by such procedures. Besides, there are many other variables to be considered when it comes to designing a desirable hydrogel for a specific application especially in tissue engineering. This will be as discussed in the following section.

1.2. Design criteria for hydrogel scaffolds in tissue engineering

In the most general sense, tissue engineering seeks to fabricate, living replacement parts for the body. In order to create such biologically and functionally active replacements, numerous strategies have been currently used including incorporation of cells, various growth factors and other bioactive signals into a material scaffold such as the hydrogels discussed above. These hydrogels serve as a synthetic extracellular matrix (ECM) to organize cells into three-dimensional (3D) architecture and to present stimuli, which

guide the regulation of the cellular functions during formation of a desired tissue. Therefore, the hydrogel is expected to provide a specific biological and mechanical environment to the encapsulated cells. The scaffold also assigns a predefined architecture to the regenerated tissue. Thus, the selection of the appropriate hydrogel scaffold materials is governed by the physical property, the mass transport property, and the biological interaction requirements of each specific application. These properties or design variables are specified by the intended scaffold application and environment into which the scaffold will be placed [2, 38, 106].

Towards a rational design of hydrogels for tissue engineering, several variables must be considered in the aspect of both biochemical and physical properties [2, 106]. In general, all hydrogels used in biomedical applications must be biocompatible and should promote cell growth. Those involving encapsulation of cell or bioactive agents must be capable of being formed into gels without damaging the cells or compromising activities of bioactive agents. They should degrade into non-cytotoxic segments for easy elimination. Ideally, the rate of scaffold degradation should mirror the rate of new tissue formation or be adequate for the controlled release of bioactive molecules. They must have adequate mass transport properties to allow diffusion of nutrients and metabolites to and from the encapsulated cells and the surrounding tissues. They are required to not only have sufficient mechanical integrity and strength to withstand manipulations associated with implantation and *in vivo* existence until the cells have produced their own functional ECM once placed at the application, but also provide an appropriate mechanical environment to support cell migration, proliferation, and differentiation [14]. As each tissue provides its own mechanical microenvironment, the mechanical characteristics of

hydrogels used in tissue engineering have to be adapted to the intended application in light of physical cues regulating cell function and tissue morphogenesis. Therefore, the physical characteristics of hydrogels used in tissue engineering applications should no longer be neglected with respect to their biological effects. The following section illustrates the role of stiffness in regulating cell functions.

1.3. The role of substrate stiffness in regulating cell behavior

As discussed in section **1.2.**, the previous approaches to engineer artificial tissues have focused largely on optimization of polymer chemistry and selection of appropriate biochemical properties to provide effective tissue regeneration. However, it is increasingly recognized that apart from biochemical conditions, physical parameters are also essential in the design variables of substrates used in tissue engineering applications [107]. Structure and function of the adherent cell depend in a crucial way on its microenvironment, including the stiffness of its substrate [108]. Recent developments in producing biocompatible materials and understanding how cells react to environmental stimuli have enabled numerous demonstrations that cells can be exquisitely sensitive to changes in the mechanical properties of their substrates even when their chemical environment is held constant.

Cells adhering to a substrate are able to sense mechanical stimuli and consequently regulate many important physiological processes including cell morphology [109, 110], adhesion [111, 112], migration [109, 113, 114], phenotype [115], differentiation [10, 116], proliferation [117], apoptosis [118] and gene expression [119]. For example, fibroblasts grown on glass were more spread but not as elongated as they

were in vivo or when grown in 3D collagen matrices [110]. It was also shown that cells generate more traction force and develop a broader and flatter morphology on stiff substrates than they do on soft but equally adhesive surfaces and cells will preferentially migrate towards stiffer regions [114]. A dependence of cell cycle rate on substrate stiffness was also demonstrated [117]. A decreased proliferation of dermal fibroblasts was found in less dense, more compliant 3D collagen matrices compared to denser, stiffer gels. It was proposed that the mechanical input associated with shape change that regulates the cell cycle [118]. Fibroblast phenotype was changed from resting to activated when the mechanical load was increased from low to high. There was marked decline in cellular DNA synthesis when the mechanical load was low [120]. In addition to the changes in cell proliferation, the biosynthetic activity of fibroblast including the release of collagenase and their response to growth factor also appeared to be mechanical load-dependent [121]. The mechanical input from the substrate, transmitted through adhesion receptors, then activates downstream signals that regulate both the degree of cell spreading and the proliferation rate. On stiff substrates, resistance to mechanical probing may lead to protein conformational changes and activation of signaling enzymes at the adhesion sites. The response in turn causes an increase in traction forces and in cell spreading, leading to increased DNA synthesis and decreased apoptosis.

The stiffness of the extracellular environment was also found to affect the phenotype and contractile properties of heart cells [115]. The substrate stiffness comparable to the native adult rat myocardium (22-50k Pa) was found to be optimal for heart cell morphology and function, with superior elongation, reasonable excitation threshold, high contractile force development and well-developed striations. The cells on

the surfaces with lower stiffness had reduced cell density and force of contraction. Those with higher stiffness exhibited poor electrical excitability.

Human mesenchymal stem cells (hMSCs) have come to play progressively prominent roles in tissue engineering due to their ability to differentiate into multiple cell lineages, including osteoblasts, chondroblasts, adipocytes, neurons, skeletal myoblasts, and cardiac myocytes [122], their relative ease of isolation and no known tumorigenic potential *in vivo* [123]. Their proliferation and differentiation was found to be responsive to substrate stiffness too. An almost complete suppression of proliferation were observed when hMSCs were cultured on or between ligand coated, soft, synthetic gels confirming that a drop in proliferation could occur independent of a change in ligand density [124]. More recently, the hMSCs provide particularly striking evidence that they sense the stiffness of their substrate. Consequently, they differentiate into specific cell lineages according to the substrate's stiffness. The hMSCs cultured on collagen-coated polyacrylamide gels of varying elasticity that correspond to the tissue elasticities of brain (0.1-1k Pa), muscle (8-17k Pa) and nascent bone (>34k Pa) respectively were found to express key markers of early neurogenic, myogenic and osteogenic lineages even though the culture media remains the same [10].

It has been found that the substrate stiffness also plays a critical role on the level of gene transfer and expression [119]. It modulated the cells' ability to take up gene carriers, and also regulated the extent of pDNA dissociation from the condensing agent and ultimate expression of the transferred gene. The endocyotsis of the pDNA condensates and their import into the nucleus increased with the increase in stiffness of the adhesion substrate.

Altogether, these suggested the existence of a fundamental micromechanical control switch that underlies tissue development. Physical properties of the substrate are potent regulators of such process. Both biochemical and mechanical signals interplay to guide cell functions and tissue regeneration. Therefore, new tissue engineering approaches aimed at regenerating lost or diseased tissues must incorporate both biochemical and physical design variables to most effectively induce tissue repair and, potentially, organ regeneration in the future.

1.4. Aims

As discussed above, it has been increasingly recognized that substrate mechanics [125] and topography of extracellular microenvironment can also modulate the tissue cell phenotype in a way similar to biochemical signals [126]. These new findings regarding the importance of the mechanical properties of a material open new possibilities, particularly in the field of biomaterials for tissue engineering. Cell-loaded biomaterials was often attempted as an advanced approach in tissue engineering to provide necessary cues for tissue regeneration with more desirable outcome. These cell therapies represent a promising way to treat a variety of diseases and injuries in the area of regenerative medicine and tissue engineering [127-129]. The full understandings of various cell functions as well as the factors that influence these physiological processes are highly crucial in advancing the cell therapies for clinical application. Thus, approaches to influence various cell functions by controlling the mechanical properties have been investigated. Most often, these studies dealt with gels of polyacrylamide and poly(dimethylsiloxane) (PDMS), which can be prepared easily and whose stiffness can be

tuned by varying the cross-linker concentration [10, 114, 130]. However, such model substrates are not designated to be used for *in vivo* applications due to its limitation to two-dimensional study (2D) as a result of its inherent toxicity of polymers and/or crosslinkers and poor cell adhesiveness owing to its nature of polymer chemistry.

Enabling a systematic study from 2D systems to three-dimensional (3D) systems is critical as recent findings suggested that cells behave more physiologically in a 3D environment compared to 2D surface [121]. When the cells are seeded within three-dimensional scaffolds, the ECM proteins produced by the cells are deposited uniformly within the scaffold, which then remodel to yield the desired cytoarchitecture [131]. It is essential to understand cell behaviors and the interaction between cells and matrix in a 3D context as cells experience a richer, more complex physical environment and markedly different geometry and behave more physiologically in 3D compared to 2D surfaces. Although, very often, given the ease of growing and observing cells on the surfaces, 2D approach was widely adopted for most research purposes. However, the extent to which observations made in 2D studies can be transferred to predict cell behavior in a 3D environment has been an active area of research.

Hydrogels have been recognized as one of the attractive candidates for cultivating cells in a 3D environment because they have high permeability for oxygen, nutrients and other water-soluble metabolites through their high water-content matrix, which is an excellent environment for cell growth and tissue regeneration [2, 5, 38, 106, 132-134]. Particularly, the use of injectable hydrogels as scaffolds in tissue engineering is advantageous compared to preformed hydrogels because they are able to fill any shape or defect, can be easily formulated with drugs, growth factors and cells by simple mixing,

and do not require a surgical procedure to be implanted or in the case of biodegradable ones, to be removed. However, a major drawback of existing injectable hydrogel systems is over the control of the gelation rate that is limited to varying the gel precursor and/or crosslinker concentration, which inevitably changes the stiffness of the hydrogel and leads to the undesirable control of the cell growth and differentiation in hydrogels. Also, such systems would require a lot of optimization in order to achieve the appropriate growth rate and control over the differentiation of stem cells, because different concentrations of precursor polymer would be used to optimize the gelation rate. Using different concentrations of the polymer precursor may cause changes in the interaction between polymer chains and cells, especially when the polymer chains are conjugated with cell adhesive ligands such as RGD peptides. As such, the stiffness of the hydrogel will vary in correspondence to the biochemical and other signals that may present in polymer chains. Thus, the need to decouple the effects of polymer concentration and the hydrogel stiffness to allow independent study on the effect of stiffness on various cell functions with minimum variation in other parameters arises.

Recently, our laboratory has developed an injectable hydrogel system with the independent tuning of stiffness and gelation rate of by utilizing a simple solution mixture of constant concentrations of hyaluronic acid-phenol conjugates, hydrogen peroxide (H_2O_2) and horseradish peroxidase (HRP) [89, 90, 105]. The hydrogels are formed *in situ* through the oxidative coupling of phenol moiety, which is catalyzed by H_2O_2 and HRP. The H_2O_2 and HRP determined the hydrogel stiffness and gelation rate of the injectable hydrogel respectively. A range of stiffness was achieved by varying the concentration of H_2O_2 while keeping the concentration of hydrogel precursor constant. At the same time, a

rapid gelation to ensure the precise location and prevent undesirable diffusion of gel precursors and encapsulated bioactive molecules to the surrounding tissues was achieved with the use of this enzyme-mediated oxidation reaction [90]. With this method, it becomes possible to address the importance of incorporating the physical variables in the design by developing a new hydrogel system with many desirable characteristics such as tunable stiffness, *in situ* forming, biocompatibility, biodegradability, excellent cell adhesion, and rapid gelation to study the cell functional responses including cell adhesion, proliferation, migration and differentiation in a 3D environment.

The objective of this study is to design and develop such hydrogel system with unique control in stiffness to meet the increasing need of understanding in the independent effect of stiffness on various cell functions in a 3D environment which proves to be very challenging using the existing hydrogel systems. This new system ensures decoupling effects of hydrogel stiffness and its precursor concentration and enables us to gain some understanding on the effect of stiffness independent of other variables on various cell functions in both 2D and 3D setting. An extension of this goal is to maximize its control in the range of stiffness to fully attain the benefits of such control in respect to cell functions. The second objective is to demonstrate the effect of stiffness on functions of human mesenchymal stem cells (hMSCs) and human fibroblast (HFF-1) including cell adhesion, migration, proliferation and differentiation and highlight their dimensionality-specific responses between the 2D and 3D studies for the cell-based therapies in tissue engineering. The ease of integration into clinical procedures allows us to further the *in vivo* therapies using such a system for tissue engineering application.

1.5. Structure of dissertation

This dissertation is divided into seven Chapters. An overview of the contents of each Chapter is provided here. The thesis is a detailed and sequential document, with each Chapter building on the conclusions of the previous Chapter. Firstly, Chapter 1 - Introduces the background on hydrogels for tissue engineering and specifically focuses on rational design variables for hydrogel as scaffold for tissue engineering that brings about our the objectives of the study. Chapter 2 – Provides details of the methodologies in our hydrogel design and discusses the synthesis and characterization of gelatin-hydroxyphenylpropionic acid (Gtn-HPA) conjugates and its hydrogel system. Chapter 3 – Describes the formation of Gtn-HPA hydrogel, composed of Gtn-HPA conjugates, by enzyme-mediated crosslinking reaction and discusses the role of stiffness in the proliferation and differentiation of hMSCs in 3D study using the Gtn-HPA hydrogels with varied stiffness. Chapter 4 – Explores the modulation of hMSCs proliferation and differentiation by hydrogel stiffness in a wide range in 2D environment and emphasizes the role of stiffness in controlling cell functions. Chapter 5 – Explores the cell-to-cell variation in cellular responses to hydrogel stiffness and describes those of human fibroblasts to stiffness in both 2D and 3D culture setting and its potential implication for wound healing application. Chapter 6 – Covers our efforts to maximize the control in stiffness range in Gtn-Phenol hydrogel system in order to fully maximize the potential of hMSCs for potential cell-based *in vivo* therapies. Chapter 7 – Appropriately summarizes and concludes this newly developed system for tissue engineering application and suggests topics and areas for further research and work.

Chapter II

Design of an injectable hydrogel system with unique tuning of stiffness

2. Design of an injectable hydrogel system with unique tuning of stiffness

2.1. Introduction

Recently, our laboratory has developed an injectable hydrogel system composed of hyaluronic acid-tyramine conjugates [89, 90, 105]. It has achieved an independent tuning of stiffness and gelation rate where concentration of H_2O_2 and HRP determined the hydrogel stiffness and gelation rate of the injectable hydrogel, respectively. The stiffness was readily tuned by the concentration of H_2O_2 without changing the concentration of hydrogel precursor solution. The gelation rate was independently controlled by the HRP concentration. This enables the formation of the hydrogel of varied stiffness with equally rapid gelation rate. The rapid gelation of an injectable hydrogel system is essential to ensure the precise location and prevent the undesirable diffusion of gel precursors and encapsulated bioactive molecules to the surrounding tissues [90].

To address the importance of incorporating the stiffness variables into the design of the hydrogels for tissue engineering as discussed in the first chapter, a hydrogel composed of gelatin-hydroxyphenylpropionic acid (Gtn-HPA) conjugates was developed in the belief that stiffness of such hydrogel can be independently controlled by the concentration of H_2O_2 without varying the concentration of Gtn-HPA conjugate. As such, the sole effect of stiffness on various cell functions can be demonstrated. *In situ* forming ability of this hydrogel system enabled us to incorporate cells into the hydrogel precursor and study the role of stiffness in a three-dimensional (3D) context. A systematic 2D study of such stiffness effect on various cell functions can be also performed as the surface of

the hydrogels strongly support the cell attachment and proliferation without additional coating of adhesive moieties owing to the inherent properties of Gtn (Figure 2-1). Taken together many other properties that Gtn-HPA hydrogel possesses, such as biocompatibility, high solubility, biodegradability, low antigenicity, this hydrogel system offers a suitable material system with unique control in stiffness for tissue engineering application.

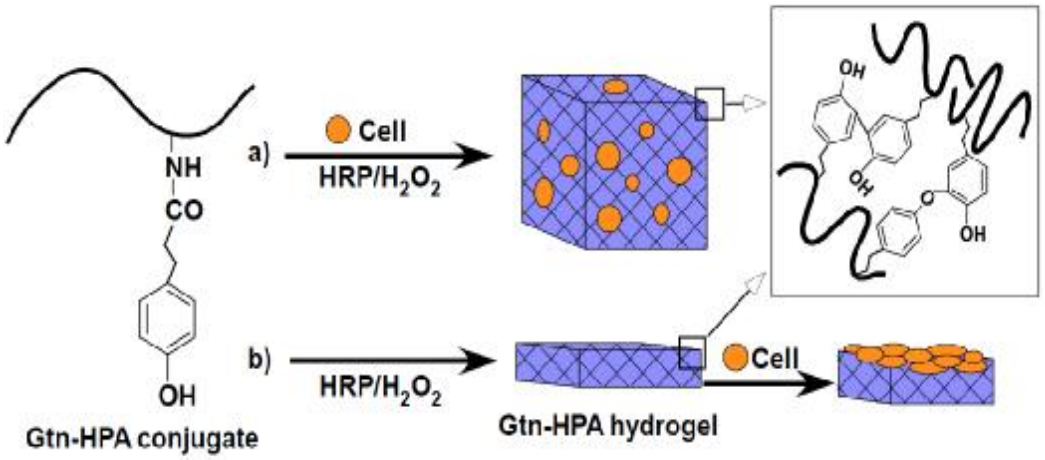

Figure 2-1. Formations of Gtn-HPA hydrogels for *in vitro* cell study.

In this chapter, the synthesis and characterization of Gtn-HPA conjugates and hydrogels are discussed. 3,4-Hydroxyphenylpropionic acid (HPA), a phenol compound, was conjugated onto Gtn by a general carbodiimide/active ester-mediated coupling reaction in distilled water. The Gtn-HPA conjugates were then purified by dialysis and characterized by the conventional 2,4,6-trinitrobenzene sulfonic acid (TNBS) method [135], UV-visible spectrometer and ^{1}H NMR to determine the percentage of HPA

conjugated to Gtn. Gtn-HPA hydrogels composed of Gtn-HPA conjugates were formed by the oxidative coupling of HPA moieties catalyzed by H_2O_2 and horseradish peroxidase (HRP). The formation of Gtn-HPA hydrogels was studied using oscillatory rheometry which measures the storage modulus (G') against the shear strain. This rheological method has been often employed to study the viscoelastic behavior of materials and G' is commonly serves an indication of stiffness of a given viscoelastic material.

2.2. Materials and methods

2.2.1. Materials

Gelatin (Gtn) (MW = 80-140k Da, pI = 5) and horseradish peroxidase (HRP) (100 units/mg) were obtained from Wako Pure Chemical Industries (Japan). 3,4-Hydroxyphenylpropionic acid (HPA), tyramine hydrochloride (Tyr·HCl), *N*-hydroxysuccinimide (NHS), 1-ethyl-3-(3-dimethylaminopropyl)-carbodiimide hydrochloride (EDC·HCl), hydrogen peroxide (H_2O_2, 30 %), 2,4,6-trinitrobenzene sulfonic acid (TNBS) and glycine were purchased from Sigma-Aldrich (Singapore). Phosphate buffer saline (PBS, 150 mM, pH 7.3) solution was supplied by media preparation facility in Biopolis (Singapore).

2.2.2. Synthesis of Gtn-HPA conjugate

3,4-Hydroxyphenylpropionic acid (HPA) was used to synthesize Gtn-HPA conjugates by a general carbodiimide/active ester-mediated coupling reaction in distilled water. HPA

(3.32 g, 20 mmol) was dissolved in 250 ml of mixture of distilled water and *N*, *N*-dimethylformamide (DMF) (3:2). To this *N*-hydroxysuccinimide (3.20 g, 27.8 mmol) and 1-ethyl-3-(3-dimethylaminopropyl)-carbodiimide hydrochloride (3.82 g, 20 mmol) were added. The reaction was stirred at room temperature for 5 h, and the pH of the mixture was maintained at 4.7. Then, 150 ml of Gtn aqueous solution (6.25 wt.%) was added to the reaction mixture and stirred over night at room temperature at pH 4.7.

2.2.3. Purification of Gtn-HPA conjugate

The solution was transferred to dialysis tubes with molecular cut-off of 1000 Da. The tubes were dialyzed against 100 mM sodium chloride solution for 2 days, a mixture of distilled water and ethanol (3:1) for 1 day and distilled water for 1 day, successively. The absorbance spectrum of dialysate was monitored using UV spectrometer. The purified solution was lyophilized to obtain the Gtn-HPA. The success of conjugation was further confirmed by 2,4,6-trinitrobenzene sulfonic acid (TNBS) method, UV-visible spectrometer measurement and ^{1}H NMR.

2.2.4. Characterization of Gtn-HPA conjugates

2,4,6-trinitrobenzenesulfonic acid (TNBS) was used as a regent to determine the concentrations of amines. Twenty-five microliters of aqueous 0.03 M TNBS was added to 1 ml of aqueous solution of Gtn-HPA conjugates in a cuvette, agitated to ensure complete mixing, and allowed to stand for 30 mins at room temperature. The reagent blank consisted of 25 µl of 0.03 M TNBS in 1 ml of 0.10 M borate. Absorbance was

recorded at 420 nm. The percentage of HPA was determined by comparing the free amine available in the Gtn-HPA to glycine standard curve prepared by a set of solutions known concentration. For quantification of phenol content in the Gtn-HPA conjugates, UV measurement study was employed. The wavelength ranging from 230 to 350 nm was scanned for aqueous solution of Gtn-HPA using UV spectrometer. A standard curve for HPA was generated by obtaining absorbance values for the corresponding different concentrations between 0.01 and 1 mM. Spectra of Gtn were also obtained and served as background. The effective concentration of HPA in Gtn-HPA conjugates was determined by absorbance measurement of the sample solution along with known concentration of HPA standards. The experiment was performed in three replicates.

2.2.5. Scale-up synthesis of Gtn-HPA conjugates

Ten times scale-up synthesis of Gtn-HPA conjugates was performed to evaluate the feasibility of production in a larger scale. HPA (33.2 g, 0.2 mol) was dissolved in 2.5 L of mixture of distilled water and *N*, *N*-dimethylformamide (DMF) (3:2). To this, *N*-hydroxysuccinimide (32 g, 0.278 mol) and 1-ethyl-3-(3-dimethylaminopropyl)-carbodiimide hydrochloride (38.2 g, 0.2 mol) were added. The reaction was stirred at room temperature for 5 h, and the pH of the mixture was maintained at 4.7. Then, 1.5 L of Gtn aqueous solution (6.25 wt.%) was added to the reaction mixture and stirred over night at room temperature at pH 4.7. The Gtn-HPA conjugates were purified and lyophilized using the same protocol as mentioned in **2.2.2.1.**. The total phenol content in

Gtn-HPA conjugates from a scale-up set up was compared with that of smaller scale by UV spectrometer measurement.

2.2.6. Rheological measurement

Rheological measurements of the hydrogel formation were performed with a HAAKE Rheoscope 1 rheometer (Karlsruhe, Germany) using a cone and plate geometry of 35 mm diameter and 0.945° cone angle. The measurements were taken at 37°C in the dynamic oscillatory mode with a constant deformation of 1 % and frequency of 1 Hz. To avoid slippage of samples during the measurement, a roughened glass bottom plate was used. The solution of HRP and H_2O_2 with different concentrations was added sequentially to an aqueous solution of Gtn-HPA (2 wt.%, 250 µl in PBS). The solution was vortexed and then immediately applied to the bottom plate. The upper cone was then lowered to a measurement gap of 0.024 mm and a layer of silicon oil was carefully applied around the cone to prevent solvent evaporation during the experiment. The measurement parameters were determined to be within the linear viscoelastic region in preliminary experiments.

2.3. Results and discussion

2.3.1. Purification of Gtn-HPA conjugates

The purification protocol was adopted from the previous publication for efficient removal of small molecules by extensive dialysis for four days [136]. Dialysis against a 100 mM NaCl solution will decrease the viscosity of solution, thus helping to remove small molecular impurities. Subsequently, dialysis against 25% EtOH significantly decreases

the volume of solution inside and finally dialysis against water rehydrates the solution and refills the dialysis tubing. By alternating these dialysis conditions, the exchange rate inside and outside the dialysis tubing is maximized. Our results show that the amount of detectable unreacted HPA in the dialysate was dramatically decreased from day 1 to day 4 (Figure 2-2). It was not detectable by day 4 after dialysis against distilled water. It suggested this dialysis routine was sufficiently effective to remove the unreacted HPA.

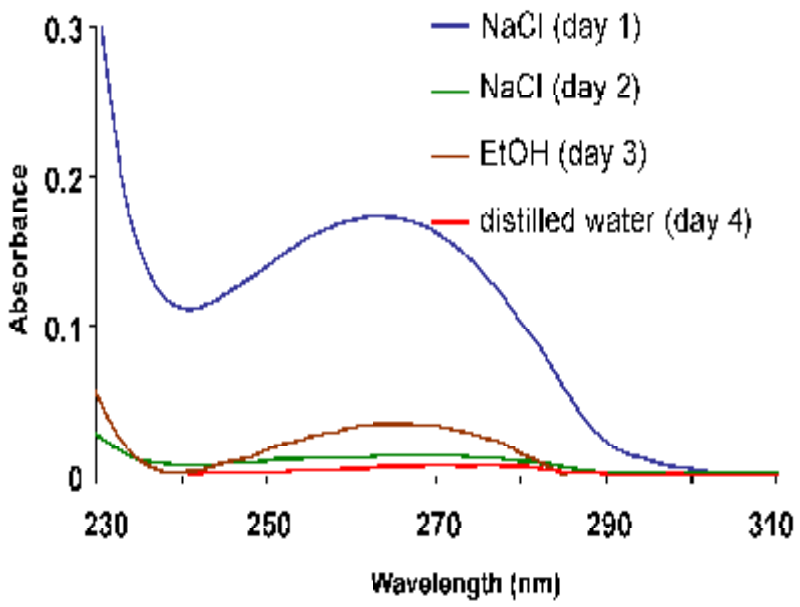

Figure 2-2. UV spectrometric analysis of the dialysates purity. NaCl dialysates (day 1 and day 2) were diluted 20 times to enable optimal detection by UV.

2.3.2. Synthesis of Gtn-HPA conjugates

Gtn-HPA conjugates were successfully synthesized by a general carbodiimide/active ester-mediated coupling reaction in distilled water. The percentage of HPA introduced to the amine groups of Gtn was determined by the conventional 2,4,6-trinitrobenzene sulfonic acid (TNBS) method. The result showed 90 % of the amine group in Gtn was conjugated with HPA. The success of this conjugation was further confirmed by ^{1}H NMR measurement. From the ^{1}H NMR spectrum of Gtn-HPA, the peaks at chemical shift (δ) 6.8 ppm and 7.1 ppm indicate the presence of the aromatic protons of HPA, in addition to the aromatic protons of phenylalanine and tyrosine residues of Gtn (δ=7.3 ppm) (Figure 2-3). The conjugation of phenol molecules was quantitatively analyzed by measuring the absorbance values at 276 nm. The total phenol content of Gtn-HPA conjugate and Gtn-HPA conjugate from a ten times scale-up setting was determined to be 4.44×10^{-7} and 4.38×10^{-7} mol/mg conjugate respectively. Therefore, the scale-up synthesis of Gtn-HPA conjugate was deemed successful without compromising the conjugation degree of HPA to the Gtn. The high batch-to-batch reproducibility and ease of scale-up has suggested that the Gtn-HPA conjugates synthesis are clearly feasible for mass production if the need arises.

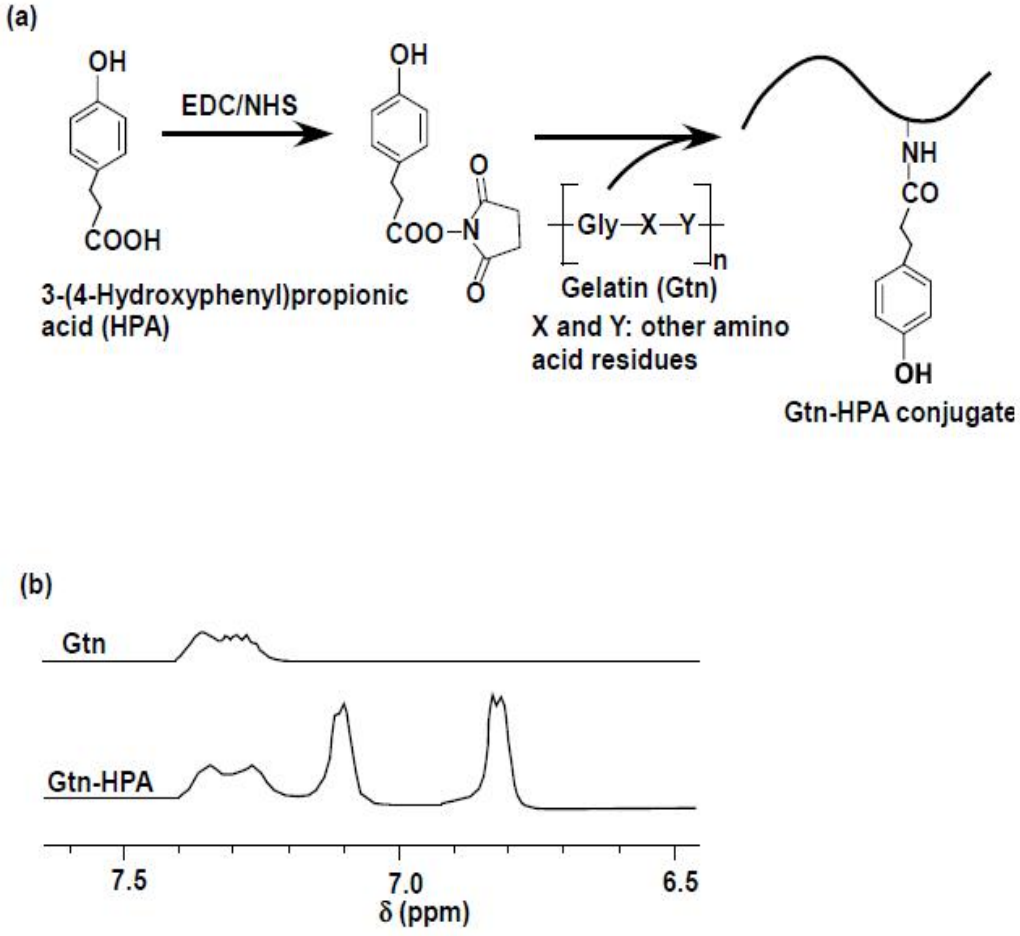

Figure 2-3. Synthesis of Gtn-HPA conjugates. (a) Synthetic scheme for Gtn-HPA conjugate; (b) ^{1}H NMR spectra of Gtn-HPA .

2.3.3. Hydrogel formation

In this section, the Gtn-HPA hydrogel formation is described. It was formed using the oxidative coupling of HPA moieties catalyzed by H_2O_2 and HRP. The gelation of Gtn-HPA conjugates was illustrated in Figure 2-4. It is well known that phenols crosslink through either a more common C-C linkage between the ortho-carbons of the aromatic ring or a C-O linkage between the ortho-carbon and the phenolic oxygen [137].

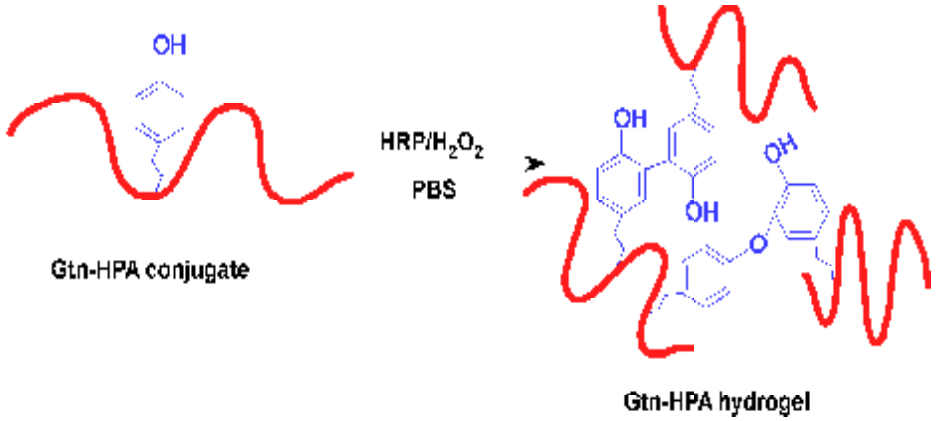

Figure 2-4. Gelation of Gtn-HPA conjugates.

The formation of Gtn-HPA hydrogels was studied using oscillatory rheometry which measures the storage modulus (G') and loss modulus (G'') against the shear strain. Rheological method has been often employed to study the viscoelastic behavior of materials and G' is commonly served an indication of stiffness of a given viscoelastic material. Also, the gel point, defined as the crossover of G' and G'', is employed to evaluate the gelation rate of hydrogel. The value of G' was recorded when it reached a

plateau, which indicated that crosslinking had been completed. Figure 2-5a shows the effects of H_2O_2 concentration on the gel point, the time required for G' to reach plateau and the G' value when HRP concentration was kept at 0.06 units/ml. It was found that G' which ranged from 10 to 1000 Pa was tunable by H_2O_2 concentration when an aqueous solution of Gtn-HPA conjugate (2 wt.%) was utilized. G' increased with the increase of H_2O_2 concentration from 0.5 mM to 1.7 mM suggesting higher crosslinking density was achieved when H_2O_2 concentration increased. However, further increase of H_2O_2 concentrations resulted in a decline of G' which was likely due to the deactivation of the HRP by an excess amount of H_2O_2 [138]. Interestingly, the gel point of hydrogels with different H_2O_2 concentrations remained at around 70 seconds, indicating that gelation rate was independent of H_2O_2 concentration. In addition, the time required for G' to reach plateau increased with the increase of H_2O_2 concentration. These results indicate that HRP was continuously oxidized by H_2O_2 and reduced by HPA moieties, until all H_2O_2 had been depleted in the process of Gtn-HPA hydrogel forming. Thus, it is considered that higher crosslinking density was achieved as a result of a higher amount of oxidized HPA, when the concentration of H_2O_2 increased. As a result, the hydrogel with higher stiffness was obtained. In this thesis, unless otherwise stated, the stiffness of hydrogel was consistently evaluated in the form of G', which is directly correlated to crosslinking density in our hydrogel system. Figure 2-5b shows the effects of HRP concentration on hydrogel formation while H_2O_2 concentration was fixed at 1.7 mM. G' remains almost constant when the HRP concentration was above 0.02 units/ml.

In contrast to the effect of H_2O_2, the gelation rate of Gtn-HPA hydrogels very much depended on the HRP concentration. Both the gel point and the time required for G' to

reach plateau decreased concomitantly as HRP concentration increased. These results are in a good agreement with an earlier report of hyaluronic acid–tyramine (HA-Tyr) hydrogel system using the same enzymatic oxidation reaction [89]. The mechanism of the independent tuning of gelation rate and stiffness of hydrogel has been explained in detail [90]. In this catalytic system, HRP catalyzed the crosslinking reaction with H_2O_2 as the oxidant. After successive oxidations of two phenol molecules, HRP returned to its original state and re-entered the crosslinking cycle. Thus, the independent tuning achieved in Gtn-HPA hydrogels is considered to be due to the catalytic reaction of HRP and H_2O_2.

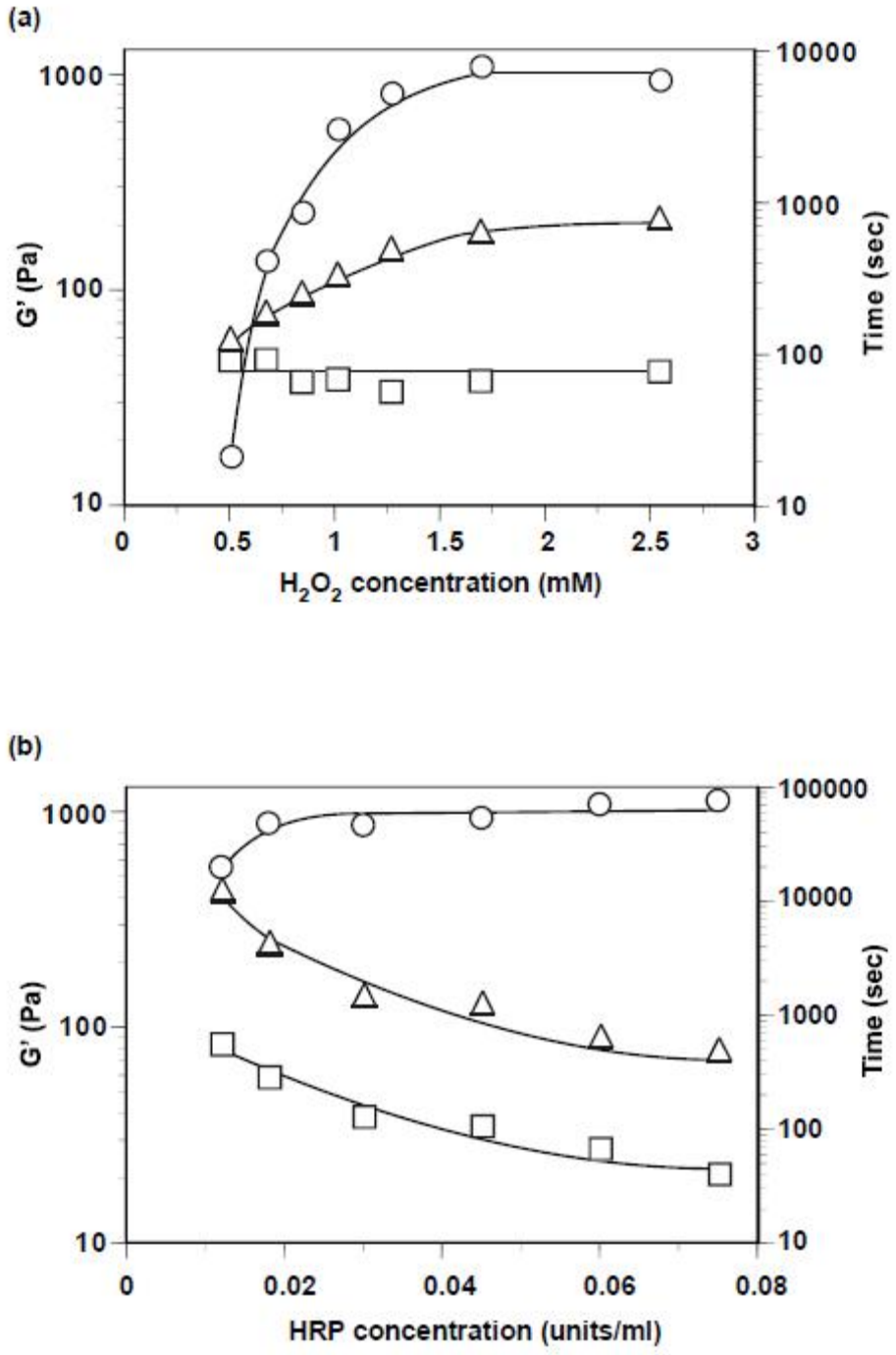

Figure 2-5. Effects of (1) H_2O_2 and (b) HRP concentration on the storage modulus G' (○), the gel point (□) and the time needed for G' to reach plateau (Δ). HRP and H_2O_2 concentrations are fixed at 0.06 units/ml for (a) and 1.7 mM for (b) respectively.

2.4. Conclusion

The synthesis and purification of Gtn-HPA conjugate were successfully performed. ^{1}H NMR and UV measurement confirmed the success of the synthesis. TNBS method revealed that about 90 % of amine in the Gtn has been conjugated. The synthesis of Gtn-HPA process was able to be scaled up without compromising the conjugation degree of HPA for easy mass production. The Gtn-HPA hydrogels were formed by the oxidative coupling reaction of phenol moiety in the presence of H_2O_2 and HRP. The stiffness of the hydrogel was well controlled by the H_2O_2 concentration, while HRP determined the gelation rate of the hydrogel. This unique independent tuning has not been seen in existing injectable hydrogel systems where the gelation rate is often closely correlated to the stiffness. The independent tuning of the Gtn-HPA hydrogel is expected to be useful as an injectable hydrogel system as such hydrogels can be formed at an efficient gelation rate with a wide range of stiffness. In the following three chapters, this Gtn-HPA hydrogel with unique tuning in stiffness was employed to study various cell functional responses to the hydrogel stiffness.

Chapter III

The role of stiffness in cell functions of hMSCs in 3D culture

3. The role of stiffness in cell functions of hMSCs in 3D culture

3.1. Introduction

Human mesenchymal stem cells (hMSCs) have generated a great deal of excitement and promise as a potential source of cells for cell-based therapeutic strategies, primarily owing to their intrinsic ability to self-renew and differentiate into functional cell types, including osteoblasts, chondroblasts, adipocytes, neurons, skeletal myoblasts, and cardiac myocytes. Stem cell-based tissue regeneration strategies have been widely investigated for the treatment of various diseases [139]. The precisely controlled differentiation of hMSCs to various cell phenotypes might become an important alternative source for cell therapy. For example, it has been also suggested that controlled neural differentiation of hMSCs might be an alternative source of cells other than neural stem cells for cell therapy of neurodegenerative disease due to the ease of harvest and expansion [140].

The differentiation of hMSCs is often stimulated by biochemical signals, for example, growth factors. However, the recent finding suggested that substrate mechanics and topography of extracellular microenvironment can modulate the tissue cell phenotype in a way similar to biochemical signals [125, 141]. hMSCs on the stiffest substrates expressed early markers of osteogenesis, whereas these cells on intermediated stiffness gels expressed myogenic markers and cells on the softest gels expressed neuronal marker [10]. Another study reported the interplay between the substrate stiffness and the surface adhesion chemistry. The stiffness regulation of lineage specific markers depended on which extracellular matrix (ECM) ligand was attached to the substrate [116]. When the

substrate was coated with collagen I, expression of the myogenesis marker MyoD was highest in hMSCs cultured on the stiffest gels, however, if the substrate was coated by collagen IV or fibronectin, expression was highest on intermediated stiffness gels. These findings underline the importance of incorporating both physical and biochemical variables into materials design particularly for tissue engineering application. An appropriate material system is greatly needed to understand and demonstrate role of stiffness in various cell functions not only in a two-dimensional environment but also in a three-dimensional (3D) one for furthering the cell-based therapies *in vivo* as the cells behave more physiologically and their functions were found to be enhanced in 3D [109, 142-144].

Gtn-HPA hydrogels are formed by an enzyme-mediated oxidation reaction as discussed in Chapter II. The *in situ* forming ability of this hydrogel system enables ease of cell encapsulation during the formation. Coupled with its inherent excellent cell adhesion properties of Gtn, biodegradability and the unique independent control in stiffness, it offers an excellent platform to study the role of stiffness in the functions of hMSCs in a 3D context.

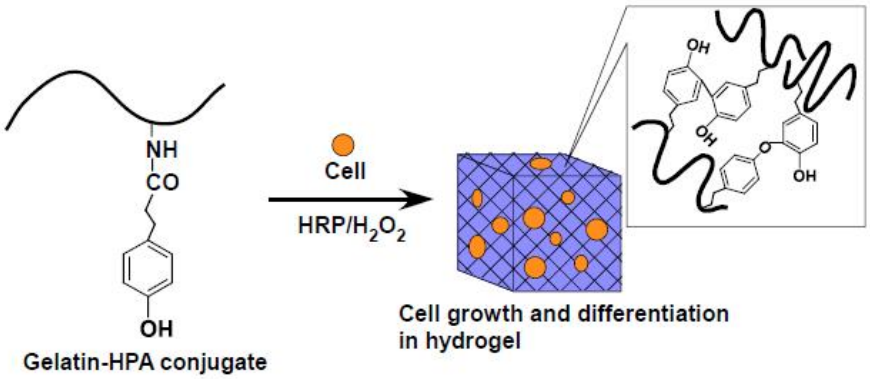

Figure 3-1. *In situ* forming of Gtn-HPA hydrogel by an enzyme-catalyzed oxidation for 3D cell growth and differentiation.

In this chapter, controls of hMSCs cell adhesion, proliferation and differentiation by the stiffness of this hydrogel system are demonstrated. The proliferation of hMSCs inside the Gtn-HPA hydrogel increased with the decrease in hydrogel stiffness and the neurogenic differentiation was also enhanced when the cells were cultured in hydrogels with lower stiffness.

3.2. Materials and methods

3.2.1. Materials

Triton X-100, bovine serum albumin (BSA), anti-β-tubulin, anti-neurofilament light chain (NFL) and anti-microtubule associated protein 2 (MAP2) were purchased from Sigma-Aldrich (Singapore). Anti-neurofilament heavy chain was obtained from Zymed (USA). Human mesenchymal stem cells (hMSCs) were provided by Cambrex Bio

Science Walkersville, Inc. (USA). Mesencult human basal medium supplemented with Mesencult human supplement was purchased from Stem Cell Technologies (Canada). Calcein acetoxymethyl ester, 4',6-diamidino-2-phenylindole (DAPI) and fluorophore-conjugated secondary antibodies were provided by Invitrogen (Singapore). HRP-conjugated secondary antibodies and Amersham ECL plus™ were purchased from GE Healthcare (Singapore).

3.2.2. Revitalization and culture of hMSCs

The cryovials containing hMSCs were retrieved from the liquid nitrogen tank and immediately incubated at 37°C in a water bath. The cryovials were transferred directly to the biohazard hood which had earlier been swabbed with 70 % alcohol. The cell suspension was transferred to a T-75 cm^2 cell culture flask using a sterile disposable pipette, followed by the addition of 12 ml of sterile supplemented hMSCs culture medium. The cells were incubated in 5 % CO_2 at 37°C. The medium was replaced after 24 h, and every 2-3 days subsequently. Cells in confluent state without signs of any form of contamination were ready for sub-culturing. The spent medium in the flask was pipetted out, followed by the addition of 5 ml of PBS (pH=7.4) to wash out cell debris and other residual substances produced by both live and dead cells. After removal of the PBS solution, 5 ml trypsin-EDTA solution (0.0125 %) was added to detach the cells from the substratum. The detached cells could be observed as separated and floating masses of round-shaped cells under the inverted microscope. Twenty ml of sterile culture medium was added to inactivate the activity of trypsin. The cell suspension was centrifuged at

1500 rpm and cell pellet was harvested after centrifugation. It was resuspended in culture medium and added to a 75 cm^2 T-flask in 5 % CO_2 at 37°C. Replenishing of fresh medium was conducted after 24 h and at subsequent 2-3 day intervals until the cells reached confluent state for the following *in vitro* study. Cells were observed under the inverted microscope at each of these time intervals to ensure they are healthy and uncontaminated. hMSCs with passage number less than 6 were used during the entire course of study.

3.2.3. Rheological measurement

Rheological measurements of the hydrogel formation were performed using the same settings and procedure as described previously in section **2.2.6.**. Briefly, the solution of HRP in 0.15 units/ml and H_2O_2 in final concentrations of 0.85 mM and 1.7 mM were added sequentially to an aqueous solution of Gtn-HPA (2 wt.%, 250 µl in PBS). The solution was vortexed and then immediately applied to the bottom plate. The upper cone was then lowered to a measurement gap of 0.024 mm and a layer of silicon oil was carefully applied around the cone to prevent solvent evaporation during the experiment. The gel point, Time needed for G' to reach plateau and G' were recorded. This experiment was performed in four replicates.

3.2.4. Enzymatic degradation of Gtn-HPA hydrogels

For the preparation of slab-shaped Gtn-HPA hydrogels, lyophilized Gtn-HPA was dissolved in PBS at a concentration of 2 wt.%. Six microliters of HRP was added to 1 ml of Gtn-HPA solution to give a final concentration of 0.15 units/ml. Crosslinking was initiated by adding 6 µl of different concentrations of H_2O_2 solution to give final concentrations of 0.85 and 1.7 mM. The mixture was vortexed vigorously before it was injected between two parallel glass plates clamped together with 1 mm spacing. The crosslinking reaction was allowed to proceed for 2 h. Then, round hydrogel disks with diameters of 1.6 cm were cut out from the hydrogel slab using a circular mold. The hydrogel disks were swollen in PBS for 24 h to reach swelling equilibrium and then sandwiched between plastic nets to facilitate retrieval of the hydrogels during degradation. The hydrogels were immersed in 20 ml of PBS containing 0.61 units/ml of type I collagenase and incubated at 37°C in an orbital shaker at 100 rpm. The degree of degradation of the hydrogels was estimated by measuring the residual hydrogel weight. For measuring the residual weight, the hydrogels were removed from the solution, blotted dry and weighed at specific time points.

3.2.5. Two-dimensional (2D) cell attachment study

For the preparation of Gtn-HPA hydrogels in the 24-well plate, lyophilized Gtn-HPA was dissolved in PBS at a concentration of 2 wt.%. Six microliters of HRP was added to 1 ml of Gtn-HPA solution to give a final concentration of 0.15 units/ml. Crosslinking was initiated by adding 6 µl of different concentrations of H_2O_2 solution to give final concentrations of 0.85 and 1.7 mM. The hydrogels were allowed to set for 4 h. Five

hundred µl of hMSCs in Mesencult human basal medium supplemented with Mesencult human supplement (passage number <6) at cell density of 3×10^5 cells/ml were seeded onto the hydrogels. The hydrogels were incubated at 37°C for 1 h and 6 h. After the incubation, the media with unattached cells were aspirated and the wells were washed with PBS. A culture plate without hydrogel served as a comparison. The cells attached on the hydrogels were harvested by incubating the hydrogels with collagenase solution at concentration of 6.7 units /ml. The cells attached on the culture plate were harvested with the aid of trypsin at concentration of 0.0125 %. To determine the number of attached cells on the hydrogels and culture well plate, the quantification of DNA was performed. The cell pellets were lysed by a freeze-thaw cycle in 200 µl of DNA-free lysis buffer. Samples were then incubated with 200 µl of PicoGreen working solution. The number of cells attached on the surfaces was then determined by the fluorescence measurement of the sample solution along with the known concentration of cell suspension for the standard curve. The fluorescence measurement was performed using a microplate reader with excitation and emission at 480 and 520 nm, respectively. This experiment was performed in four replicates.

3.2.6. Preparation of Gtn-HPA hydrogels encapsulated with hMSCs

To prepare hydrogel encapsulated with hMSCs, hMSC were harvested and mixed with 1 ml of Gtn-HPA solution (2 wt.%) in 6-well plate at final concentrations of 1×10^5 cells /ml. To initiate gel formation, 6 µl of H_2O_2 with concentrations of 142 mM and 284 mM

and 6 µl of HRP (25 units /ml) were added to the solution. The hydrogels were allowed to set for 4 h before being maintained in culture medium.

3.2.7. hMSCs proliferation on the Gtn-HPA hydrogels (2D)

For 2D cell proliferation on the surface of hydrogels, the hydrogels were prepared in 24-well plate using the same protocol as described above and allowed to set for 4 h. Five hundred microliters of hMSCs in mesencult human basal medium supplemented with mesencult human supplement (passage number <6) at cell density of 2×10^4 cells/ml were seeded onto the hydrogels and maintained in culture medium. The culture medium was changed every 2-3 days. The cell numbers were determined by the quantification of DNA. The PicoGreen assay to quantify DNA amount was performed using the same protocol as described above.

3.2.8. hMSCs proliferation in the Gtn-HPA hydrogels (3D)

For 3D cell proliferation in the hydrogels, hMSC encapsulated hydrogels were prepared as described above. The hydrogels were allowed to set for 4 h before being maintained in culture medium. The culture medium was changed every 2-3 days. To evaluate the cell proliferation in hydrogels, the cell pellets were harvested by incubating the gels with collagenase solution (6.7 units/ml) for digestion of Gtn-HPA hydrogels. The cell numbers were determined by the quantification of DNA. The PicoGreen assay to quantify DNA amount was performed using the same protocol as described above. For the observation of cell morphology in hydrogels, cell-encapsulated hydrogels were incubated with 2 µM

of calcein acetoxymethyl ester (Calcien AM) for 1 h at 37°C. The morphology of fluorescently labeled cells was accessed using fluorescence microscope (Olympus 71, Japan).

3.2.9. Degradation of hydrogel encapsulated with hMSCs

To monitor the change of water uptake in Gtn-HPA hydrogel over time, cell-encapsulated hydrogels were prepared as described above in section **3.2.6.**. Gtn-HPA hydrogels in the absence of cells were also prepared and maintained in the same culture medium as comparison. At each time interval, the hydrogels were removed from medium, blotted to remove excess aqueous medium and immediately weighed. Water uptake was calculated from the equation $W=(M_s-M_d)/M_d$, where M_s is the weight of the hydrogel in swollen state, and M_d is the dry weight of the hydrogel obtained by lyophilization. Three replicates were performed for this experiment.

3.2.10. hMSCs focal adhesion study

Both 2D and 3D cultures of hMSCs were performed using Gtn-HPA hydrogels for 2 weeks before being immunostained using an actin/focal adhesion stain kit. Prior to it, the hydrogels together with the cells were fixed with 4 % formaldehyde solution at room temperature for 20 min. After washing, the cells were permeabilized using 0.5 % Triton X-100 in PBS solution at room temperature for 5 min. The cells were then blocked in 0.05 % Triton X-100 containing 1 % bovine serum albumin at room temperature for 1 h. The samples were then incubated with anti-vinculin in blocking buffer solution at 4°C

overnight. After washing, the cells were incubated with the FITC-conjugated secondary antibody in the dark for 30 min. For double labeling, TRITC-conjugated phalloidin was incubated simultaneously with the secondary antibody. The cell nuclei were counterstained with DAPI (1:15,000 in water of 5 mg/ml stock). Confocal images were taken with a confocal laser scanning microscope (Olympus FV300, Japan).

3.2.11. Three-dimensional (3D) hMSCs differentiation

For studies involving hMSC differentiation in Gtn-HPA hydrogels, the cells were pre-treated with mitomycin C (10 μg/ml) for 2 h to inhibit proliferation and washed three times with culture medium. The hydrogels containing mitomycin C treated hMSCs at final density of 1×10^5 cells/ml were prepared as described above in section **3.2.6.**. The culture was maintained for 3 weeks. Prior to confocal imaging, the cells were fixed, permeabilized and blocked using the same protocol as described above. The samples were then incubated with the primary antibody in blocking buffer solution at 4°C overnight. After washing, the cells were incubated with the fluorophore-conjugated secondary antibodies in the dark for 30 min. The cell nuclei were counterstained with DAPI (1:15,000 in water of 5 mg/ml stock). Confocal images were taken with confocal laser scanning microscope (Olympus FV300, Japan). For western blotting, cells were harvested using collagenase as described above. The cells in buffer (4 % SDS, 20 % glycerol and 0.02 % bromophenol blue in Tris-HCl (0.125 M, pH 6.8)) were sonicated for 30 seconds. Cell lysate was boiled for 5 min, and was subjected to SDS-polyacrylamide gel electrophoresis. The separated proteins were transferred onto nitrocellulose, blocked with 5 % milk, and immunoblotted with specific primary antibodies, and detected using

HRP-conjugated secondary antibodies and Amersham ECL plus™ as a chemiluminescent substrate. Blot for β-actin was served as a control to ensure constant protein loading level. All western blottings were performed in duplicate.

3.3. Results and discussion

3.3.1. Gtn-HPA hydrogel formation

The composition of hydrogel formation was optimized for *in vitro* study. The hydrogels with the values of G' less than 1K Pa were selected because poor cell proliferation was observed in the hydrogels with higher stiffness in our preliminary 3D cell culture study. The rheological properties of selected hydrogels for the subsequent *in vitro* study were summarized in Table 3-1**.** G' of the hydrogels was significantly increased with increasing H_2O_2 concentrations which is in good agreement with previous findings that the concentration of H_2O_2 is primary factor in controlling the stiffness. When 0.85 and 1.7 mM of H_2O_2 concentration were used, the values of G' were 281+19 and 841+45 Pa, respectively. The hydrogels with different stiffness (281 and 841 Pa) are abbreviated respectively, as Gtn-HPA-2A and Gtn-HPA-2B.

Table 3-1. Rheological properties of Gtn-HPA hydrogels used in the 3D cell proliferation and differentiation study[a]

Sample	Gtn-HPA (wt.%)	HRP (units/ml)	H_2O_2 (mM)	G' (Pa)	Gel point (sec)[b]	Time needed for G' to reach plateau (sec)
Gtn-HPA-2A	2	0.15	0.85	281 ± 19[†]	<30	78 ± 12
Gtn-HPA-2B	2	0.15	1.7	841 ± 45	45 ± 5	251 ± 29

[a] Measurement was taken with constant deformation of 1 % at 1Hz and 37°C (n=4). Results are shown as the average values ± standard deviation.

[b] Gel point is defined as the time at which the crossover of storage modulus (G') and loss modulus (G'') occurred. Herein, it is used as an indicator of the rate of gelation.

[†] Means that the stiffness of Gtn-HPA-2A was significantly lower than that of Gtn-HPA-2B. Differences between the values were assessed using Student's unpaired *t*-test and $p < 0.05$ was considered statistically significant.

3.3.2. Enzymatic degradation of Gtn-HPA hydrogels

Matrix metalloprotease (MMP) has been reported to degrade the extracellular matrix, leading to cell migration and growth in the body [145] and affect the degradability of proteolysis-sensitive hydrogels [15]. We assessed the enzymatic degradability of Gtn-HPA hydrogels using type-1 collagenase, one of MMP family (Figure 3-2). Gtn-HPA-2A degraded much faster than Gtn-HPA-2B. This result suggests that the degradability can be well controlled by hydrogel stiffness and is expected to affect the proliferation rate of cells in hydrogels.

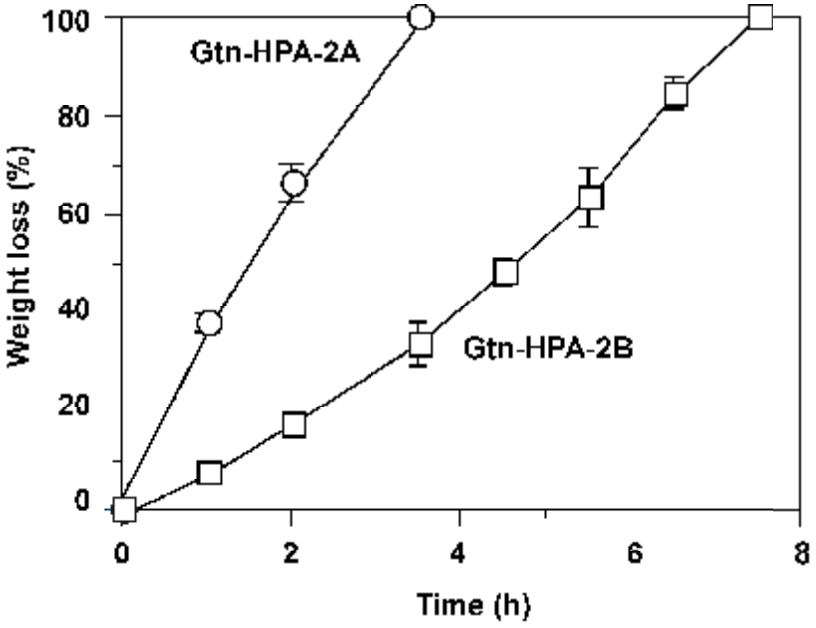

Figure 3-2. Enzymatic degradation of Gtn-HPA hydrogels in the presence of 0.61 units/ml of type I collagenase at 37°C. Results are shown as the average values ± standard deviation (n=3).

3.3.3. Cell attachment and proliferation on Gtn-HPA hydrogels

Prior to performing 3D cell culture in hydrogels, hMSCs were seeded on the surface of the hydrogels to evaluate cell attachment properties. Figure 3-3a shows cell numbers of cells attached on culture plate, Gtn-HPA-2A and Gtn-HPA-2B hydrogels expressed as a percentage with respect to the initial seeding number. The Gtn-HPA hydrogels provided an excellent support for cell attachment. The cell attachment on the Gtn-HPA hydrogels regardless of their stiffness after 1 h incubation was significantly greater compared to the cell culture plate, and the hMSCs attached on the hydrogels continued to outnumber the ones on the culture plate during 6 h incubation. This good cell attachment behavior supported by the Gtn-HPA hydrogels is considered to be due to the positively charged residues and RGD peptide sequences of Gtn [146]. Also, the Gtn-HPA-2B hydrogel achieved higher cell attachment after 1 h incubation compared to Gtn-HPA-2A. The cell attachment between hydrogels with different stiffness showed no significant difference after 6 h incubation. It has been reported that matrix stiffness affects morphology of hMSCs; the focal adhesion growth and elongation of the cell are promoted with increasing matrix stiffness ranging from 1K Pa to 34K Pa [10]. It is noteworthy that even though both hydrogels in our study are of G' less than 1K Pa, a significant difference in cell attachment was found for the first hour of incubation. Nevertheless, the difference was not significant after 6 h incubation.

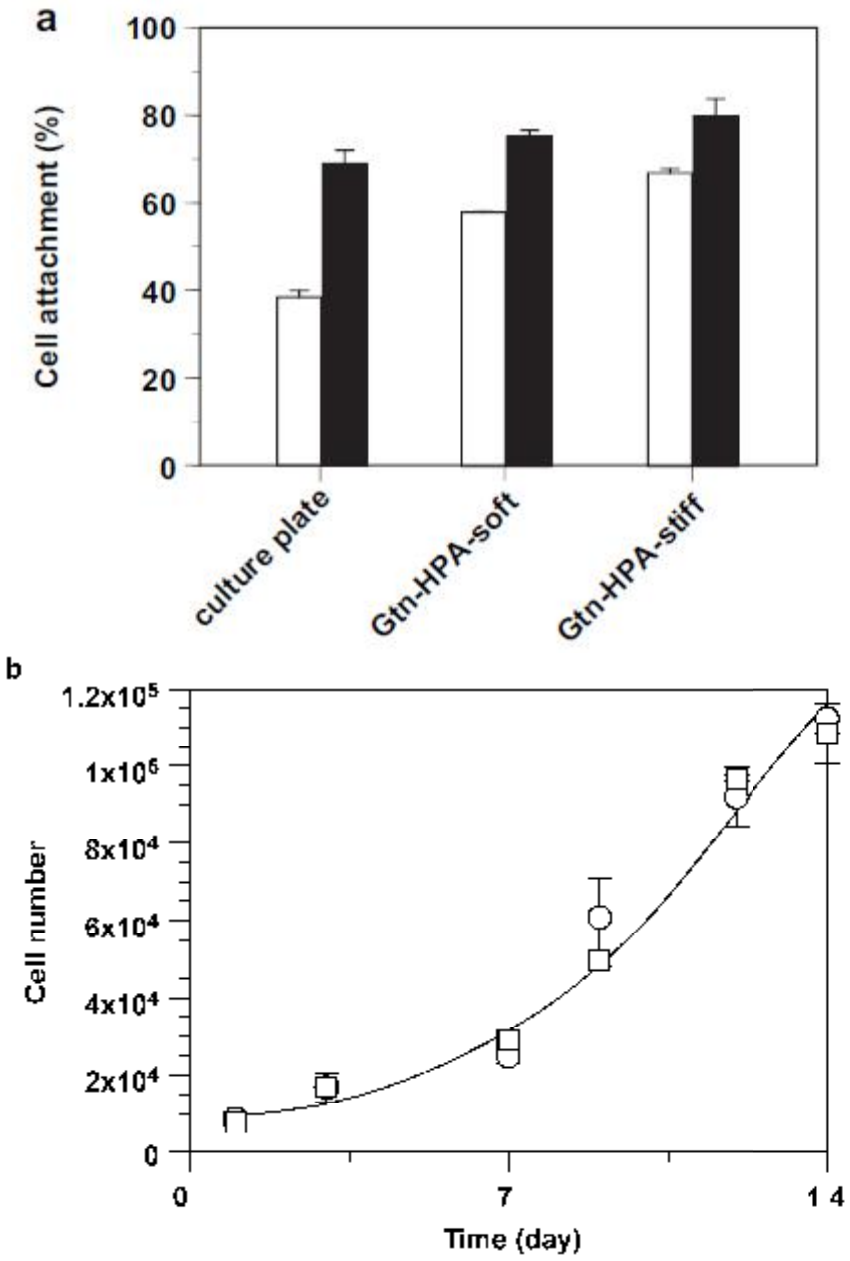

Figure 3-3. (a) hMSCs attachment on the surface of Gtn-HPA hydrogels after 1 h (open bar) and 6 h (filled bar) incubation. (b) 2D hMSCs proliferation on Gtn-HPA-2A (™) and Gtn-HPA-2B (□). Results are shown as the average values ± standard deviation (n=4).

Figure 3-3b shows the proliferation of hMSCs on the surface of Gtn-HPA hydrogels with different stiffness. During 2 weeks culture of hMSCs on the hydrogel, cells continued to grow on both hydrogels without showing much difference in terms of the proliferation rate. As discussed above, there was no significant difference in cell numbers attached on the surface after 6 h between the two Gtn-HPA hydrogels. Hence, these results indicate that within the range of G' (280-840 Pa), stiffness of these hydrogels has little effect on the proliferation rate of hMSCs cultured on the hydrogel surface.

3.3.4. 3D culture of hMSC in Gtn-HPA hydrogels

Given the evidence that Gtn-HPA hydrogel can be prepared under mild conditions, pairing with its biodegradability as well as cell adhesion property, the 3D culture of hMSCs inside Gtn-HPA hydrogels with different stiffness was explored. It was found that the cell proliferation was dependent on the stiffness of Gtn-HPA hydrogels (Figure 3-4a). The rate of hMSCs proliferation increased with the decrease of the hydrogel stiffness, unlike the cell proliferation on the surface of the Gtn-HPA hydrogels discussed above. It suggested that this difference in the cell proliferation rate is attributed to the stiffness in a 3D environment, while the cells proliferated well on hydrogels regardless of their stiffness in a 2D context within the same stiffness range.

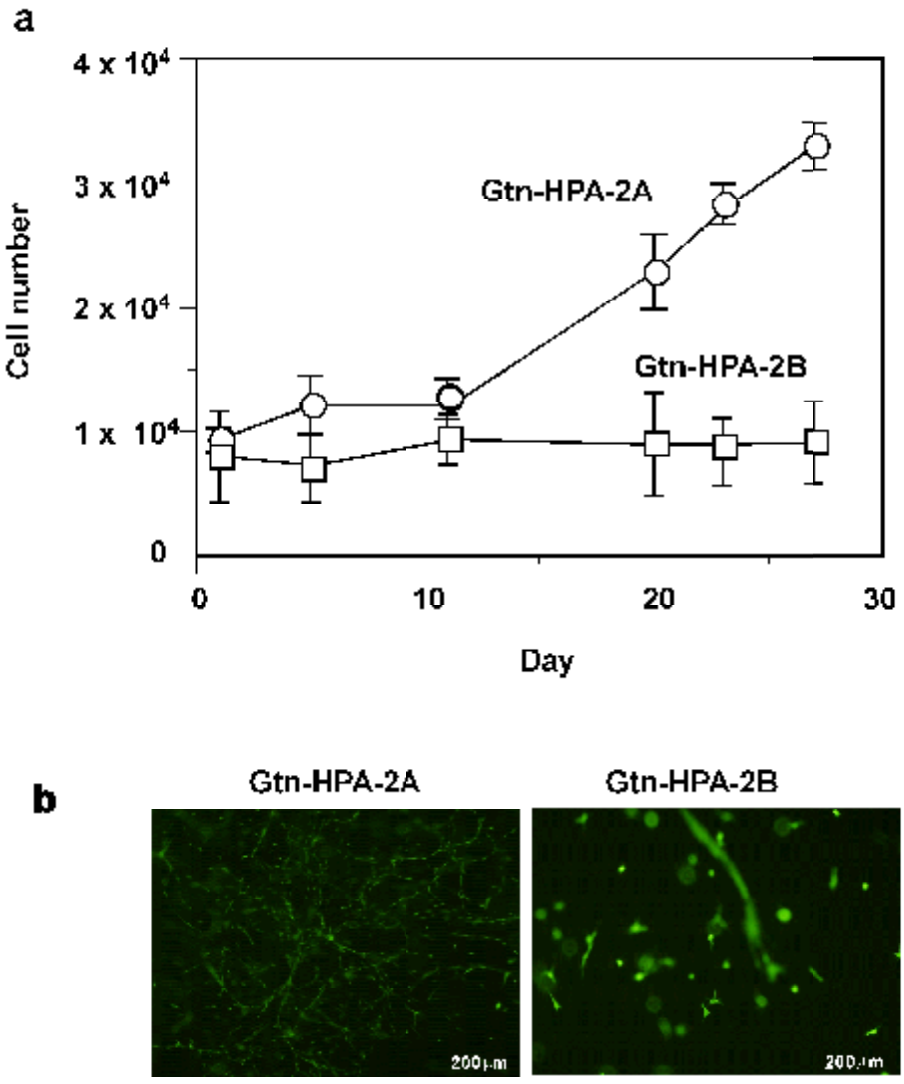

Figure 3-4. (a) 3D hMSC proliferation in Gtn-HPA hydrogels. Results are shown as the average values ± standard deviation (n=6). (b) Fluorescence images of hMSCs cultured in Gtn-HPA hydrogels. The cells were stained by calcein AM.

Figure 3-4b represents the morphology of cells cultured in hydrogels after 2 weeks. The cells were stained by calcein acetoxymethyl ester (Calcein AM). hMSCs were allowed to grow inside the hydrogels. In the case of Gtn-HPA-2A, the hMSCs proliferated and formed inter-cell connections in the hydrogels with filopodia-rich morphology. However, the hMSCs in Gtn-HPA-2B appeared to be much smaller due to the stiffer property resulting in a slower proliferation.

To understand the effects of hydrogel stiffness on cell proliferation in Gtn-HPA hydrogels, the water uptake of Gtn-HPA hydrogels with and without cells was measured (Figure 3-5). For Gtn-HPA-2A without cells, the water uptake increased during the first week before reaching a plateau. In contrast, the water uptake in Gtn-HPA-2A with cells kept increasing and showed higher water uptake in comparison to Gtn-HPA-2A without cells. In the case of Gtn-HPA-2B hydrogels, no significant difference in water uptake was found between the hydrogels with or without cells. The change of water uptake over time could be attributed to swelling of the hydrogel as a result of degradation or crosslinking efficiency.

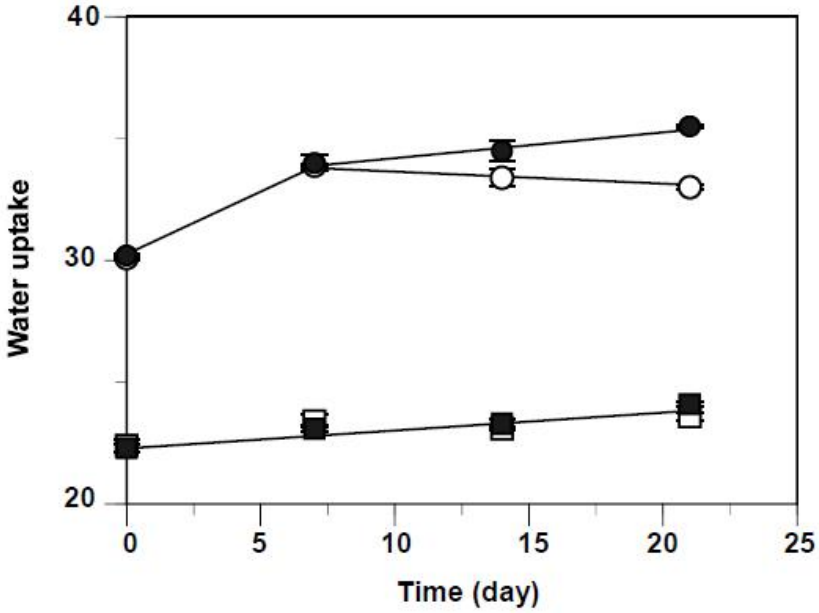

Figure 3-5. Water uptake of Gtn-HPA-2A without cells (○), Gtn-HPA-2A with cells (●), Gtn-HPA-2B without cells (□) and Gtn-HPA-2B with cells (■). Results are shown as the average values ± standard deviation (n=3).

In a separate experiment, crosslinking efficiency for Gtn-HPA-soft and Gtn-HPA-stiff was determined. The dry weight of Gtn-HPA hydrogels obtained by lyophilization was recorded after the hydrogels were soaked in water for 48 h. The dry weight without soaking in water served as a control. It was found that 89 % Gtn-HPA conjugate remained after soaking in the case of Gtn-HPA-2A. Whereas, there was 95 % left for Gtn-HPA-2B. Thus, it is suggested that for the Gtn-HPA-2A hydrogels, the increase of water uptake in the first week may be attributed to the leaching of uncrosslinked polymers. The continued increase in water uptake of the cell-encapsulated Gtn-HPA-2A for the subsequent two weeks is most likely due to the degradation of the hydrogels. For the stiffer hydrogels, it is considered that the difference in the change of water uptake over time was much smaller compared to soft ones largely due to the higher stiffness resulting in a slower degradation. These results indicate that both appropriate stiffness and degradability of the hydrogels play important roles in controlling 3D cell proliferation in hydrogels.

3.3.5. Focal adhesion study

To further study how the cells responded to the substrate stiffness, immunostaining of focal adhesion and actin cytoskeleton was performed. Figure 3-6 shows the confocal fluorescence images of focal adhesion and actin cytoskeleton in hMSCs when the cells were cultured using Gtn-HPA hydrogels. These images revealed focal contacts in green using an anti-vinculin monoclonal antibody. Also, F-actin was detected in red and nuclei were stained in blue. In the 2D study, the cells appeared to be more spread out when they

were cultured on a stiffer surface. Both focal contact and F-actin organization show a progressive trend, from diffuse when in contact with soft hydrogels to a more organized arrangement in the case of stiffer ones. These results are in good agreement with the earlier reports on hMSC responding to matrix elasticity on collagen coated polyacrylamide gels [10]. Despite the difference in the focal contact and F-actin arrangement between Gtn-HPA-2A and Gtn-HPA-2B, it did not exert much influence on proliferation rate in 2D as shown above.

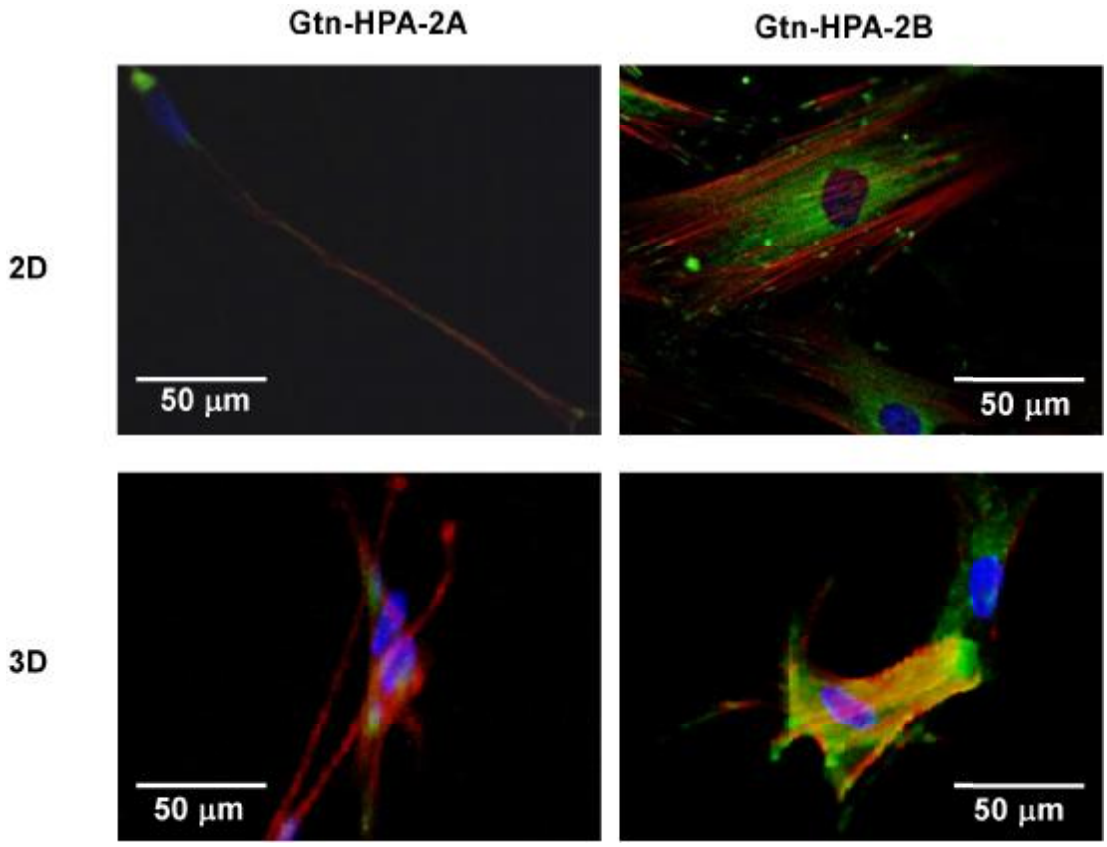

Figure 3-6. Confocal fluorescence microscopy of focal adhesion and actin cytoskeleton in hMSCs cultured using Gtn-HPA hydrogels.

When the cells were cultured in a 3D environment, the focal contact and F-actin organization showed a similar trend compared to the observations from the 2D study. However, the proliferation rate of hMSCs in a 3D context was strongly affected by stiffness as discussed above. Thus, it is considered that the degradability of hydrogels is a dominant factor in controlling the cell proliferation, rather than the focal contact presentation and F-actin arrangement. These responses to substrate stiffness through focal contact presentation and F-actin arrangement may affect the differentiation of hMSCs, and are to be discussed in the following study.

3.3.6. hMSCs differentiation in Gtn-HPA hydrogels

To develop Gtn-HPA hydrogels for the neurogenesis of hMSCs in the 3D context, the cells were pre-treated with mitomycin C to inhibit proliferation and maintained inside the hydrogels with different stiffness in normal culture medium for 3 weeks. Mitomycin C has been shown to have little impact on average cell shape and morphology [10]. Cells were then immunostained with neuron-specific antibodies: neurofilament light chain (NFL), late neuronal marker neurofilament heavy chain (NFH), mid/late neuronal marker microtubule associated protein 2 (MAP2) and neuron-specific marker 3 tubulin. Nuclei were counterstained with 4',6-diamidino-2-phenylindole (DAPI). In immunofluorescence images, cells in Gtn-HPA-2A revealed expression of these neuron-specific proteins (Figure 3-7a). On the contrary, cells cultured on plastic culture plate over the same period of culture did not express the neuron-specific proteins.

Western blotting was employed to quantify these expressed proteins. For cells harvested after 1 week of culture inside the Gtn-HPA hydrogels, only β-tubulin was

detectable in western blots. The period of hMSCs culture in Gtn-HPA hydrogels was optimized to be 3 weeks to quantify protein markers of mid/late neurons (MAP2) and even mature neurons (NFL and NFH) (Figure 3-7b). The expression of these protein markers was normalized to that of β-actin. The result confirmed that the hMSCs cultured inside the Gtn-HPA hydrogels for 3 weeks expressed protein markers for neuronal commitment, NFL, NFH, MAP2, and β3-tubulin, while cells cultured on plastic culture plate for the same period of time showed no neuronal protein marker expression.

As mentioned, it has been reported that the differentiation of hMSCs on the surface of collagen-coated polyacrylamide gels [10]. Our results indicate that the neurogenesis of hMSCs in hydrogels can be also achieved if the appropriate stiffness of hydrogel is provided. The neurogenesis was also strongly affected by hydrogel stiffness. Gtn-HPA-2A expressed much more neuronal protein markers compared to the Gtn-HPA-2B. It has been suggested that the focal contact and F-actin arrangement could affect the differentiation of hMSCs [10]. As discussed above, the hMSCs responded to substrate stiffness through the focal contact and F-actin arrangement. Thus, it is considered that neurogenesis in the Gtn-HPA hydrogels was largely affected by cell response in the focal adhesion due to stiffness. It is increasingly evident that cells do sense and respond to mechanical properties of the substrate in respect to a variety of cell functions, such as cell migration, spreading, growth and differentiation [2]. The result of cell proliferation and differentiation in Gtn-HPA hydrogels indicates that the design of a hydrogel scaffold with well-controlled mechanical properties is crucial in tissue engineering applications. Physical parameters are as important as biological and chemical parameters to effectively repair, regenerate or engineer tissues.

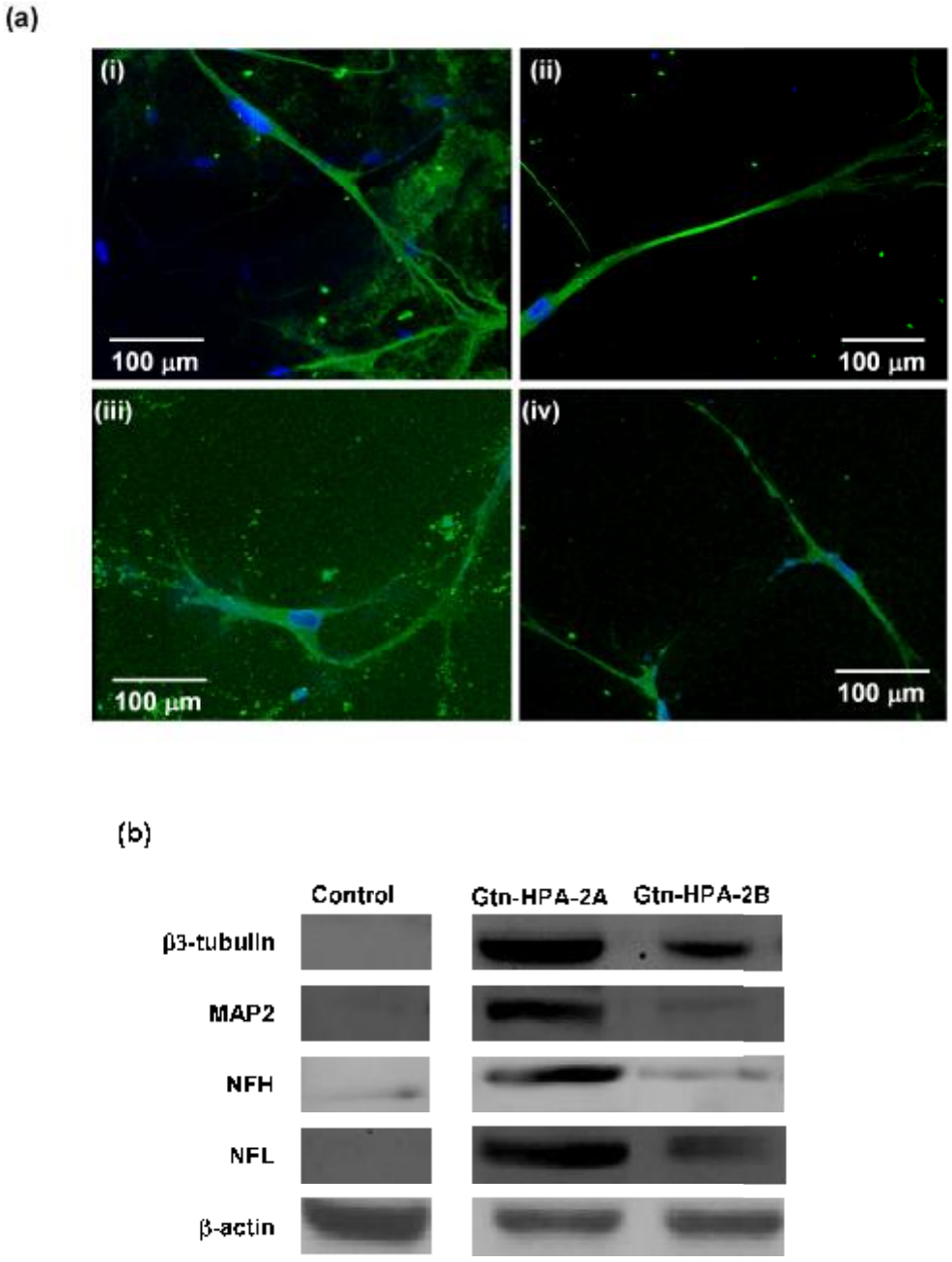

Figure 3-7. (a) Immunofluorescence images of (i) β3-tubulin, (ii) NFL, (iii) MAP2, and (iv) NFH expressed in Gtn-HPA-2A hydrogels. (b) Western blotting of proteins expressed in Gtn-HPA hydrogels. Cells cultured on plastic culture plates were used as a control.

3.4. Conclusion

An injectable and biodegradable Gtn-HPA hydrogel was formed by the oxidative coupling reaction of phenol moiety in the presence of H_2O_2 and HRP. The stiffness of the hydrogel was well controlled by the H_2O_2 concentration. The ease of cell encapsulation into Gtn-HPA provided a simple and effective mean to study the cell functions in a 3D environment. It was found that the proliferation rate of 3D hMSC cultured in Gtn-HPA hydrogels was tuned by the hydrogel stiffness. Neurogenesis of hMSCs in 3D was demonstrated using this hydrogel system, and the degree of neurogenesis was affected by the stiffness of hydrogel without the use of any biochemical signal, as confirmed by immunostaining and western blotting. This Gtn-HPA hydrogel system offers an excellent platform to study cell functional responses in a 3D environment, given its *in situ* forming ability, excellent cell adhesion and tunable mechanical properties. With its biocompatibility and biodegradability, the Gtn-HPA hydrogel presents a promising system for regenerative applications of stem cells in tissue engineering and has the potential to further stem cell-based *in vivo* therapies. In the future, injectable Gtn-HPA hydrogels with tunable mechanical properties for 3D cell culture and differentiation would be an important strategic tool to treat neurological disorders or brain injuries.

Chapter IV

The role of stiffness in cell functions of hMSCs in 2D study

4. The role of stiffness in cell functions of hMSCs in 2D study

4.1. Introduction

In the previous chapter, controls of the proliferation rate and differentiation of hMSCs in a three-dimensional (3D) context in normal growth media by hydrogel stiffness was successfully demonstrated using the Gtn-HPA hydrogels. However, due to the inherent difficulties in 3D culture systems such as poor transportation of nutrients and low degradability of hydrogels as a result of increasing stiffness, the culture and differentiation of hMSCs in hydrogels with storage modulus (G') higher than 1000 Pa appeared to be challenging. As described in previous chapters, hMSCs were clearly responsive to substrate stiffness and differentiated to different phenotypes by collagen-coated polyacrylamide gels of varying stiffness [10]. Thus, it is important to design an appropriate system to attain the full benefits of stem cell differentiation for tissue regeneration. The Gtn-HPA hydrogel, being able to achieve wide range of control in stiffness, would be a good candidate for such need useful as a hydrogel scaffold system. The hMSCs cultured on Gtn-HPA hydrogels with appropriate stiffness could be differentiated to specific phenotypes according to the need and the hydrogels could be subsequently degraded after the differentiation of cells for an intended application.

In this chapter, we prepared Gtn-HPA hydrogels with a wide range of stiffness and cultured hMSCs on the hydrogels (Figure 4-1). The rate of cell proliferation in 2D was remarkably different to that in 3D. The gene expressions of the hMSCs cultured on the hydrogels with varied stiffness were compared. We observed not only neuronal but also myogenic differentiation of hMSCs on the hydrogel surfaces as the hydrogel

stiffness was increased. We believe that this Gtn-HPA hydrogel system with tunable mechanical properties provides a simple and effective 2D platform to study cell functional responses by hydrogel stiffness as well, besides its successful application in 3D discussed in Chapter III.

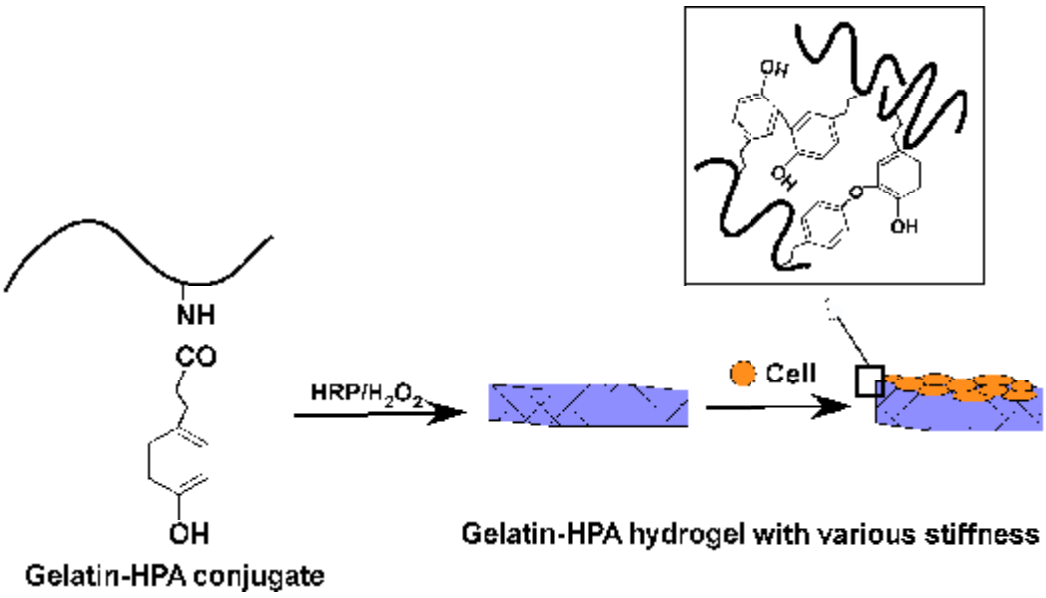

Figure 4-1. Schematic presentation of 2D cell study using Gtn-HPA hydrogels.

4.2. Materials and methods

4.2.1. Materials

Anti-myogenic transcription factor (MyoD) and Desmin antibody was purchased from Chemicon (USA). TRIzol reagent was obtained from Invitrogen (Singapore). RNeasy Minikit was purchased from Qiagen (USA) and RT² *Profiler*™ PCR array is from

SABiosciences™ (USA). The other materials used in this chapter are the same as described in the previous chapter.

4.2.2. Rheological measurement

Gtn-HPA conjugates were synthesized as described previously in section **2.2.2.**. Rheological measurements of the hydrogel formation were performed as described in section **2.2.6.** with minor change in hydrogel formulation. The aqueous solution of Gtn-HPA used in this chapter was 5 or 10 wt.% instead of 2 wt.% used in chapter III. The concentration of H_2O_2 was altered accordingly in an attempt to obtain the Gtn-HPA hydrogel with much higher stiffness.

4.2.3. Enzymatic degradation of Gtn-HPA hydrogels

Slab-shaped Gtn-HPA hydrogels were prepared as described previously in chapter III with some minor change in hydrogel formulation. Briefly, lyophilized Gtn-HPA was dissolved in PBS at a concentration of 5 wt.%. 6 µl of HRP was added to 1 ml of Gtn-HPA solution to give a final concentration of 0.15 units/ml. Crosslinking was initiated by adding 6 µl of different concentrations of H_2O_2 solution to give final concentrations of 1.7, 3.4 and 8.5 mM. The mixture was vortexed vigorously before it was injected between two parallel glass plates clamped together with 1 mm spacing. Then, round hydrogel disks with diameters of 1.6 cm were cut out from the hydrogel slab using the same circular mold prior to degradation study. The protocol of degradation study was described in section **3.2.4.**.

4.2.4. Time course assay on cell attachment

Gtn-HPA hydrogels were prepared in the 24-well plate in a similar manner as described in section **3.2.5.**. The same experimental protocol and DNA quantification assay to determine the cell number were followed to monitor the cell attachment over culture time as described in the section **3.2.5.**. In this experiment, the hMSCs (passage number <6) at cell density of 3×10^5 cells/ml was seeded onto the hydrogels.

4.2.5. Cell proliferation assay

For 2D cell proliferation on the surface of hydrogels, 250 µl of hMSCs in Mesencult human basal medium supplemented with Mesencult human supplement at cell density of 6×10^5 cells/ml was seeded onto the Gtn-HPA hydrogels for this study. The same experimental protocol was employed to evaluate the cell proliferation on the hydrogels with varied stiffness as described in section **3.2.7.**.

4.2.6. Cell migration assay

Cell migration assay was performed in a 24-well plate. 20 µl of hMSCs in mesencult human basal medium supplemented with Mesencult human supplement at cell density of 1×10^6 cells/ml were seeded onto the center of Gtn-HPA hydrogels. The cells were allowed to attach onto the surface overnight. Unattached cells were removed by washing with PBS before 250 µl of culture medium was added to each well. The plate was incubated in a humidified chamber (37°C, 5 % CO_2) to allow cell migration. At selected

time intervals, the cells were examined microscopically to record the distance they had travelled from the center of the circle. This experiment was performed in three replicates.

4.2.7. Cell focal adhesion study

The same imunostaining protocol was employed to study the cell focal adhesion of the hMSCs cultured on the Gtn-HPA hydrogels as described in section **3.2.10.**.

4.2.8. RNA preparation

Gtn-HPA hydrogels were prepared in the 6-well plate in the similar manner as described above. One milliliter of hMSCs in Mesencult human basal medium supplemented with Mesencult human supplement at cell density of 2×10^6 cells/ml was seeded onto the hydrogels. The cells on Gtn-HPA hydrogels and a culture plate were both harvested by trypsinization after the samples were incubated at 37°C for 2 days. The total RNA was extracted from the samples with TRIzol reagent (Invitrogen) according to the manufacturer's protocol, based on an estimate of 1×10^7 cells. After washing the RNA with 75 % ethanol, the samples were cleaned using the RNeasy Minikit (Qiagen), according to the manufacturer's protocol. The RNA yield, purity and concentration were determined using a NanoDrop® ND-1000 UV-Vis Spectrophotometer.

4.2.9. PCR array analysis

Screening for the expression of 84 genes associated with cell adhesion and ECM molecules in hMSCs cultured on Gtn-HPA hydrogels was performed in triplicate using the human ECM and adhesion molecules RT² *Profiler*™ PCR array (SABiosciences™, USA) according to manufacturer's instructions. In brief, cDNA was prepared from 1 μg total RNA by using a RT^2 PCR array first strand kit. PCR amplification was conducted with an initial 10 min step at 95ºC followed by 40 cycles of 95ºC for 15 s and 60ºC for 1 min on a MyiQ2 Real Time PCR machine (Bio-Rad, USA). Melting curves were obtained using the following conditions: 95°C, 1 min; 65°C, 2 min (OPTICS OFF); 65°C to 95°C at 2°C / min (OPTICS ON). Data was imported into an Excel worksheet and analyzed using the Web-based PCR Array Data Analysis from SABiosciences with normalization of the raw data to β-actin.

4.2.10. 2D cell differentiation

As described in section **3.2.11.**, the hMSCs were again pre-treated with mitomycin C (10 μg/ml) for 2 h to inhibit their proliferation and washed three times with culture medium. The cell density of 1×10^5 cells/ml was seeded on the Gtn-HPA hydrogels. The same immunostaining and western blotting protocols were used to detect the protein expression in the hMSCs. Besides the neurogenic protein markers used in previous chapter, myogenic antibodies including anti-myogenic transcription factor (MyoD) and desmin were used in both immunostaining and western blotting.

4.3. Results and discussion

4.3.1. Preparation and degradation of Gtn-HPA hydrogels with varied stiffness

In the previous chapter III, the G' value of Gtn-HPA hydrogels ranged from around 20 to 1000 Pa when 2 wt.% of the Gtn-HPA conjugate was utilized. The stiffness of Gtn-HPA hydrogels was controlled by varying the H_2O_2 concentration without affecting the gelation rate. In this chapter, the Gtn-HPA hydrogels were prepared by using 5 wt.% of Gtn-HPA conjugate to provide an even wider range of stiffness.

Table 4-1 summarizes the rheological properties of Gtn-HPA hydrogels formed with different H_2O_2 concentrations. The G' of the hydrogels was significantly raised by increasing the H_2O_2 concentration; and when 1.7, 3.4 and 8.5 mM of H_2O_2 concentrations were used, the values of G' were 629 ± 71, 2529 ± 290, and 8172 ± 1338 Pa, respectively. A further increase in H_2O_2 concentration from 8.5 mM to 10.2 mM did not increase the stiffness of the resultant hydrogels, instead, a decrease in the stiffness was found. This decrease might to due to the deactivation of HRP by an excess amount of H_2O_2 [147]. The hydrogels with different stiffness (629, 2529 and 8172 Pa) are abbreviated as Gtn-HPA-5A, Gtn-HPA-5B and Gtn-HPA-5C, respectively. A wide range of G' was readily tuned by H_2O_2 concentration, in contrast, little effect was observed on the gel point, defined as the crossover of G' and loss modulus (G''). Except that when the H_2O_2 concentration was increased from 3.4 to 8.5 mM, a slight rise in the gel point was observed mostly attributed to the deactivation of HRP by higher amount of H_2O_2. Nevertheless, the efficient gelation rate of less than 1 min was achieved regardless of the H_2O_2 concentration. In addition, the time required for G' to reach a plateau increased

with the increase in H_2O_2 concentration. These results are in good agreement with previous reports on the independent tuning of hydrogel mechanical properties and gelation rates [89, 148, 149]. They indicate that the mechanical strength (i.e. crosslinking density) of the hydrogel could be tuned by H_2O_2 concentration without compromising the rapid gelation rate. H_2O_2 decomposes to water after oxidizing HRP which in turn oxidizes the HPA. Thus, the percentage of HPA moieties that actually participated in the crosslinking reaction would depend on the amount of H_2O_2 available.

Table 4-1. Rheological properties of Gtn-HPA hydrogels used in the 2D cell proliferation and differentiation study[a]

Sample	Gtn-HPA (wt.%)	HRP (units/ml)	H_2O_2 (mM)	G' (Pa)	Gel point (sec)[b]	Time needed for G' to reach plateau (sec)
Gtn-HPA-5A	5	0.15	1.7	629±71	<30	79 ± 13
Gtn-HPA-5B	5	0.15	3.4	2529±290	<30	172 ± 10
Gtn-HPA-5C	5	0.15	8.5	8172±1338	36 ± 10	1282 ± 129
Gtn-HPA-10A	10	0.16	10.2	12780 ± 1540	<30	109 ± 25

[a] Measurement was taken with constant deformation of 1 % at 1Hz and 37oC (n=4). Results are shown as the average values ± standard deviation.

[b] Gel point is defined as the time at which the crossover of storage modulus (G') and loss modulus (G'') occurred. Herein, it is used as an indicator of the rate of gelation.

In addition, a Gtn-HPA hydrogel was prepared using 10 wt.% of Gtn-HPA conjugate to increase the G' further. The G' was increased to around 12800 Pa. This hydrogel is abbreviated as Gtn-HPA-10A. The increase in G' achieved by using a higher concentration of Gtn-HPA conjugate indicates that a higher number of HPA moieties participated in the crosslinking reaction. It is also noteworthy that the viscosity of the Gtn-HPA solution is directly proportional to its concentration. Preparation of 15 wt % of Gtn-HPA solution in an attempt to maximize the stiffness control in its hydrogel system yielded a highly viscous solution. A hydrogel precursor solution with high viscosity may impose difficulties in measurement of rheological properties and handling particularly in the process of injection for an injectable hydrogel system. Therefore, the concentration of Gtn-HPA conjugates was limited to 10 w.t % in this study in view of its potential application as an injectable hydrogel system.

It is well known that the stiffness of a hydrogel affects its enzymatic degradation. We assessed the enzymatic degradation of Gtn-HPA hydrogels using type-1 collagenase, a member of the matrix metalloproteases (MMP) family. MMP degrades the extracellular matrix, leading to cell migration and growth in the body [150] . Accordingly, they can digest proteolysis-sensitive hydrogels [151]. Figure 4-2 shows that the rate of hydrogel degradation decreased with increased hydrogel stiffness. This result suggests that the enzymatic degradability of Gtn-HPA hydrogels can be well-controlled by hydrogel stiffness.

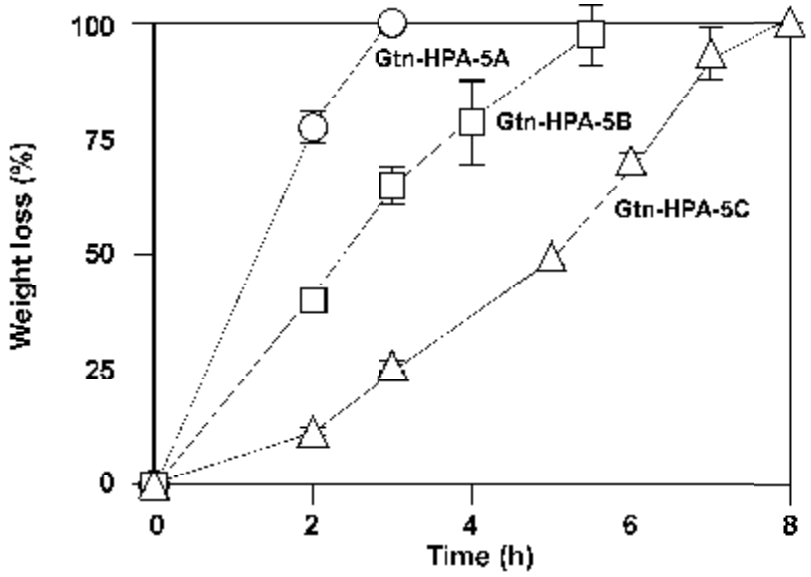

Figure 4-2. Enzymatic degradation of Gtn-HPA-5A (™), Gtn-HPA-5B (£) and Gtn-HPA-5C (r) hydrogels in the presence of 6.7 units/ml of type I collagenase at 37°C. Results are shown as the average values ± standard deviation (n=3).

4.3.2. Cell attachment, migration and proliferation

The role of substrate stiffness on cell functions such as adhesion, migration, differentiation, or spreading has been demonstrated for various cell types that have been cultured on different substrates [2, 118, 125, 152]. Although there is cell-to-cell variability, it is generally found that cells growing on stiffer surfaces have a larger spreading area, more organized cytoskeletons and more stable focal adhesions. Across the range of stiffness studied in this chapter, Gtn-HPA hydrogels have provided an excellent support for cell attachment. As shown in Figure 4-3, the number of hMSCs attached to hydrogels with different stiffness was significantly higher than the hMSCs attached to a NUNC® culture well-plate during the initial 6 h of incubation although there was not a significant difference found when the hydrogel stiffness between Gtn-HPA-5B and Gtn-HPA-5C when the stiffness of hydrogel was above 2.5k Pa. The cells were found to be firmly attached to surfaces of the Gtn-HPA hydrogels. Also, the cell anchorage of Gtn-HPA hydrogels was progressively enhanced by increasing the stiffness of the hydrogels, which was most likely attributed to the enhancement in cell proliferation with higher stiffness as discussed below.

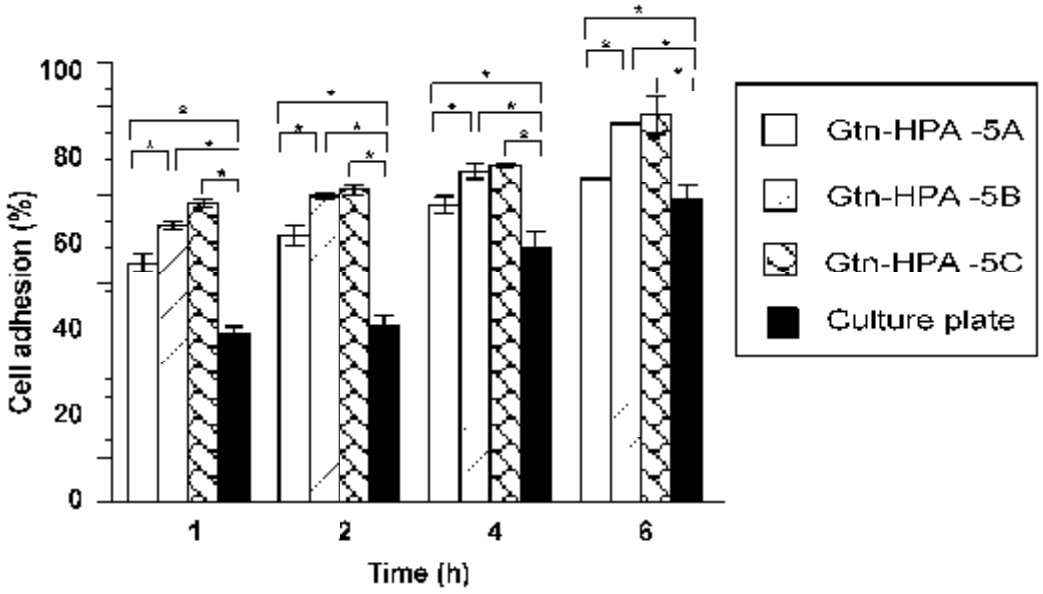

Figure 4-3. hMSCs attachment on the surface of Gtn-HPA hydrogels after different incubation periods. Results are shown as the average values ± standard deviation (*$p<0.05$, n=3).

Next, the proliferation rate of hMSCs grown on Gtn-HPA hydrogels was monitored. A good correlation between the proliferation rate and hydrogel stiffness was found (Figure 4-4). The hMSCs cultured on Gtn-HPA-5B and Gtn-HPA-5C hydrogels grew much faster than the ones grown on Gtn-HPA-5A. We attribute this observation to firmer adhesion, decreased apoptosis and a greater proportion of phosphorylated focal adhesion kinases (FAK) as a result of higher spreading [153-156]. To confirm our hypothesis, we performed immunostaining on the hMSCs to detect their focal adhesion actin cytoskeleton. Confocal fluorescence microscopy of the stained cells revealed focal contacts in green using an anti-vinculin monoclonal antibody and a FITC-conjugated secondary antibody (Figure 4-5). F-Actin was stained in red, and the nuclei were stained with 4',6-diamidino-2-phenylindole (DAPI) and appear in blue. The cells appeared to be more spread out when they were cultured on a stiffer hydrogel. The F-actin was much more organized when the cells were in contact with a stiff hydrogel. Both the focal contact and F-actin organization showed a progressive trend, from being diffuse when in contact with soft hydrogels to having a more structured arrangement when the cells were attached to the stiffer ones. These observations are in good agreement with the earlier reports of stem cells responding to matrix elasticity on both synthetic and naturally-derived material [10, 116, 156, 157]. These various responses to substrate stiffness through the focal contact patterns and the F-actin arrangement of hMSCs may induce their differentiation as discussed in the following experiment.

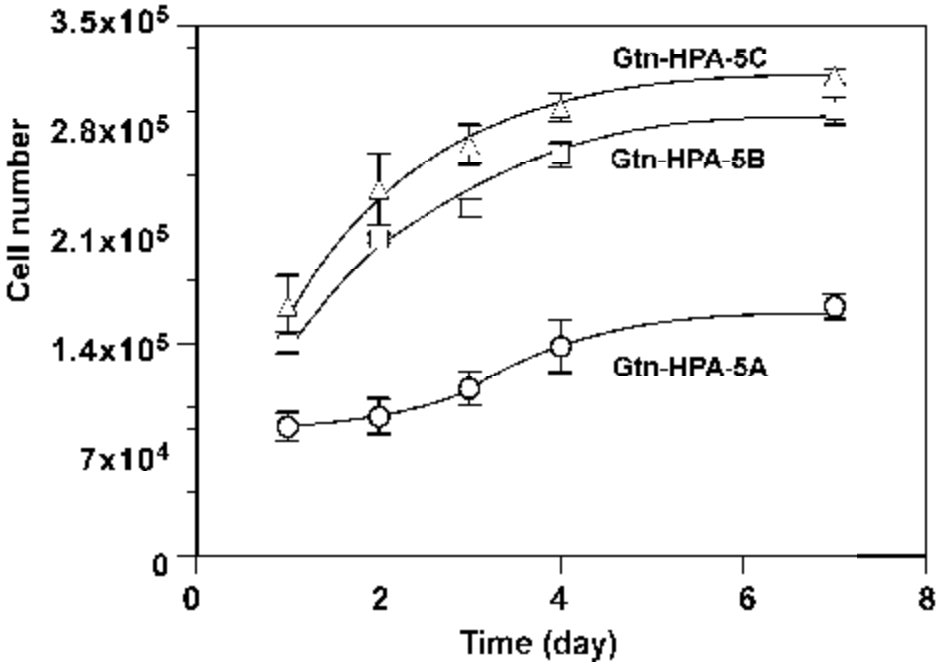

Figure 4-4. 2D hMSCs proliferation on Gtn-HPA hydrogels with different stiffness. Results are shown as the average values ± standard deviation (n=4).

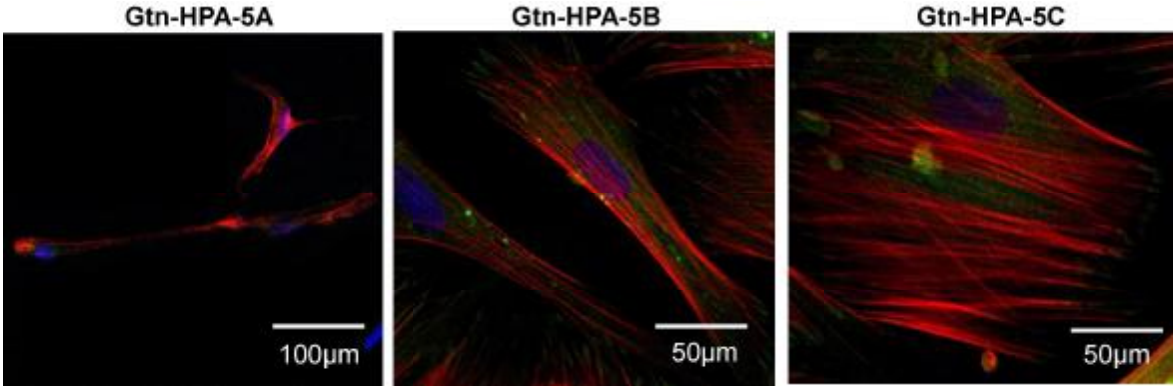

Figure 4-5. Confocal fluorescence microscopy of focal adhesion and actin cytoskeleton in hMSCs cultured on Gtn-HPA hydrogels.

To further investigate the effect of hydrogels stiffness on cell function, analysis on the migration of hMSCs was performed. A previous report by Lo et al. has revealed that fibroblasts moved with a higher average migration rate when grown on stiffer surfaces [114]. We performed a migration assay and we found that the migration distance calculated from the seeding site of hMSCs was twice that of Gtn-HPA-5A when cells were grown on Gtn-HPA-5C (Figure 4-6a). The difference in migration rate between Gtn-HPA-5B and Gtn-HPA-5C was insignificant. However, an analysis of the cross-sectional distribution of the cells revealed that the cell migration depended on cell culture conditions. The hMSCs growing on Gtn-HPA-5A migrated in a 3D plane (Figure 4-6b). That is, in conjunction to the horizontal displacement on the surface of the hydrogels, the cells also moved in a Z direction into the hydrogel. However, the majority of the hMSCs seeded on Gtn-HPA-5B and Gtn-HPA-5C remained on their surfaces. The high stiffness restricted the cells from moving into the hydrogel. As the enzymatic degradability of Gtn-HPA hydrogel increased with decreasing the stiffness of hydrogel (Figure 4-2), we consider that the cell migration in a Z direction was affected by the degradation of the hydrogel.

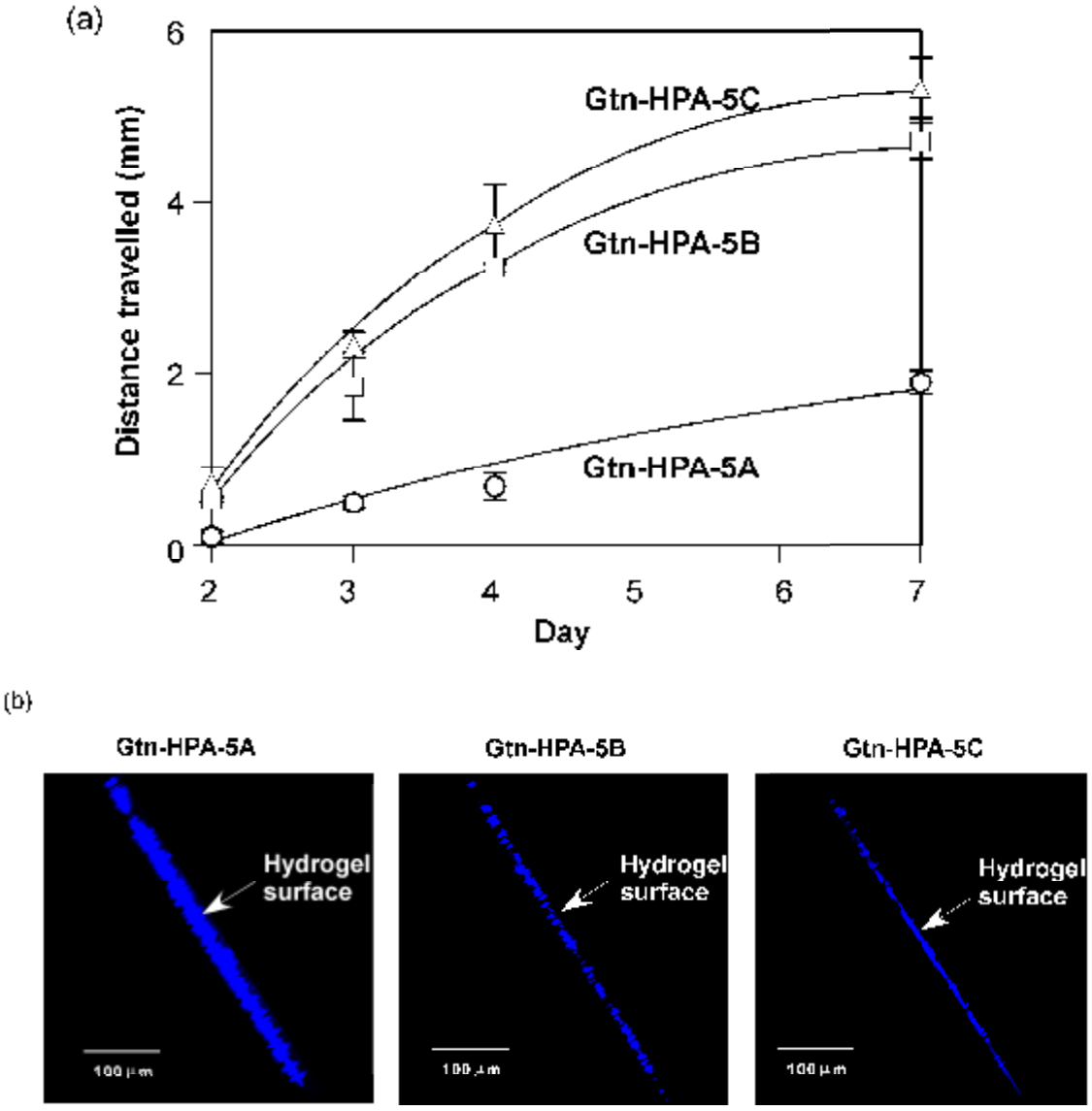

Figure 4-6. (a) The distance that hMSCs migrated on Gtn-HPA hydrogels with different stiffness. (b) Cross-sectional image of the hydrogels. Results are shown as the average values ± standard deviation (n=4).

To understand the behavior of cells cultured on Gtn-HPA hydrogels with different stiffness, the gene expression profiles of the cells were examined by using human ECM and adhesion molecules RT² *Profiler*™ PCR array [158]. There was a set of primers for 84 genes related to ECM and adhesion molecules in the assay plate. There were 67 genes detected in the culture well plate, 69 in the Gtn-HPA-5-soft, 68 in the Gtn-HPA-5-medium and 68 in the Gtn-HPA-5 stiff, respectively. Out of the 84 genes, 66 (79 %) were detectable in all 4 samples.

Table 4-2 summarizes gene's expression with a greater than 2-fold change in hMSCs cultured on the hydrogels compared to those cultured on the well plate. It was found that 11, 9 and 5 genes were up-regulated at least 2-fold when hMSCs were cultured on Gtn-HPA-5A, Gtn-HPA-5B and Gtn-HPA-5C hydrogels, respectively. MMP1, SPP1, ITGB4, ADAMTS13 and CLEC3B were among those genes whose expression was up-regulated at least 2-fold, and were commonly upregulated on all the Gtn-HPA hydrogels regardless of their stiffness. Four genes (TNC, ICAM1, VCAM1 and LAMA1) were commonly up-regulated in Gtn-HPA-5A and Gtn-HPA-5B. Only two genes (MMP-8 and MMP-13) were uniquely up-regulated on Gtn-HPA-5A. SPP1, ITGB4, TNC and ICAM1 are reported to mediate cell-matrix and cell-cell interactions [159-161]. Interestingly, the change in expression of the genes was enhanced as the stiffness of Gtn-HPA hydrogels was decreased. As described earlier, cell attachment on Gtn-HPA hydrogel dropped with decreasing stiffness. Therefore, it is considered that such an up-regulation of gene's expression might be affected by hydrogel stiffness. Consequently, cell attachment on the hydrogels with lower stiffness may be encouraged with enhanced adhesive protein molecules. It is known that MMPs are not constitutively expressed by cells *in vivo* [162].

However, alterations in the cell matrix interactions regulate MMP expression [163]. Furthermore, MMPs degrade ECM proteins to expose the RGD sequence in the protein and enhance cell-matrix interactions [162]. We found that the change in the expression of MMPs increased with the decrease in hydrogel stiffness. In particular, MMP1 was highly up-regulated by a hydrogel with lower stiffness. These results indicate that the stiffness of Gtn-HPA hydrogel could affect cell attachment and migration due to the regulation of adhesive protein and MMPs.

These results present further evidence that cells can sense and respond to the environment of their substrate's stiffness, by regulating their spreading, attachment, migration and proliferation. The extent to which cells can sense their substrate stiffness and how cells respond to changes in their substrate stiffness can have profound implications for tissue engineering and regeneration.

Table 4-2. Gene expression profiling in hMSCs cultured on Gtn-HPA hydrogels with different stiffness.

	Gene symbol	Fold change in gene expression[a)]		
		Gtn-HPA-5A	Gtn-HPA-5B	Gtn-HPA-5C
Matrix metallopeptidase 1 (interstitial collagenase)	MMP1	10.5	7.1	2.3
Secreted phosphoprotein 1	SPP1	9.8	6.3	3.3
Integrin, beta 4	ITGB4	3.5	2.2	2.1
Matrix metallopeptidase 8 (neutrophil collagenase)	MMP8	3.3	1.6	1.0
Tenascin C	TNC	3.2	2.0	1.6
Intercellular adhesion molecule 1	ICAM1	3.0	2.2	1.7
Vascular cell adhesion molecule 1	VCAM1	2.8	2.2	1.7
ADAM metallopeptidase with thrombospondin type 1 motif, 13	ADAMTS13	2.6	2.7	3.2
C-type lectin domain family 3, member B	CLEC3B	2.4	2.8	2.6
Laminin, alpha 1	LAMA1	2.3	2.3	1.9
Matrix metallopeptidase 13 (collagenase 3)	MMP13	2.0	1.3	-2.2

[a] The fold change for each gene is calculated as the average expression using hydrogels divided by the average expression using cell culture plates.

4.3.3. hMSCs differentiation on Gtn-HPA hydrogels

The differentiation of hMSCs in response to stiffness of Gtn-HPA hydrogel in 2D is evaluated and discussed in this chapter. For this purpose, the cells were pre-treated with mitomycin C to inhibit proliferation and they were cultured on hydrogels with different stiffness in the presence of a normal culture medium for 3 weeks. Mitomycin C is proven to have little impact on average cell shape and morphology [10]. Cells on the hydrogels with different stiffness were then stained with a group of neuron-specific antibodies consisting of neurofilament light chain (NFL), late neuronal marker neurofilament heavy chain (NFH) and neuron-specific marker β3-tubulin, or with a group of myogenic markers consisting of myogenesis differentiation protein 1 (MyoD1) and desmin. Nuclei were counterstained with DAPI and images were collected by immunofluorescent microscopy. Cells grown on both Gtn-HPA-5A and Gtn-HPA-5B revealed the expression of neuron-specific proteins (Figure 4-7a). On the contrary, cells cultured on Gtn-HPA-5C did not express any of the neuron-specific proteins over the same period of time. These results indicate that Gtn-HPA hydrogels with a stiffness of less than 2500 Pa stimulated the neurogenesis of the hMSCs. Western blotting was used to confirm expression of the same group of protein markers. hMSCs cultured on the Gtn-HPA-5A and Gtn-HPA-5B for 3 weeks expressed neuronal markers, whereas cells cultured on Gtn-HPA-5C for the same period of time showed a much reduced amount of neuronal protein marker expression (Figure 4-7b). The expression level of these proteins was normalized to that of β-actin. These qualitative results strongly suggest that the commitment of hMSCs differentiation to a given lineage is influenced by the stiffness of the hydrogel. Indeed,

these findings are in agreement with previous results that showed that hMSCs underwent neurogenesis when grown on 2D collagen-coated polyacrylamide gel.

In chapter III, we have discussed on the neurogenic differentiation of hMSCs in 3D culture. The cells which were cultured in the Gtn-HPA-2A hydrogel (G' = 280 Pa) expressed much more neuronal protein markers compared to those cultured in Gtn-HPA-2B hydrogel where G' = 840 Pa. In contrast, the neurogenic differentiation of hMSCs was observed when the cells were cultured on the surface of Gtn-HPA-5B (G' = 2529 Pa). These results indicate that the range of stiffness of Gtn-HPA hydrogels that induces neurogenesic differentiation depends on the cell culture mode (2D or 3D), although the commitment of hMSCs to a neuronal phenotype is generally affected by hydrogel stiffness. It is worthwhile to note that in a 3D culture, the degradability and nutrient transportation in hydrogels, often linked to changes in hydrogel stiffness, also affect cell behavior. Thus, we consider that the ranges of hydrogel stiffness that induce neurogenic differentiation are different between 2D and 3D cultures.

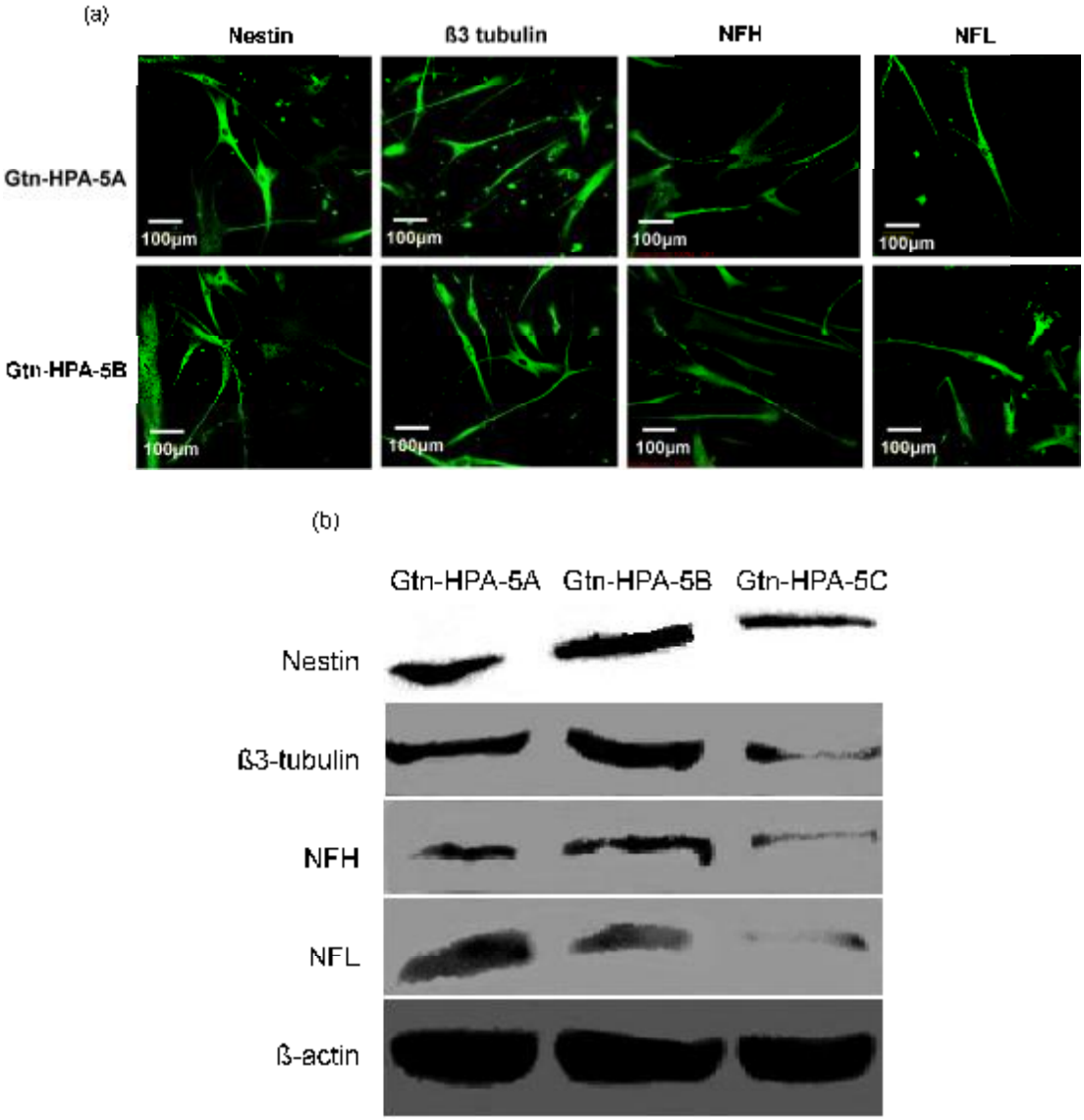

Figure 4-7. (a) Immunofluorescence images of neurogenic protein markers and (b) western blotting of proteins expressed in hMSCs cultured on Gtn-HPA hydrogels with different stiffness.

When the cells were stained with myogenic markers, they also showed a stiffness-dependent pattern of expression. The hMSCs cultured on Gtn-HPA-5C showed positive staining for myogenic markers such as MyoD1 and desmin (Figure 4-8a). MyoD1 stained in green co-localized with the nuclei stained in blue. Co-staining the cells with MyoD1 and DAPI reveals their expression in light blue, and desmin was stained in red. In an attempt to further define the range of stiffness that promotes myogenesis of hMSCs, we utilized a hydrogel of higher stiffness (Gtn-HPA-10A). Western blot results corroborated the up-regulation of myogenic protein markers when the hMSCs were cultured on these hydrogels (Figure 4-8b). Conversely, cells that were cultured on the Gtn-HPA-5B showed little of these proteins.

The result of cell proliferation and differentiation on Gtn-HPA hydrogels indicates that the design of a hydrogel scaffold with well-controlled mechanical properties is crucial for tissue engineering applications. Physical parameters are as important as biological and chemical parameters, to effectively repair, regenerate or engineer tissues.

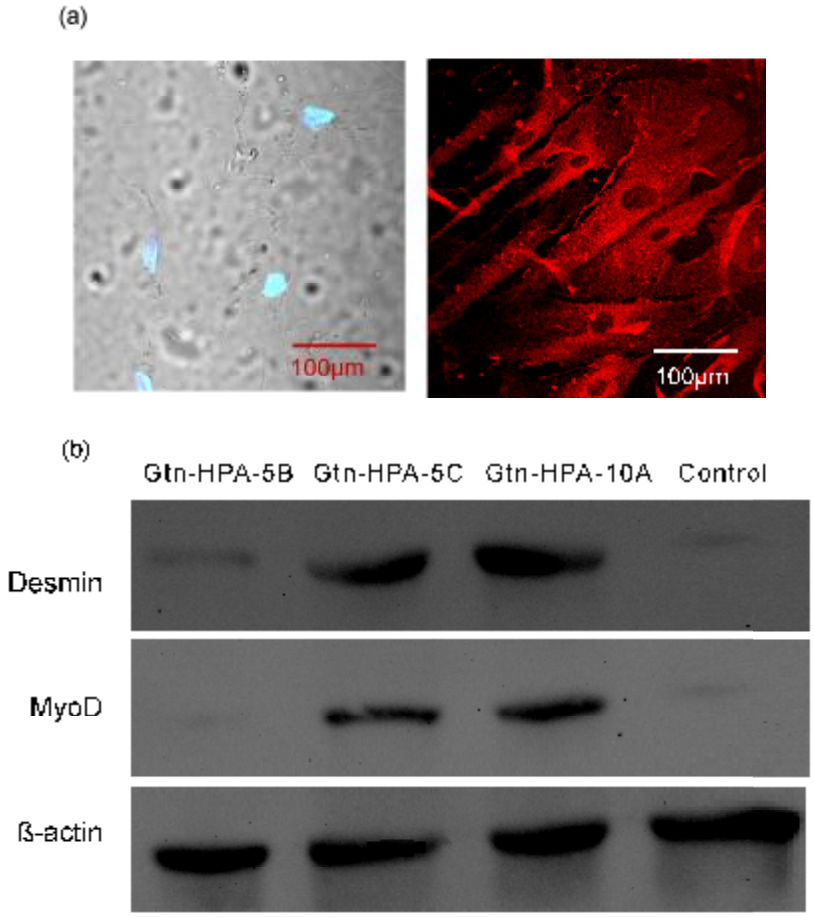

Figure 4-8. (a) Immunofluorescence images of myogenic protein markers and (b) western blotting of proteins expressed in hMSCs cultured on Gtn-HPA hydrogels with different stiffness.

4.4. Conclusion

Biodegradable Gtn-HPA hydrogels were formed by the oxidative coupling reaction of HPA moiety in the presence of H_2O_2 and HRP. The stiffness of the hydrogel was well-controlled by the H_2O_2 concentration without changing the concentration of polymer precursor solution. The hydrogels supported cell attachment and cell proliferation in a stiffness-dependent manner. It was found that hMSCs on stiffer hydrogels have a higher proliferation rate, larger spreading area, more organized cytoskeletons, more stable focal adhesions and faster migration rate. The stimulation of both neurogenic and myogenic differentiation of hMSCs on Gtn-HPA hydrogels exhibited a stiffness-dependence without the additional use of any biochemical signal. Neurogenesis of hMSCs was observed when the hydrogel stiffness was in the range of 600 to 2500 Pa. The cells on a softer hydrogel (600 Pa) expressed more neurogenic protein markers. The myogenesis of hMSCs was achieved instead when the hydrogel stiffness is greater than 8000 Pa. We have demonstrated that Gtn-HPA hydrogels with tunable mechanical properties offer a promising system for cell therapy. Their excellent cell adhesion without coating with additional adhesive ligands, biodegradability and optical transparency are the added advantages for the use of Gtn-HPA hydrogels in tissue engineering.

Chapter V

Cell responses of human fibroblast to hydrogel stiffness for wound healing application

5. Cell responses of human fibroblast to hydrogel stiffness for wound healing application

5.1. Introduction

Hydrogels have attracted intensive attention for wound healing applications as they can provide aqueous environment, enhancing the healing process of wound [164, 165]. Many clinical studies demonstrate that hydrogel dressings healed the wound quicker and reduced pain, compared to saline dressings [164, 166]. Moreover, *in situ* forming hydrogel dressings create minimally invasive methods that offer advantages over the use of preformed dressings such as conformability in any wound bed of irregular shape particularly, convenience of application, and improved patient compliance and comfort. Cultivation of either fibroblasts or keratinocytes, or a combination of both, to regenerate the structural complexity and heterogeneity of the skin was also attempted to promote healing in the wounds and improve the clinical outcome of healed skin. The closure of cutaneous wounds involves three processes: epithelization, connective tissue deposition and contraction. Dermal fibroblasts normally are sessile and quiescent, while they become activated after cutaneous wounding. Activated fibroblasts migrate to the fibronectin-fibrin wound interface, proliferate, and synthesize a new collagen-containing matrix called granulation tissue. During the events, wound contraction begins. The proliferation of fibroblasts is terminated and regresses and extracellular matrix remodeling commences when the wound defect is replaced.

As mentioned in chapter I, III and IV, the mechanical property of substrates influences the function, proliferation, and differentiation of cells and tissue

morphogenesis [2, 10, 106, 115, 116, 125, 128, 167-169]. It has also become evident that gene expression and proliferation of fibroblasts is regulated by mechanical force in the course of wound contraction [121]. Mechanical load plays an important role in regulating cell phenotype from resting to activated when the mechanical load changed from low to high [170]. These findings suggested that matrix stiffness is a key component of contractile behaviors during the wound healing process.

To address the importance of wound contraction for wound healing, many systems have been created as two- or three-dimensional substrates of controlled stiffness including collagen- and other natural polymer based matrixes to study the influence of such mechanical properties on the functions of fibroblast. The functions of fibroblast were closely dependent on the microenvironment where they reside including their physical properties and dimensionality. It is ultimately important to understand such effects in a 3D context as cells experience a richer, more complex physical environment and markedly different geometry and behave more physiologically in 3D compared to 2D surfaces. Nevertheless, very often, given the ease of growing and observing cells on the surfaces, 2D approach was widely adopted for most research purposes. However, the extent to which observations made in 2D studies can be transferred to predict cell behavior in a 3D environment has been an active area of research. It is well documented that fibroblasts embedded in collagen gels show distinct morphologies from those cultured on tissue-culture plastic [171]. Cells on free-floating collagen gels lack the pronounced F-actin stress fibers that are seen on tissue-culture plastic [172]. These findings highlighted the importance of incorporating the physical variables into designing ideal wound dressing to control the functions of fibroblast for acceleration of the wound

healing process and reduction in scar formation. The limitation in controlling the stiffness together with other drawbacks associated with the current hydrogel systems including fragility of the graft, poor mechanical stability, difficulties in integrating into clinical procedure and the toxicity of the materials have rendered them limited their use as potential wound dressing materials [173-175].

In the previous chapters, the role of stiffness in various cell functions including focal adhesion, proliferation rate and differentiation of hMSCs in both 2D and 3D contexts was clearly demonstrated using the Gtn-HPA hydrogel system with tunable stiffness. It has provided a simple and effective means to study cell functional responses to stiffness both in 2D and 3D culture environments given its *in situ* forming ability, excellent cell adhesion, tunable mechanical properties and stability. In this chapter, the Gtn-HPA hydrogels with varied stiffness were employed to study human fibroblast (HFF-1) cell behaviors in 2D and 3D cell culture environments to gain more understanding on the effect of stiffness on cell responses using the same material system for potential wound healing application. It would also provide an insight into the possible optimization of physical properties of wound dressing material when cell-loaded hydrogels are attempted to minimize the wound contraction and scar formation.

5.2. Materials and methods

5.2.1. Materials

The materials used to synthesize the Gtn-HPA conjugates and Gtn-HPA hydrogels remained the same as described in section **2.2.1.**. Human fibroblast (HFF-1) cells were

obtained from ATCC (USA). Dulbecco's modified eagle medium (DMEM) and fetal bovine serum (FBS) were provided by Invitrogen (Singapore). The remaining reagents mentioned in this chapter in the course of *in vitro* study were described in sections **3.2.1** and **4.2.1.**.

5.2.2. Revitalization and culture of HFF-1

The protocol followed for the revitalization and culture of HFF-1 were the same as described in section **3.2.2.**. The supplemented HFF-1 culture medium used to maintain the culture of HFF-1 contains DMEM, 15 % FBS, 1.0 mM sodium pyruvate. Penicillin at 100 units/ml and streptomycin 100 μg/ml were supplemented to complete the culture medium.

5.2.3. Preparation of Gtn-HPA and cell-capsulated Gtn-HPA hydrogels

Gtn-HPA conjugates were synthesized and rheological properties of their hydrogels were measured as described previously in section **2.2.2.** and **2.2.6.**. The compositions of the hydrogels and their rheological properties used in this study were the same as listed in Table 3-1 and Table 4-1. For the preparation of Gtn-HPA hydrogels encapsulated with cells, HFF-1 at final concentrations of 2×10^5 cells/ml was used.

5.2.4. Cell focal adhesion study

Both 2D and 3D cultures of HFF-1 involving Gtn-HPA hydrogels were maintained for 2 weeks before being immunostained using an actin/focal adhesion stain kit as described previously in section **3.2.8.**.

5.2.5. Time course assay on cell attachment

To prepare Gtn and Gtn-HPA coated surfaces, 5 wt.% of Gtn and Gtn-HPA was prepared and transferred to 24-well plates. After 1 h incubation, the solutions were removed and the plates were allowed to dry overnight. The same protocol was followed to study the time course assay on the HFF-1 attachment using Gtn-HPA hydrogels as described in section **3.2.5.** with minor change. In this study, 500 µl of HFF-1 in DMEM supplemented with 15 % FBS at cell density of 1×10^6 cells/ml was seeded onto various surfaces including the Gtn and Gtn-HPA coated plates and the Gtn-HPA hydrogels, respectively.

5.2.6. Cell proliferation assay

For 2D cell proliferation on the surface of hydrogels, 250 µl of HFF-1 in complete medium at cell density of 1×10^5 cells/ml was seeded onto the Gtn-HPA hydrogels. For 3D cell proliferation in the hydrogels, the hydrogel encapsulated with cells was prepared as described in section **5.2.3.**. The same protocols to harvest the attached cells with the aid of collagenase, label the cells by calcien AM and to determine cell number using DNA quantification assay were followed as described in section **3.2.5.**.

5.2.7. Degradation of hydrogel encapsulated with cells

To monitor the degradation of the hydrogel in the culture medium, HFF-1 were mixed with 1 ml of Gtn-HPA solution (2 wt.%) in 6-well plate at final concentrations of 2×10^5 cells/ml, the hydrogel was then cast into a disk with a diameter of 20 mm and a thickness of 1.5 mm. They are maintained in the culture medium. At each time interval, the stiffness of the hydrogels was measured using the HAAKE Rheoscope 1 rheometer. The measurement gap was optimized and maximum G' was recorded for each sample. At the same time interval, the change of water uptake in cell-encapsulated Gtn-HPA hydrogels over time was monitored as described as section **3.2.9.**. Three replicates were performed for both experiments.

5.3. Results and discussion

5.3.1. Hydrogel formation

As demonstrated in the previous two chapters, the *in situ* forming characteristic of this hydrogel allowed *in vitro* studies on various cell functions in response to hydrogel stiffness in both 2D and 3D culture environment. hMSCs adhering to a Gtn-HPA hydrogels are able to sense the mechanical stimuli and consequently regulate many important physiological processes such as adhesion, migration, proliferation and differentiation. In the case of human fibroblasts, it was clearly evident that those cultured in collagen matrices acquire tissue-like phenotypic characteristics not typically observed in cells in monolayer culture [121].

In this study, both 2D and 3D studies on the stiffness effect of hydrogel were performed and compared using the same Gtn-HPA systems. In a 2D cell culture study, the hydrogels were allowed to set before seeding of cells on their surfaces. While in a 3D cell culture study, the cells of interest were suspended in Gtn-HPA hydrogel precursor solution before enzyme catalytic reaction occurred, therefore, the cells were encapsulated inside the Gtn-HPA hydogels for further 3D studies. The very same groups of Gtn-HPA designated for 3D and 2D *in vitro* studies for hMSCs were used in this study for HFF-1. They are abbreviated as Gtn-HPA-2A and Gtn-HPA-2B in 3D studies as listed in Table 3-1. Those used in 2D studies are abbreviated as Gtn-HPA-5A, Gtn-HPA-5B and Gtn-HPA-5C as listed in Table 4-1. With an efficient gelation rate of less than 45 sec regardless of its stiffness, the Gtn-HPA hydrogel system would be a promising injectable hydrogel system for wound dressing application with or without cells. The uncontrolled diffusion of gel precursors to the surrounding tissues in relevant clinical situations can be easily avoided with this efficient gelation process.

5.3.2. Cell attachment

Prior to studying cell attachment on Gtn-HPA hydrogels, human fibroblast (HFF-1) were first seeded on the surface of culture plate coated with Gtn and Gtn-HPA conjugate to evaluate the cell adhesiveness of the test materials. It was found that the difference in cell attachment percentage of HFF-1 between the Gtn coated and Gtn-HPA conjugate coated surfaces was not significant throughout the entire course of study as shown in Figure 5-1a. They greatly supported the cell attachment comparable to the commonly used culture

plates. This indicated that the modification done to Gtn by the conjugation of HPA to it did not alter the inherent cell adhesiveness of Gtn. It was reported that this was due to its positively charged residues and embedded RGD peptide sequences in the Gtn [146].

In contrast, when the HFF-1 was seeded onto Gtn-HPA hydrogels with varied stiffness instead of coated culture plates with Gtn or Gtn-HPA conjugates, the percentage of cells attached over time differed greatly among the hydrogels (Figure 5-1b). The cells on the softer Gtn-HPA showed much slower progress in the attachment over time. Only 40 % of the cells attached on the Gtn-HPA hydrogels of G' value less than 1k Pa including Gtn-HPA-2A, Gtn-HPA-2B and Gtn-HPA-5A after 6 h of incubation. However, a vast majority of HFF-1 had firmly attached to Gtn-HPA-5C of G' value 8 kPa at merely 4 h incubation. The cells showed progressive improvement on the cell attachment when hydrogel stiffness was increased from 600 Pa (Gtn-HPA-5A) to 8 kPa (Gtn-HPA-5C) despite the fact that the same concentration of Gtn-HPA conjugates was used to prepared them. However, there was not much difference in the cell adhesiveness among Gtn-HPA-2A, Gtn-HPA-2B and Gtn-HPA-5A regardless of the concentration of Gtn-HPA conjugates used. It suggested that the stiffness of the hydrogel was the determining factor in manipulating the cell attachment in this study. It might be also the cause of insignificant differences observed in the previous experiments on the Gtn and Gtn-HPA conjugates coated plastics where the cells were cultured on the culture plastic with a thin layer of coating of Gtn or Gtn-HPA cojugates instead of Gtn-HPA hydrogels. The thin layer of coating did not significantly change the mechanical properties of the underneath plastic plate where the cells were cultured on.

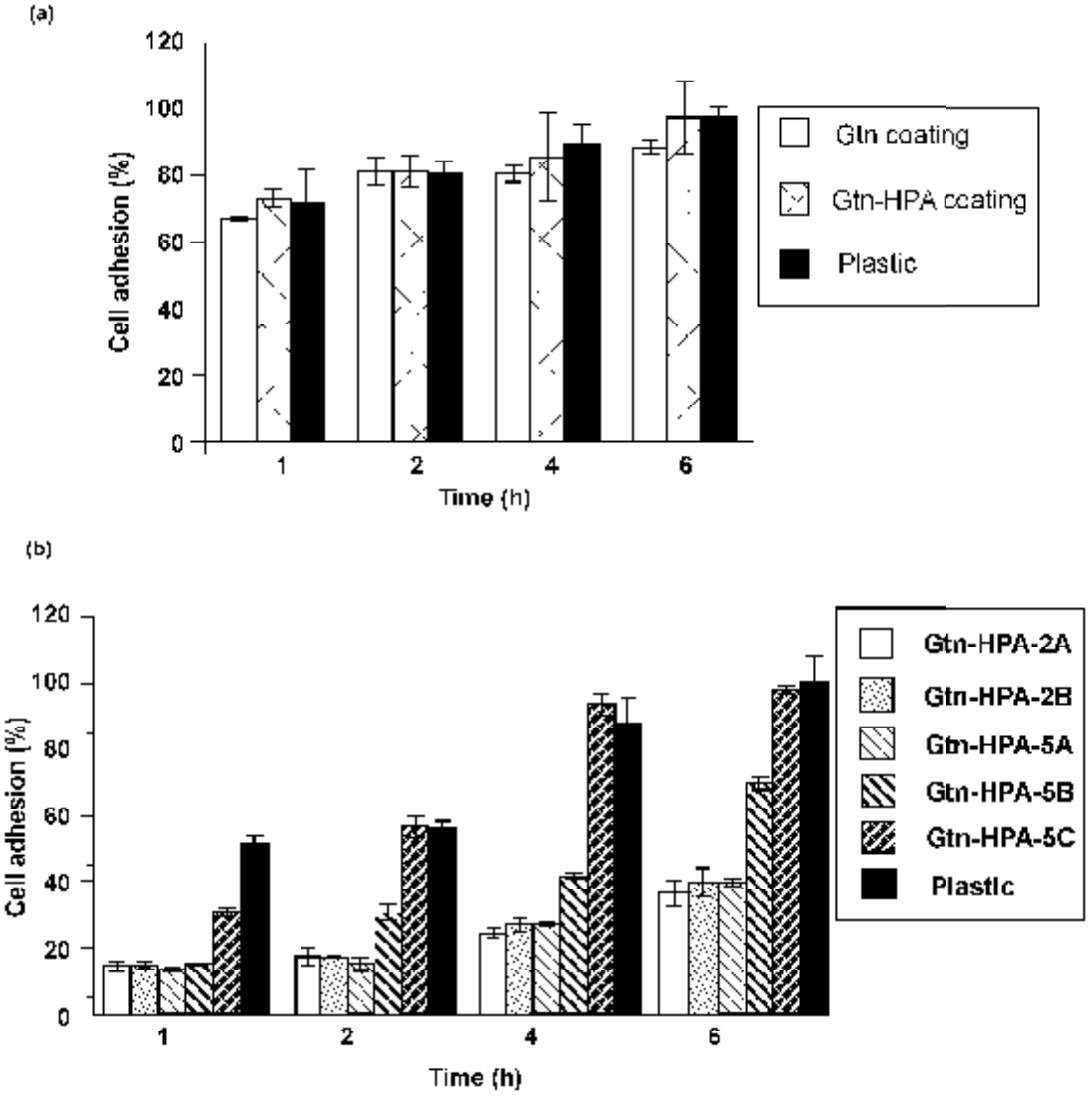

Figure 5-1. HFF-1 attachment on the surfaces (a) coated with Gtn and Gtn-HPA conjugates, (b) of Gtn-HPA hydrogels with varied stiffness after different incubation periods. Results are shown as the average values ± standard deviation (n=3).

5.3.3. Focal adhesion and proliferation in 2D study

After the HFF-1 was seeded onto the Gtn-HPA hydrogels (2D), it was observed that those attached to the softer hydrogels appeared to be more elongated compared to the ones on the stiff hydrogels microscopically. To confirm the observation, immunostaining on the fibroblast was performed to detect their focal adhesion actin cytoskeleton. Confocal fluorescence microscopy of the stained cells revealed focal contacts in green using an anti-vinculin monoclonal antibody and a FITC-conjugated secondary antibody. F-actin was shown in red and nuclei in blue (Figure 5-2). For the hydrogels with stiffness less than 1 kPa including Gtn-HPA-2A, Gtn-HPA-2B and Gtn-HPA-5A, no visual difference in the images was observed for the fibroblasts grown on them. They shared the same observation of a diffuse organization of focal contacts and F-actin fibers. The fibroblasts cultured on stiffer substrates including Gtn-HPA-5B and Gtn-HPA-5C had developed more spread-out morphology, more organized actin fibers and focal contacts compared with cells cultured on the soft counterparts. This increased cytoskeleton organization on stiffer substrates resembles the response observed in previous studies on various cell type [117, 176] including our own observation on the hMSCs discussed in the previous two chapters. An increase in stiffness of hydrogel seems to enhance stress fiber formation in cells which promotes the entry into the cell cycle as reported earlier [117]. Our experiment was consistent with these findings that a stiffer matrix led to a more organized cytoskeleton arrangement and an increased proliferation rate as a result of firmer adhesion. The changes in cell morphology and adhesion as a response to hydrogel stiffness most likely led to differences in cell proliferation as discussed below.

Indeed, despite the Gtn-HPA hydrogels being a great support for fibroblast attachment and proliferation regardless of their stiffness, a measurable effect on the proliferation rate of fibroblast influenced by stiffness of Gtn-HPA hydrogel was found. The proliferation rate of fibroblasts was progressively increased with an increase in the stiffness of the hydrogel where they were grown on (Figure 5-3a). It was also found that the cells cultured on the surface of Gtn-HPA-5A also moved in a Z direction into the hydrogel (Figure 5-3b). The nuclei of cells were stained in blue. The distance travelled along the Z direction was much longer compared to that of hMSCs as shown in Figure 4-6 given the same culture time which is attributed to cell-to-cell variation. However, such movement was not seen in the ones on the surface of Gtn-HPA-5B and Gtn-HPA-5C resembling the observation found on hMSCs. It validated that this migration was most likely associated with the degradability of the hydrogels.

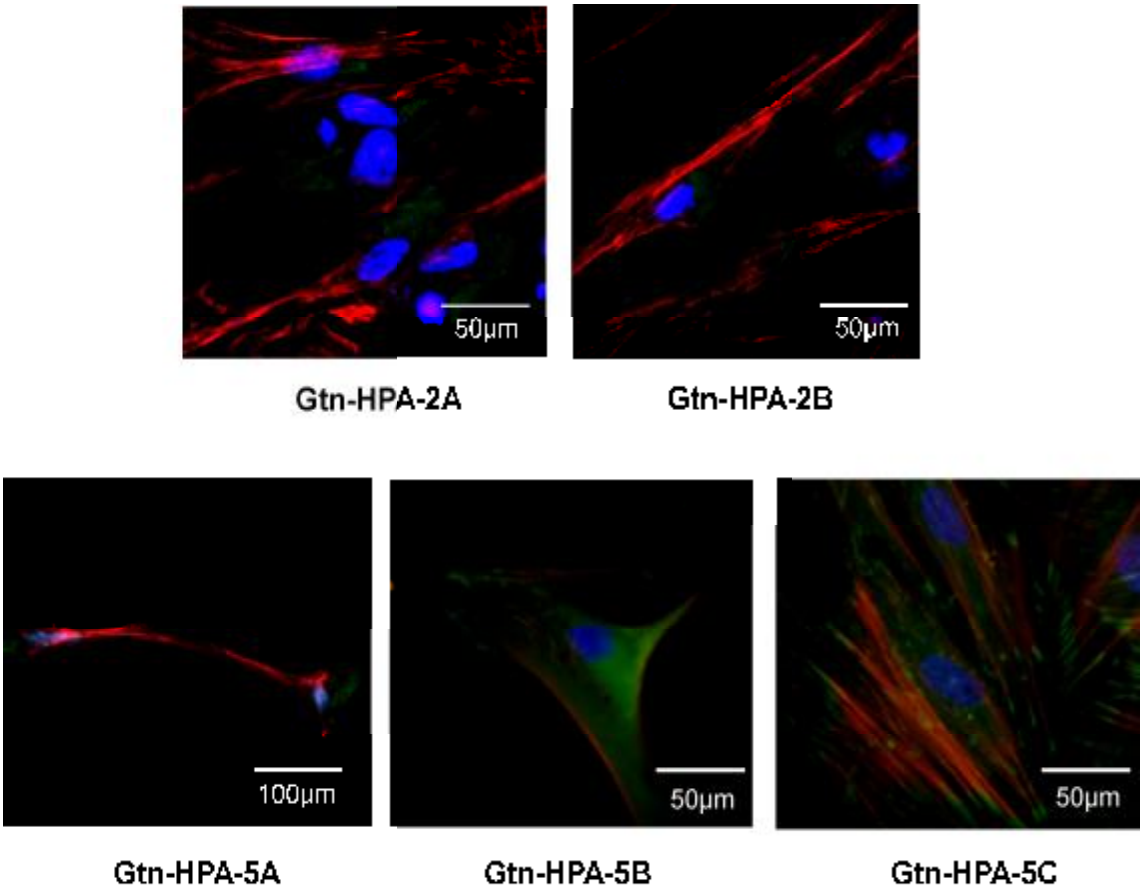

Figure 5-2. Confocal fluorescence microscopy of focal adhesion and actin cytoskeleton in HFF-1 cultured on Gtn-HPA hydrogels.

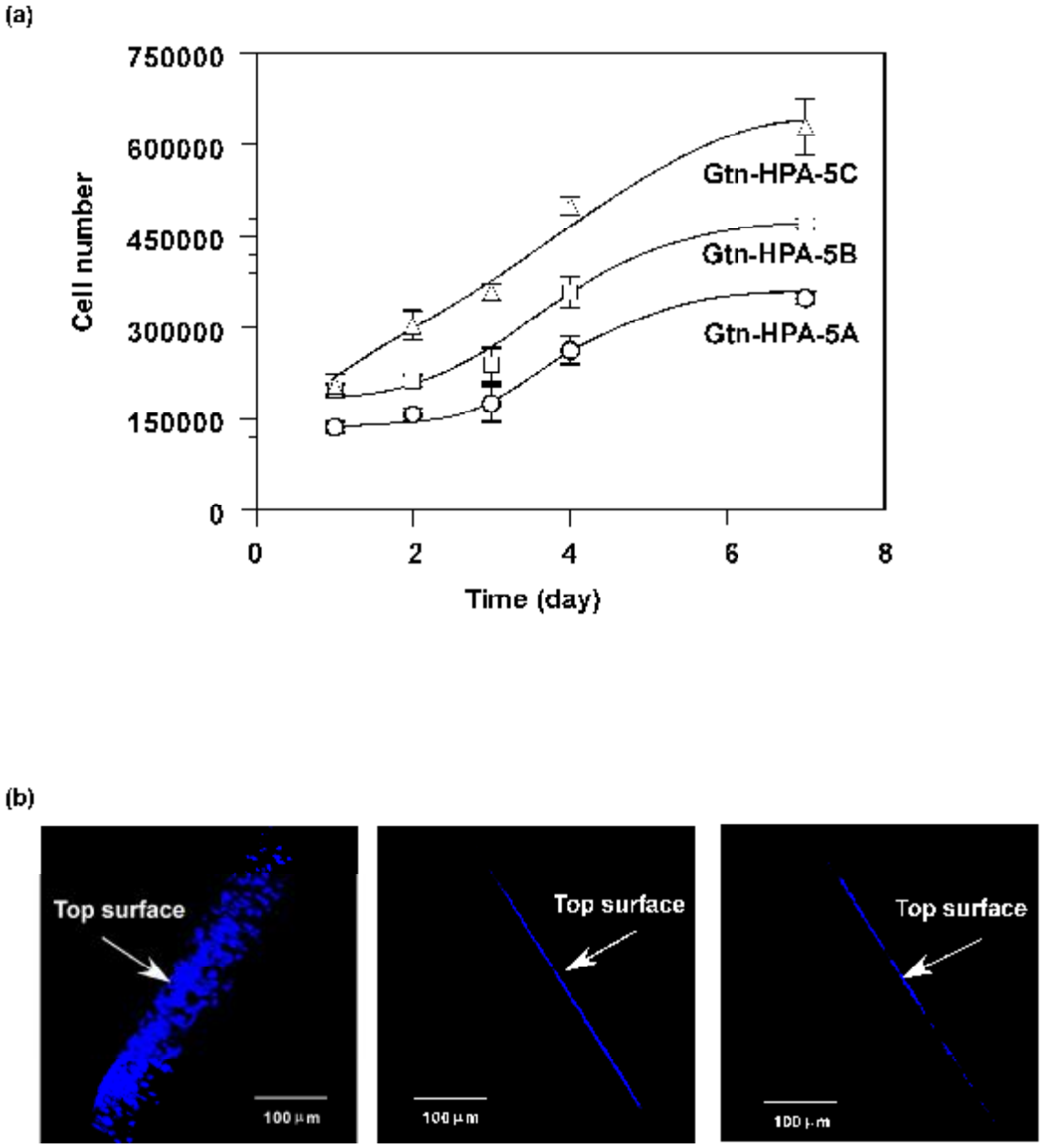

Figure 5-3. HFF-1 proliferation on Gtn-HPA hydrogels with different stiffness. Results are shown as the average values ± standard deviation (n=4). (b) Cross-sectional image of hydrogel with HFF-1 cultured on the surfaces.

5.3.4. Focal adhesion and proliferation in 3D study

Given the evidence that Gtn-HPA hydrogel strongly supports cell attachment and proliferation in the 2D cell culture setting, the 3D culture of HFF-1 inside Gtn-HPA hydrogels was explored in an attempt to develop cell-encapsulated construct in a tissue-like environment whose stiffness can be controlled to allow detailed correlation with cell responses. The hydrogel encapsulated with HFF-1 was formed *in situ* by suspending the cells in the hydrogel precursor solution prior to activation by HRP and H_2O_2. Gtn-HPA-2A and Gtn-HPA-2B of G' value less than 1 kPa was chosen to study the stiffness effect in a 3D environment. Figure 5-4a represents the morphology of cells cultured in Gtn-HPA hydrogels after 2 weeks. Hydrogels comprising of hyaluronic acid- Tyramine (HA-Tyr) with similar G' value of 614 Pa were used a comparison. The preparation of HA-Tyr was performed as reported previously [89]. The cells were stained by calcein AM. It was found that HFF-1 proliferated and interconnected inside the Gtn-HPA hydrogels with filopodia-rich morphology. Whilst the HFF-1 in HA-phenol hydrogels appeared to be rounded over time, largely due to the poor spreading of cells despite being of similar stiffness to the Gtn-HPA-2B hydrogels. This observation was attributed to highly negatively charged polymer chain in hyaluronic hydrogels resulting in poor cell adhesiveness [177].

It was also shown that the cell proliferation was dependent on the stiffness of Gtn-HPA hydrogels (Figure 5-4b). It is noteworthy that there was a striking difference between the fibroblasts proliferation profiles obtained from the 3D and 2D studies. Firstly, a very slow proliferation was observed in the first 12 days of culture in the 3D

experiment; however the same fibroblast seemed to experience continuous growth over the entire culture period when they were cultured on 2D surfaces. The initial low proliferation rate uniquely found in the 3D culture system might be due to a largely differed environment the cell has experienced in 3D. It is reported that fibroblast exhibited a marked decline in cellular DNA synthesis when fibroblasts were cultured in 3D floating collagen matrixes with elaborated dendritic network of extensions [120]. Secondly, the proliferation rate of HFF-1 found at the later stage of cell culture decreased with the increase of the hydrogel stiffness. However, no noticeable cell proliferation of HFF-1 was found in hyaluronic acid hydrogel through out the four weeks of culture. It suggested that for the fibroblast, cell adhesiveness of the materials was prerequisite for supporting cell proliferation and the rate of cell proliferation was affected by the stiffness of material surrounding it.

Immunostaining on the fibroblast which was cultured inside the Gtn-HPA hydrogels with varied stiffness was also performed to detect their focal adhesion and actin cytoskeleton. These images reveal focal contacts in green using an anti-vinculin monoclonal antibody. F-Actin was detected in red and nuclei shown in blue. As shown in Figure 5-4c, the cells in Gtn-HPA-2A hydrogel appeared more elongated with diffuse organization of actin filaments and focal contacts. However, the cells inside Gtn-HPA-2B appeared to be more compact and more organized in actin and focal contacts presentation. This distinct difference was not found when the fibroblasts were cultured on surfaces of the same hydrogels in the 2D study as shown in Figure 5-2.

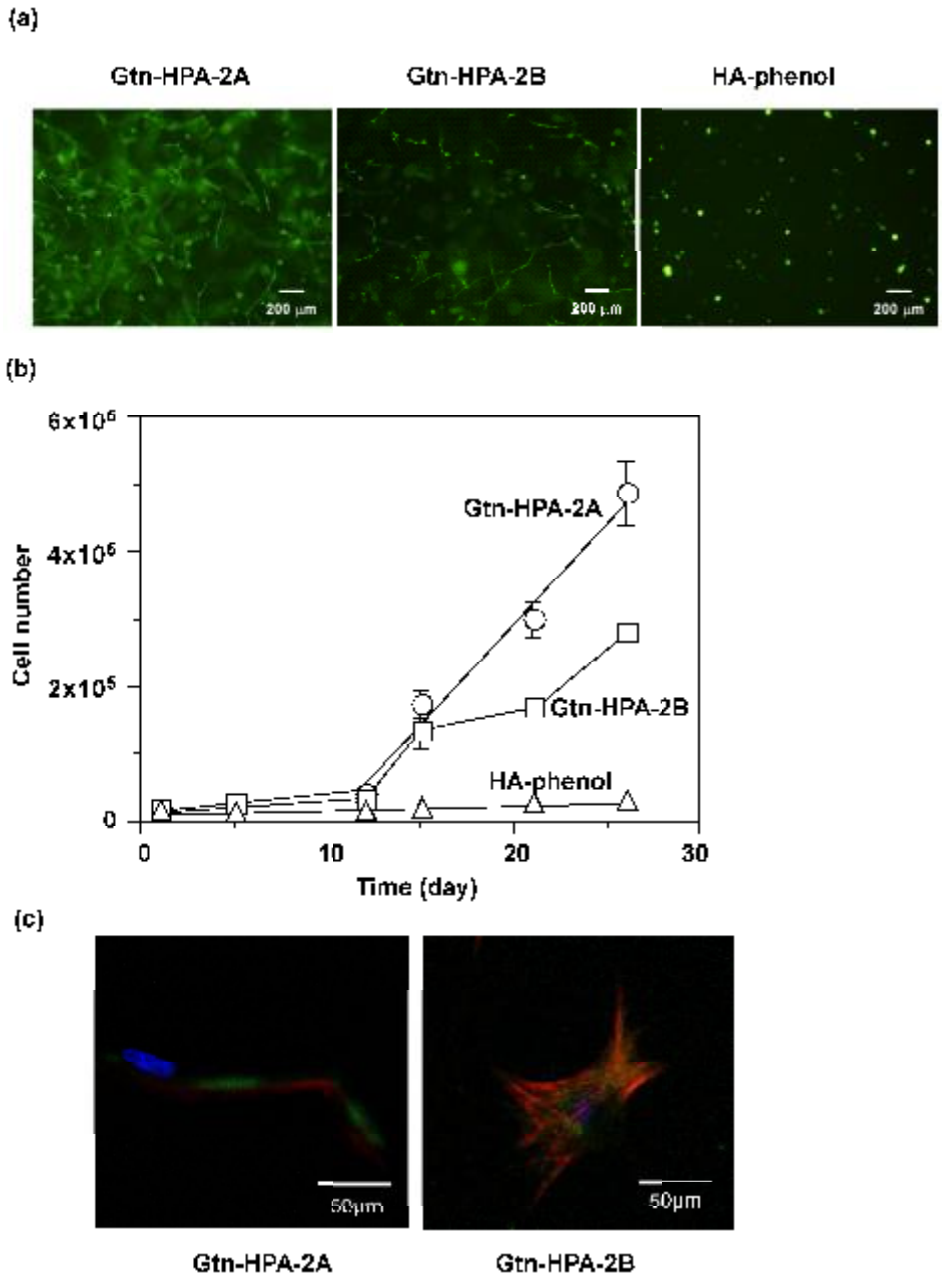

Figure 5-4. (a) Fluorescence images of HFF-1 cultured in Gtn-HPA hydrogels. The cells were stained by calcein AM. (b) 3D HFF-1 proliferation in Gtn-HPA hydrogels. Results are shown as the average values ± standard deviation (n=6) (c) Confocal fluorescence microscopy of focal adhesion and actin cytoskeleton in HFF-1 cultured in Gtn-HPA hydrogels.

In this 3D study, the proliferation rate was adversely affected by the increase of stiffness, unlike the findings from the 2D study that higher stiffness accelerated cell proliferation, even though both studies showed the similar trend in focal contacts and actin organization when the stiffness changed. Thus, it was considered that lower water uptake of the hydrogel as a result of high stiffness and the degradability of the hydrogel also play an important role in the cell proliferation in a 3D context as discussed in the following study. Understanding of the interactions between the cells and properties of the surrounding matrix in a tissue-like 3D environment is essential for a rational design in the tissue engineering application.

5.3.5. Degradation of hydrogels encapsulated with HFF-1

The changes in water uptake and stiffness of Gtn-HPA hydrogels encapsulated with HFF-1 over culture were closely monitored to understand the effect of hydrogel degradability on cell proliferation. The hydrogel degradability in the presence of cells was strongly correlated to its stiffness. As shown in Figure 5-5a, The hydrogels without the cells regardless of their stiffness did not change significantly in the respect of water uptake over three weeks of culture except in the case of Gtn-HPA-2A at week one. As discussed in section **3.3.4.**, about 89 % Gtn-HPA conjugate remained after soaking in the case of Gtn-HPA-2A. Whereas, there was 95 % left for Gtn-HPA-2B. Therefore, this abrupt change observed in water uptake was most likely due to the leaching of uncrosslinked polymers as value of water uptake was stabilized in the following two weeks. The leach-out of uncrosslinked polymers was well controlled in the case of Gtn-HPA-2B, as a result, little variation was shown in the water uptake.

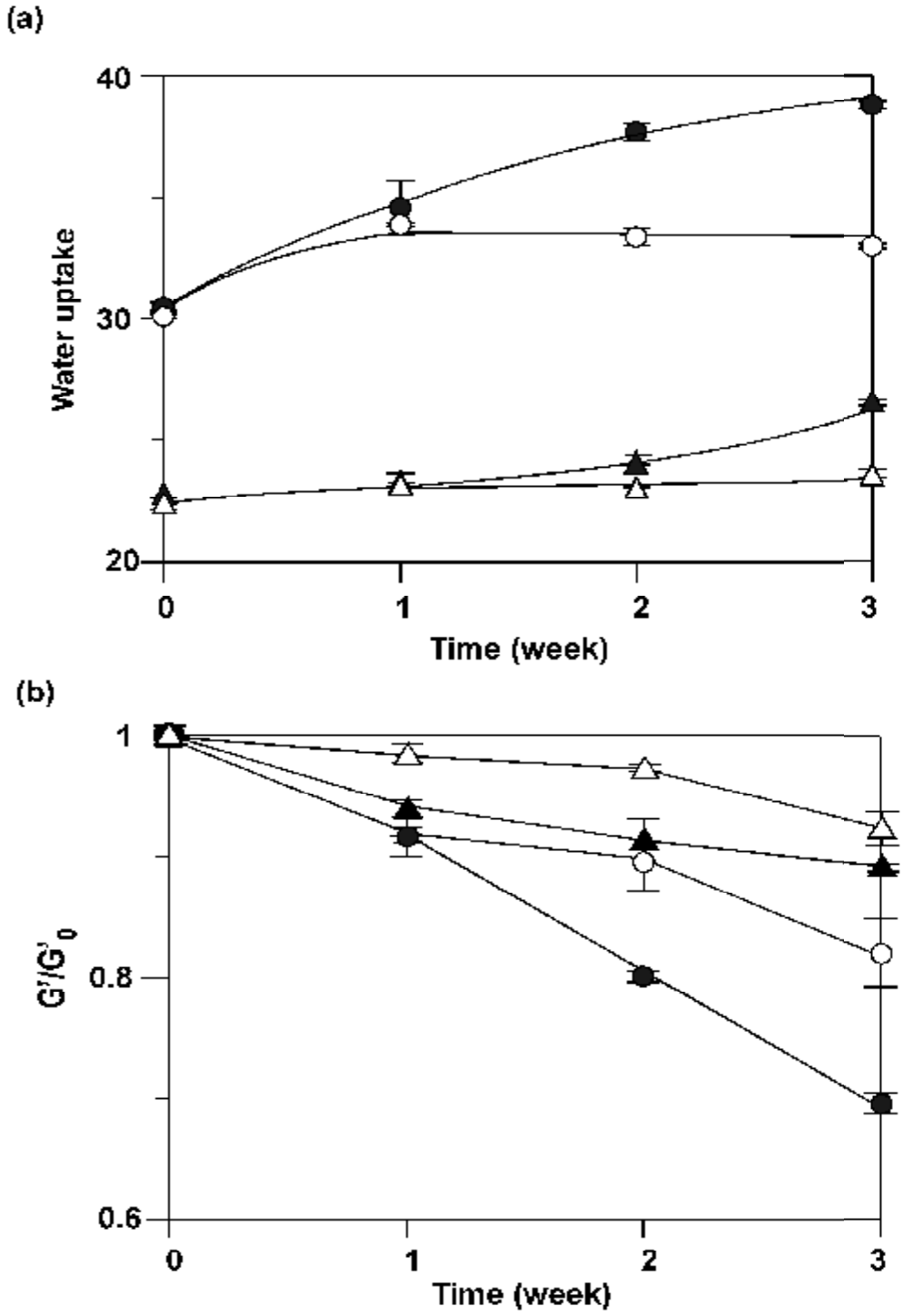

Figure 5-5. Change in (a) water uptake and (b) storage modulus of Gtn-HPA-2A without cell (™), Gtn-HPA-2A with cell (●), Gtn-HPA-2B without cell (△) and Gtn-HPA-2B with cell (▲). Results are shown as the average values ± standard deviation (n=3).

However, when the cells were encapsulated inside the hydrogels, the increase in water uptake was distinct over culture. The difference in the change of water uptake over time was much larger in the case of softer hydrogel, which is largely attributed to the faster degradation as a result of lower stiffness. A similar observation was made when the stiffness of the cell-encapsulated hydrogels were recorded at each time interval (Figure 5-5b). Up to 90 % of G' was maintained in the case of Gtn-HPA-2B, however, the G' of the softer counterpart, Gtn-HPA-2A lost 30 % in the value of G'. This suggested that the degradation process occurred when the cells are cultured inside the hydrogel, inevitably, resulting in a change in stiffness. It was also reported that in addition to changes in cell proliferation, fibroblasts in 3D floating collagen matrixes also show decreased collagen biosynthesis and increased release of collagenase compared with cells in anchored matrices [121]. Taken together, it is believed that the degradability of the hydrogels and change in cell biosynthesis in response to stiffness play important roles in cell proliferation and migration in 3D culture.

5.4. Conclusion

An injectable Gtn-HPA hydrogel was formed by the oxidative coupling reaction of phenol moiety in the presence of H_2O_2 and HRP. A wide range of stiffness of the hydrogel was readily tuned by the H_2O_2 concentration. The proliferation rate of HFF-1 in contact with Gtn-HPA hydrogels was strongly affected by the hydrogel stiffness. In the 2D studies, the fibroblasts exhibited a higher proliferation rate, more organized cytoskeletons and focal adhesion when the stiffness of the hydrogel where they were

grown on was increased. However, the cells cultured inside the hydrogel remained non-proliferative for 12 days before a stiffness-dependent proliferation profile was shown. The stiffness of hydrogel affected the proliferation rate in a different manner from the 2D studies. The marked difference in the respect of the fibroblast proliferation between 2D and 3D studies underlines the need of considering the effects of both the dimensionality and the stiffness in the design of such materials as wound dressings in order to accelerate the wound healing process and improve the clinical outcome of it. This Gtn-HPA hydrogel system provides a simple and effective means to study cell functional responses in both 2D and 3D environments, given its excellent cell adhesion and tunable mechanical properties. With its *in situ* forming ability, efficient gelling mechanism, biocompatibility, biodegradability and cost effectiveness, the Gtn-HPA hydrogel offers a great potential as wound dressing material.

Chapter VI

Synthesis and Characterization of Gtn-HPA-Tyr with broader stiffness control

6. Synthesis of characterization of Gtn-HPA-Tyr with broader stiffness control

6.1. Introduction

In the previous three chapters, an injectable hydrogel scaffold system composed of Gtn-HPA conjugates with tunable stiffness was developed for controlling the various cell functions including cell adhesion, migration, proliferation and differentiation of human mesenchymal stems cells (hMSCs) and human dermal fibroblast (HFF-1) in a two-dimensional (2D) and three-dimensional (3D) cell culture environment. The Gtn-HPA hydrogels were formed using the oxidative coupling of phenol moieties catalyzed by hydrogen peroxide (H_2O_2) and horseradish peroxidase (HRP). The stiffness of the hydrogels was readily tuned by varying H_2O_2 concentration without changing the concentration of polymer precursor. In the 3D culture setting, due to the inherent difficulties in 3D culture systems such as poor transportation of nutrients and low degradability of hydrogels as a result of increasing stiffness, the storage modulus (G') of hydrogels studied in 3D was limited to no higher than 1000 Pa. In contrast, for 2D cell culture systems, Gtn-HPA hydrogel with higher stiffness could be useful for controlling the cell functions of hMSCs and HFF-1 due to free access to nutrients. We found that the stiffness of the hydrogel strongly affected the cell proliferation rates. The rate of human fibroblast and hMSCs proliferation increased with the decrease of the hydrogel stiffness. The differentiation of hMSCs was also directed by the stiffness of the hydrogel where they resided on. The hMSCs on a softer hydrogel (G'=600 Pa) expressed more neurogenic protein markers, while cells on a stiffer hydrogel (G'=12800 Pa) showed a higher up-regulation of myogenic protein.

In light of the role of stiffness of substrate on various cell functions, and to fully maximize its potential and extend its application as an injectable hydrogel system with tunable mechanical properties in tissue engineering and regenerative medicine, there is a need to further broaden the range of control in stiffness. As discussed in the previous chapters, both H_2O_2 and Gtn-HPA concentrations were directly correlated to the stiffness of Gtn-HPA hydrogel. However, the excessive amount of H_2O_2 resulted in a decrease in the hydrogel stiffness given the same Gtn-HPA concentration. On the other hand, an increase in the concentration of Gtn-HPA significantly increased the viscosity of the solution which may impose difficulties in handling especially in the process of injection for an injectable hydrogel system like Gtn-HPA. Therefore, an increase in phenol content in the biopolymer-phenol conjugate presents as a more feasible alternative to achieve a even greater extent in stiffness control in the case of Gtn-Phenol hydrogel system.

As characterized in chapter II, the amine group in Gtn was highly conjugated with HPA. Up to 90 % of the amine group in Gtn was already utilized in Gtn-HPA conjugate. Therefore, to further increase the phenol content in the conjugates, tyramine (Tyr) was additionally conjugated to the carboxyl groups in Gtn in a similar manner by carbodiimide/active ester-mediated coupling reaction. In this chapter, the synthesis and characterization of Gtn-HPA-Tyr are discussed. The total phenol content was carefully monitored so as not to compromise the solubility of the resultant Gtn-HPA-Tyr conjugate in water. This study also explored its range of control in hydrogel stiffness in a comparison to its predecessor Gtn-HPA, its capability in supporting cell growth as well as *in vitro* cytotoxicity on its fragmented products by enzymatic degradation.

6.2. Materials and methods

6.2.1. Materials

The materials used to synthesize the Gtn-HPA conjugates and Gtn-HPA hydrogels remained the same as described in section **2.2.1.**. Tyramine hydrochloride was purchased from Sigma-Aldrich (Singapore). Inventorized primers for enolase 2 (ENO2), myogenic differentiation factor 1 (MYOD1), osteocalcin and Runt-related transcription factor 2 (anti-RUNX2) and Taqman® gene expression assay kit was provided by Invitrogen (Singapore). The remaining reagents mentioned in this chapter in the course of *in vitro* study were described in section **5.2.1.**.

6.2.2. Synthesis of Gtn-HPA-Tyr conjugate

The synthesis of Gtn-HPA-Tyr conjugate was achieved by a two-step reaction process (Scheme 1). Firstly, Gtn-HPA conjugate was synthesized as described previously in chapter I. Briefly, HPA (3.32 g, 20 mmol) was dissolved in 250 ml of mixture of distilled water and *N*, *N*-dimethylformamide (DMF) (3:2). To this NHS (3.20 g, 27.8 mmol) and EDC·HCl (3.82 g, 20 mmol) were added. The solution was stirred at room temperature for 5 h, and the pH of the mixture was maintained at 4.7. Then, 150 ml of Gtn aqueous solution (6.25 wt.%) was added to the reaction mixture and stirred over night at room temperature at pH 4.7. The solution was transferred to dialysis tubes with molecular cut-off of 1000 Da. The tubes were dialyzed against 100 mM sodium chloride solution for 2 days, a mixture of distilled water and ethanol (3:1) for 1 day and distilled water for 1 day, successively. Then, Tyr·HCl (0.50 g, 2.87 mmol), NHS (0.12 g, 1 mmol) and EDC (0.14

g, 0.75 mmol) were added to the purified Gtn-HPA conjugate solution to synthesize Gtn-HPA-Tyr conjugate. The solution was again stirred over night at room temperature at pH 4.7. Then, the solution was dialyzed in the same manner as described above. The purified solution was finally lyophilized to obtain the Gtn-HPA-Tyr conjugate. However, precipitation occurred when Tyr·HCl (1.0 g, 5.74 mmol), NHS (0.24 g, 2.0 mmol) and EDC (0.28, 1.5 mmol) were added into the purified Gtn-HPA conjugate solution under the same reaction condition. This insoluble conjugate abbreviated as Gtn-insoluble was harvested and lyophilized for characterization.

6.2.3. Characterization of Gtn-HPA-Tyr conjugates

^{1}H NMR spectra were recorded on a Bruker AV-400 (400 MHz) spectrometer at room temperature to characterize the conjugation of phenol compounds of Gtn-HPA and Gtn-HPA-Tyr conjugates (10 mg/ml in D_2O). To determine the phenol content of Gtn-Phenol conjugates, the absorbance of Gtn-HPA-Tyr and Gtn-HPA conjugates (1mg/ml) was measured at 276 nm using a UV-visible spectrophotometer (U-2810, Hitachi, Japan). The phenol content of each sample was estimated by comparing to the HPA and Tyr standards. Differential scanning calorimetry (DSC) was performed with a DSC-Q100 (TA Instruments, USA). Gtn, Gtn-HPA, Gtn-HPA-Tyr conjugates and Gtn-insoluble (6-8mg) in crimped standard aluminum pans which were heated from 35°C to 230°C at 3°C/min to obtain the DSC thermograms. The Gtn-insoluble was also characterized by DSC as a comparison.

6.2.4. Rheological measurement

Rheological measurements of the hydrogel formation were performed as described in section **2.2.6.** with minor change in hydrogel formulation. The aqueous solution of Gtn-HPA-Tyr used in this chapter was 10 wt.%. The solution of H_2O_2 with different concentrations was added to the 10 wt.% of Gtn-HPA-Tyr while HRP was kept at 0.15 units/ml.

6.2.5. Time course assay of cell attachment

This experiment was designed to assess whether further conjugation of Tyr to Gtn-HPA and the resultant increase of its hydrogel stiffness interfere with the attachment of HFF-1. The hydrogel with highest stiffness were selected according to the results of rheological measurement. Gtn-HPA and Gtn-HPA-Tyr hydrogels were prepared in the 24-well plate in a similar manner as described in section **3.2.5.** with minor change in hydrogel formation. In brief, 6 µl of HRP was added to 1 ml of Gtn-HPA and Gtn-HPA-Tyr conjugate solutions (10 wt.%) to give a final concentration of 0.15 units/ml. Crosslinking was initiated by adding 6 µl of H_2O_2 solution to give a final concentration of 13 mM. The same experimental protocol and DNA quantification assay to determine the cell number were followed to monitor the cell attachment over culture time as described in the section **3.2.5.**. Two hundred and fifty µl of HFF-1 in the complete medium at cell density of 6×10^5 cells/ml was seeded onto these hydrogels in this study.

6.2.6. Cell focal adhesion study

The same imunostaining protocol was employed to study the cell focal adhesion of the HFF-1 cultured on the Gtn-HPA hydrogels as described in section **3.2.10.**.

6.2.7. Real time PCR analysis

The hydrogels were digested with collagenase solution (0.5 wt.%) and the cells were then harvested for RNA extraction to measure the relative expression of genes of interest in hMSCs that were cultured on Gtn-HPA and Gtn-HPA-Tyr hydrogels for 3 weeks. This extraction was performed according to the protocols specified in the RNeasy Mini Kit (Qiagen, USA). The RNA samples were reverse-transcribed to cDNA using a First strand cDNA synthesis kit (Fermentas, Canada). The relative expression of enolase 2 (ENO2), myogenic differentiation factor 1 (MYOD1), RUNX2 and OC was then determined *via* real-time PCR using a Bio-Rad iQ5 multicolor real-time PCR detection system (Bio-Rad, USA). Specific primers for these genes were inventoried by Invitrogen. Each PCR reaction was performed in 20 µl of a reaction mixture containing 2 µl cDNA, 1 µl of each primer, 10 µl of Taqman® gene expression master mix (Invitrogen) and 7 µl of diethylpyrocarbonate (DEPC)-treated water (Invitrogen). The final concentration of the primers used in this study was 100 µM. The samples were then subjected to cycling conditions as specified in the TaqMan® Gene expression assay kit protocol. The experiment was performed in triplicate. The results were normalized to β-actin gene expression and were expressed as fold change values relative to undifferentiated hMSCs.

6.2.8. Enzymatic degradation of Gtn-HPA-Tyr hydrogels

Slab-shaped Gtn-HPA-Tyr hydrogels with different stiffness were prepared as described in section **6.2.5.** with some change in hydrogel formulation. The concentrations of H_2O_2 solution to give final concentrations of 1.7, 3.4, 8.5, 13 and 17 mM were used. The G' of resultant hydrogels was 600, 3200, 13500, 14600 and 26800 Pa, respectively. The protocol of degradation study was described in section **3.2.4.**.

6.2.9. Cytotoxicity study of fragmented Gtn-Phenol hydrogels

The hydrogel with highest stiffness was prepared in the same manner as described above and tested for their cytotoxicity. These hydrogels were immersed in 1 ml of PBS containing 6.7 units/ml of type I collagenase and incubated at 37°C in an orbital shaker at 100 rpm. After the hydrogels were fully degraded, the solution, containing the degraded hydrogels, was aseptically diluted at volume ratio of 1:3 and 1:9 using the culture medium to give final concentrations of 0.25 and 0.6 wt.%. HFF-1 cells in 200 µl of the respective medium containing the degraded products were added at a density of 5×10^4 cells/ml to the wells of 96-well plate. The wells containing the cells exposed to type I collagenase solutions of the same concentration were served as comparisons. The cells were incubated for 24 and 72 h. At the end of the specified exposure time, cell viability was assessed using Alamar blue assay. Briefly, at each time interval, the culture medium was aspirated and replaced with fresh medium, and incubated with Alamar blue dye (10 %) for 3 h to measure the viability of cells. Fluorescence measurement was performed with an Infinite M200 (Tecan, Switzerland). Wavelengths of excitation and emission

were set at 570 and 590 nm, respectively. The results were expressed as percentage of viability compared with untreated cells.

6.3. Results and discussion

6.3.1. Synthesis and characterization of Gtn-HPA-Tyr conjugate

As described in the chapter II, Gtn-HPA conjugate was successfully synthesized by a general carbodiimide/active ester-mediated coupling reaction in distilled water. In this study, Gtn-HPA-Tyr conjugate was synthesized to further increase the phenol content into Gtn using a 2-step reaction (Figure 6-1). Firstly, Gtn-HPA conjugate was synthesized by a reaction between amine groups of Gtn and succinimide-activated HPA. After purification of Gtn-HPA conjugate by a dialysis, Tyr was additionally conjugated to carboxyl functional groups of Gtn-HPA conjugate which is readily available in Gtn to synthesize Gtn-HPA-Tyr conjugate by reaction between the carboxyl groups in Gtn and amine groups in Tyr. As descried in the section **6.2.2.**, the conjugation of phenol was optimized so as not to compromise the water-solubility of the resultant conjugate.

^{1}H NMR measurements of synthesized bioconjugates revealed that the integrated intensities of phenol (6.8 ppm and 7.1 ppm) of Gtn-HPA-Tyr conjugate were higher than those of Gtn-HPA conjugate, confirming the conjugation of both HPA and Tyr to Gtn (Figure 6-2). Furthermore, the conjugation of phenol molecules was quantitatively analyzed by measuring the absorbance values at 276 nm. The phenol content was calculated using HPA standards with known concentrations. No significant difference in

the absorbance between HPA and Tyr standards was observed. The total phenol content of Gtn-HPA and Gtn-HPA-Tyr conjugate was determined to be 4.44 x $10^{-7}$and 7.11 x 10^{-7} mol/mg conjugate, respectively.

The DSC curves of Gtn, Gtn-HPA, Gtn-HPA-Tyr and Gtn-insoluble conjugates were compared in Figure 6-3. Two glass transition temperatures (Tgs) (first Tg; 72.2 and second Tg; 200.6°C) for Gtn were observed in the thermograms. The conjugation of HPA to Gtn seemed to have a strong influence on the second Tg. With such conjugation, the second Tg was shifted by 3.2°C, from 200.6°C to 197.4°C. Further conjugation of Tyr to Gtn-HPA conjugate decreased the second Tg even further by another 2.6°C to 194.8°C. This shift of second Tg was largely pronounced in the case of Gtn-insoluble conjugate with overly conjugated Tyr moiety. Its second Tg appeared at 157.9°C. However, the first Tg was only marginally different among all the samples. As Fraga et al. have reported the first Tg of Gtn is a minor one, observed around 80–100°C and associated with the glass transition of *a*-amino acid blocks (soft blocks) [178]. The second more intense Tg is observed around 180–200°C, and represents the blocks of imino acids, proline, hydroxyproline with glycine (rigid blocks). Therefore, the shift of second Tg by phenol conjugation suggests that majority of the conjugation was done near the rigid block of the Gtn with minimal impact on the soft block of Gtn. It is considered that the conjugation of the phenol molecules disrupted the crystalline structure mainly formed by the rigid blocks and drove the second Tg down.

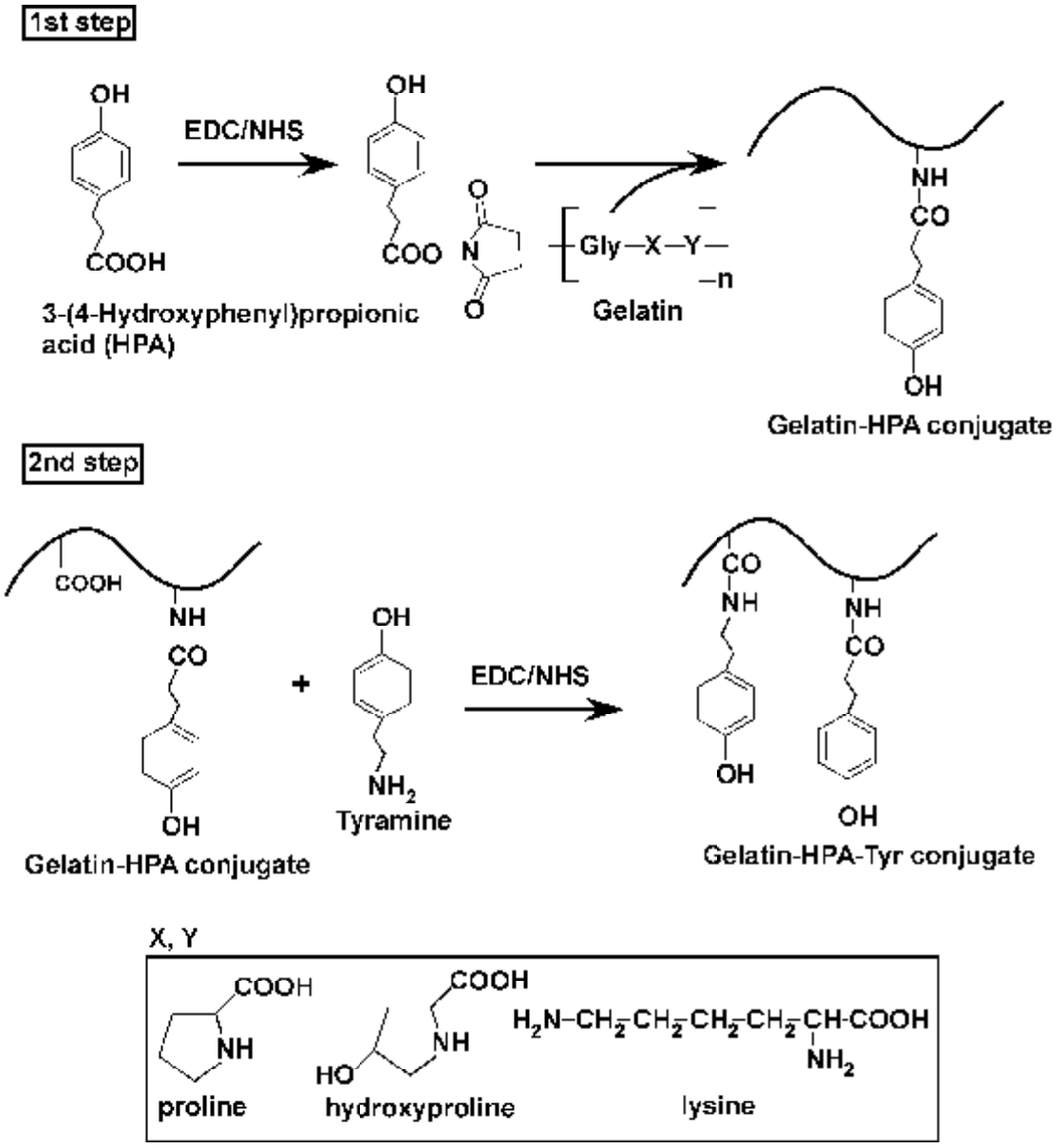

Figure 6-1. Reaction scheme for the synthesis of Gtn-HPA-Tyr conjugates.

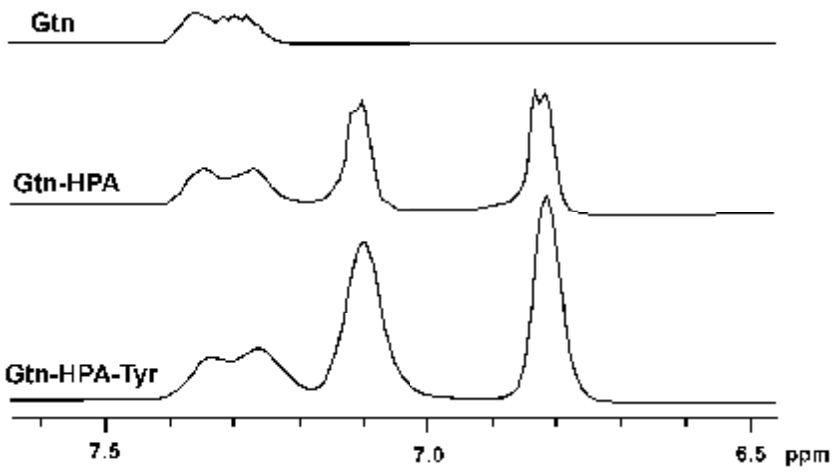

Figure 6-2. ^{1}H NMR spectra of Gtn, Gtn-HPA and Gtn-HPA-Tyr conjugates.

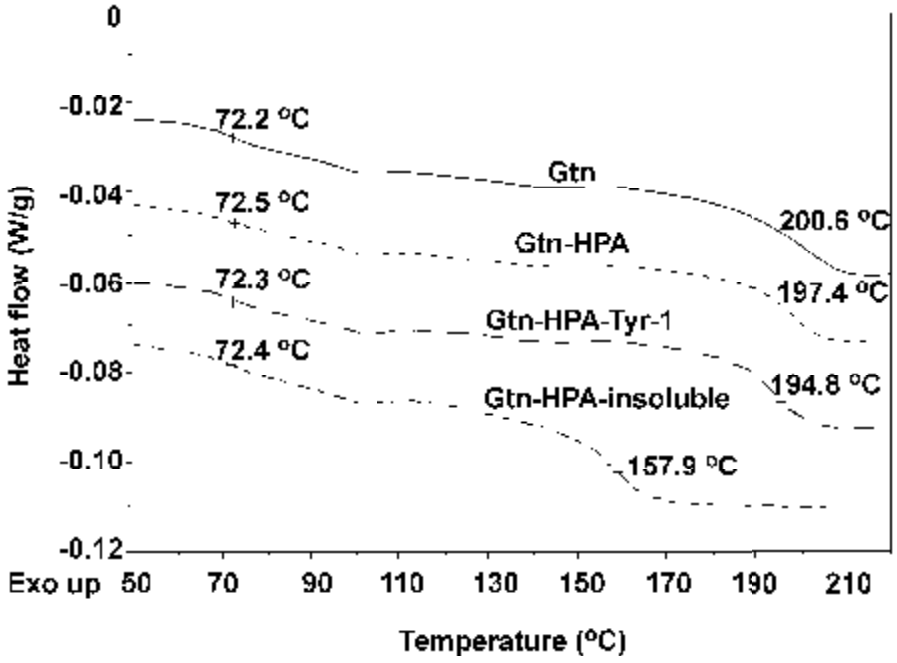

Figure 6-3. DSC thermograms of Gtn, Gtn-HPA, Gtn-HPA-Tyr and Gtn-insoluble conjugates.

6.3.2. Rheological measurement

As described in previous chapters, the hydrogel composed of Gtn-HPA conjugate was formed using the oxidative coupling of HPA moieties catalyzed by H_2O_2 and HRP. The storage modulus (G') of the Gtn-HPA hydrogels prepared by using 5 wt.% of Gtn-HPA conjugate was readily tuned from 600 to 8000 Pa by increasing H_2O_2 concentration. It peaked when 8.5 mM of H_2O_2 was used before a decline was observed with excessive amount of H_2O_2. In this study, the concentration of both Gtn-HPA and Gtn-HPA-Tyr conjugates was kept at 10 wt.% instead. The Gtn-HPA-Tyr hydrogel was formed using the oxidative coupling of both HPA and Tyr moieties catalyzed by H_2O_2 and HRP (Figure 6-4). The phenols were crosslinked through either a more common C-C linkage between the *ortho*-carbons of the aromatic ring or a C-O linkage between the *ortho*-carbon and the phenolic oxygen as discussed in section **2.3.3.**.

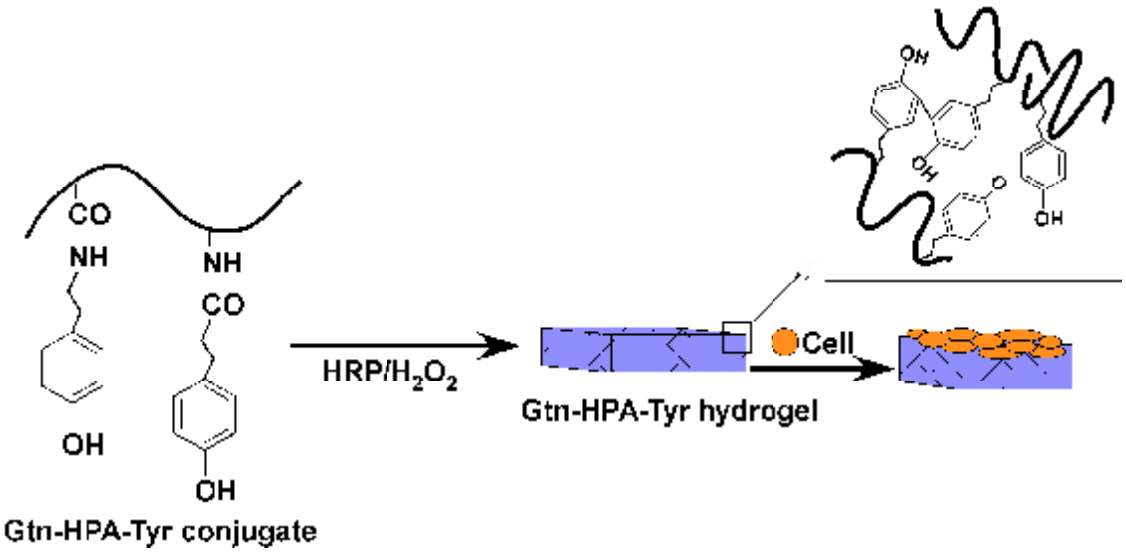

Figure 6-4. Schematic presentation of formation of Gtn-HPA-Tyr hydrogel by enzyme-catalyzed oxidation for 2D cell growth.

Figure 6-5 summarizes the rheological properties of Gtn-Phenol hydrogels formed with varied H_2O_2 concentrations. The same trend that the G' was significantly increased with the increase of the H_2O_2 concentration was found in both Gtn-HPA and Gtn-HPA-Tyr hydrogels (Figure 6-5a). The dependence of H_2O_2 concentration indicates that with more phenol moiety available in the system, more H_2O_2 were needed to maximize the crosslinking density. H_2O_2 decomposes to water after oxidizing HRP which in turn oxidizes the HPA. Thus, the percentage of phenol moieties that actually participated in the crosslinking reaction would depend on the amount of H_2O_2 available. The G' of Gtn-HPA hydrogel ranging from 998 ± 14 to 13556 ± 665 Pa was achieved when 10 wt.% of Gtn-HPA conjugate was used. In the previous chapter IV, the highest stiffness was found to be around 8000 Pa when 5 wt.% of Gtn-HPA conjugates was selected. In this study, we found the G' of Gtn-HPA hydrogel significantly increased to 14000 Pa when 10 wt.% of Gtn-HPA conjugate was utilized. It was also noted that higher amount of H_2O_2 was needed to achieve Gtn-HPA hydrogel with 14000 Pa in stiffness as the polymer concentration increased from 5 wt.% to 10 wt.%. It peaked when H_2O_2 concentration was set at 13 mM. The increase in G' achieved by using a higher concentration of Gtn-HPA conjugate (10 wt.%) indicates that a higher number of HPA moieties participated in the crosslinking reaction. As discussed in the section **6.1.**, an increase in the concentration of Gtn-HPA inevitably increased the viscosity of the solution. Sole increase in Gtn-HPA concentration may impose difficulties in handling especially in the process of injection for an injectable hydrogel system. Thus, the maximum Gtn-HPA concentration was limited to 10 wt.%.

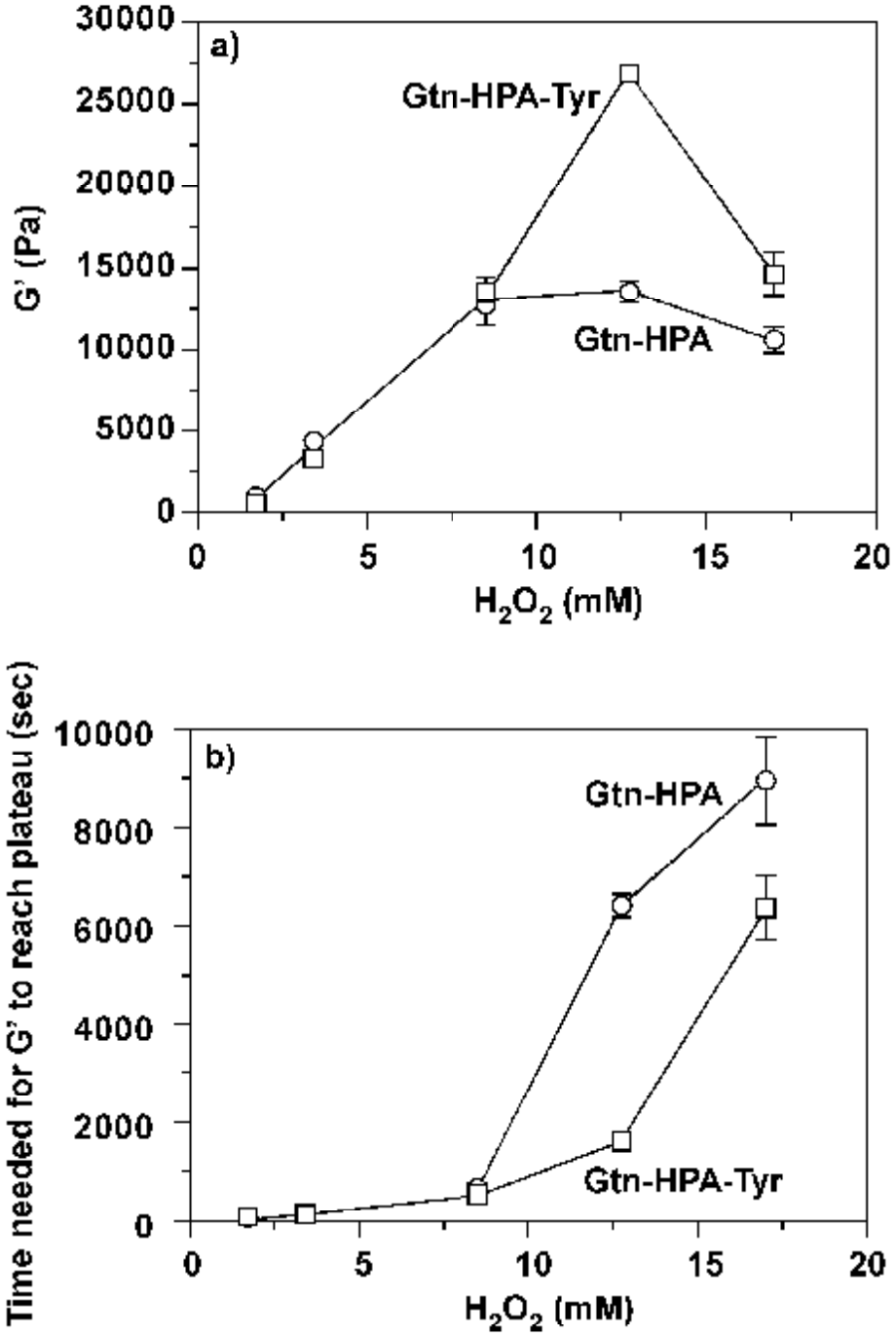

Figure 6-5. Effects of H_2O_2 on (a) the storage modulus G' and (b) the time needed for G' to reach plateau. HRP concentration is fixed at 0.15 units/ml. Results are shown as the average values ± standard deviation (n=3).

Indeed, when the same 10 wt.% polymer concentration was used, much higher G' (26830 ± 471 Pa) was achieved when 13 mM of H_2O_2 was utilized in the case of Gtn-HPA-Tyr hydrogel system. This high stiffness was not seen in the predecessor Gtn-HPA hydrogel system. The highest G' achieved in Gtn-HPA-Tyr hydrogel was almost double in comparison with Gtn-HPA hydrogel. Therefore, the increase in phenol content by additional Tyr moiety proved to be an effective way to attain an even greater extent in stiffness control. In addition, the time required for G' to reach a plateau increased with the increase of H_2O_2 concentration for both Gtn-HPA and Gtn-HPA-Tyr hydrogels (Figure 6-5b). This result is in a good agreement with our earlier reports of enzyme-mediated injectable hydrogel systems [89]. Interestingly, the time required for G' to reach a plateau of Gtn-HPA-Tyr hydrogel was lower compared to that of Gtn-HPA hydrogel when higher H_2O_2 concentration (13 and 17 mM) was utilized. This faster crosslinking achieved by Gtn-HPA-Tyr hydrogel is most likely attributed to an increase in the concentration of local phenol moiety as a result of higher phenol content in Gtn-HPA-Tyr hydrogel.

As discussed in Chapter IV, the hMSCs clearly demonstrated their capability to differentiate into specific lineages based on stiffness of the Gtn-HPA hydrogel. hMSCs on a softer Gtn-HPA hydrogel (600 Pa) expressed more neurogenic protein markers, while cells on a stiffer Gtn-HPA hydrogel (12800 Pa) showed a higher up-regulation of myogenic protein. With a much broader range in stiffness that Gtn-HPA-Tyr hydrogel system can offer, direction of osteogenic differentiation of hMSCs by the stiffness of

Gtn-HPA-Tyr hydrogel system would be possible when often much higher stiffness was required to direct such differentiation as reported previously [10].

Towards this end, the hydrogels of highest G' from Gtn-HPA and Gtn-HPA-Tyr systems were firstly selected and evaluated in the following *in vitro* cell culture studies. Their rheological properties were summarized in Table 6-1. From the measurements of gel point of hydrogels, the gel point was less than 3 mins, indicating both system offered efficient gel formation regardless of its stiffness. Rapid gel formation may minimize the uncontrolled diffusion of gel precursors and bioactive agents to the surrounding tissues when it comes to potential clinical application.

Table 6-1. Rheological properties of Gtn-HPA and Gtn-HPA-Tyr hydrogels used in the cell culture study[a]

Hydrogel	Conjugate (wt.%)	HRP (units/ml)	H_2O_2 (mM)	G' (Pa)	Gel point (sec)[b]	Time needed for G' to reach plateau (sec)
Gtn-HPA-13k	10	0.15	13	13557 ± 665	<180	6412 ± 235
Gtn-HPA-Tyr-20k	10	0.15	11	20078±576	<180	1345±45
Gtn-HPA-Tyr-26k	10	0.15	13	26830 ± 471	<180	1590 ± 29

[a] Measurement was taken with constant deformation of 1 % at 1Hz and 37°C (n=3). Results are shown as the values ± standard deviation.
[b] Gel point is defined as the time at which the crossover of storage modulus (G') and loss modulus (G'') occurred. Herein, it is used as an indicator of the rate of gelation.

6.3.3. Cell attachment

It is generally understood that cells growing on stiffer surfaces have a larger spreading area, more organized cytoskeletons and more stable focal adhesion although there is cell-to-cell variability. In our studies in previous chapters on Gtn-HPA hydrogel system, the same correlation was found between the hMSCs focal contact and the hydrogel stiffness across the range of stiffness studied (600 Pa to 12800 Pa).

In this study, Gtn-HPA-13k hydrogel (G' = 13500 Pa) and Gtn-HPA-Tyr-26k hydrogel (G' = 26800 Pa) were chosen to investigate the effect of further increase in hydrogel stiffness as a result of further conjugation of Tyr moieties on the cell attachment and spreading. The number of adherent HFF-1 cell increased over incubation time. After 4 h incubation, the vast majority of HFF-1 was attached to the hydrogel surfaces, with the percentage of adhered cells similar to that on the culture plate as shown in Figure 6-6a. Within the range of hydrogel stiffness studied in this report, the effect of further increase in hydrogel stiffness on the course of cell attachment and its focal contact was not significantly different in a comparison with that found in previous study using hydrogels with stiffness ranging from 600 Pa to 8000 Pa. No significant difference was observed in time course cell attachment and its focal contact between the two stiff hydrogel surfaces. The cells were found to be tightly adherent onto both hydrogel surfaces with organized structural arrangement of F-actin and focal contact (Figure 6-6b), indicating that the further conjugation of Tyr moiety to Gtn-HPA conjugate did not affect cell attachment behaviors. After 1 week , the HFF-1 on both surfaces attained confluence indicating the adhesion of the cells is strong and stable enough to induce steady cell growth.

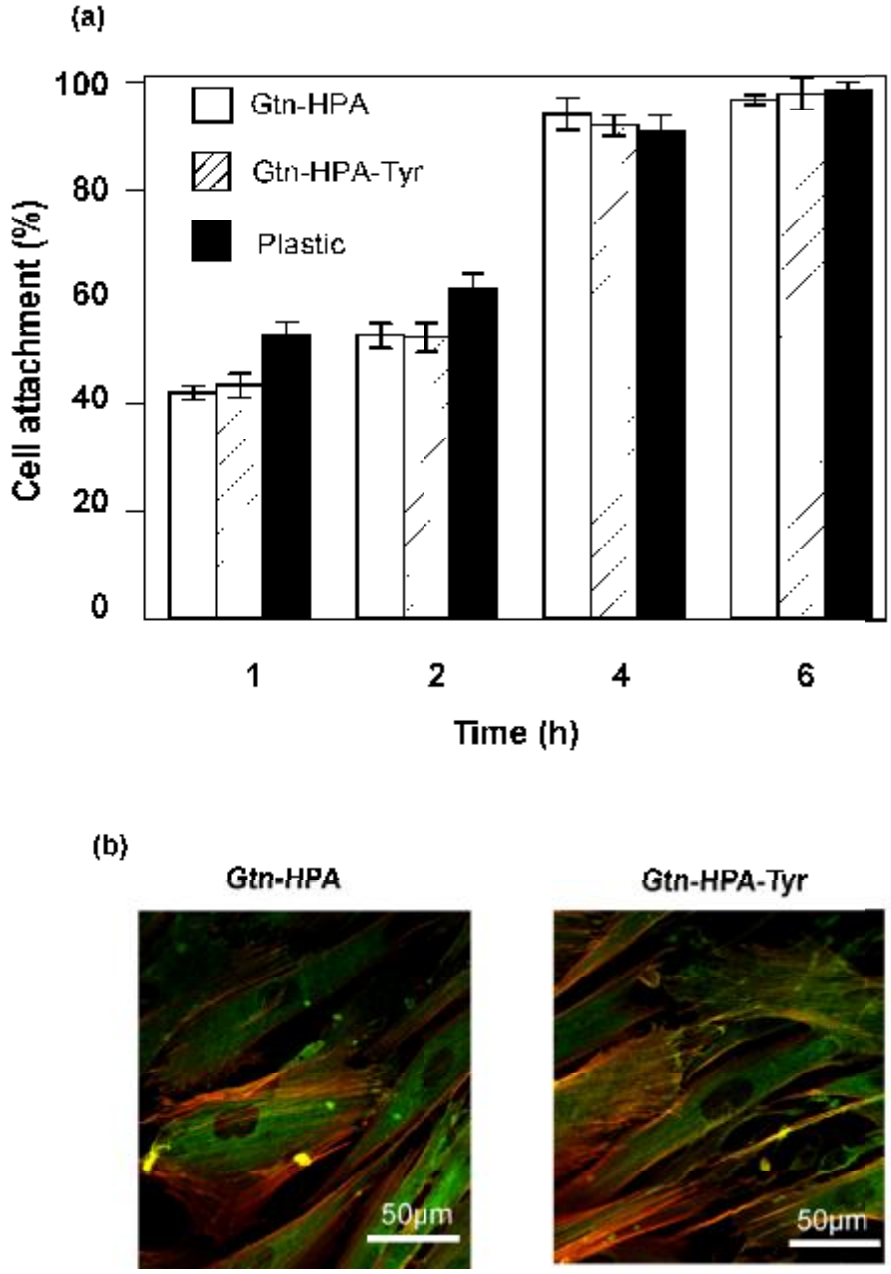

Figure 6-6. HFF-1 (a) attachment and (b) its confocal fluorescence microscopy of focal adhesion and actin cytoskeleton on the surface of Gtn-HPA and Gtn-HPA-Tyr hydrogels.

This result suggested that when hydrogel stiffness was above 8k Pa, fibroblast became less responsive to further increase of the stiffness. The cells exerted firm adhesion to the substrate above this threshold stiffness of 8k Pa with not much changes in focal contact behavior when stiffness was further increased. Thus, the changes in cell morphology as a result of the difference in focal contact were prominent in consequently regulating cell proliferation.

6.3.4. Stimulation of osteogenic differentiation of hMSCs

Although not much difference was observed on the cell attachment and focal adhesion when they were cultured on the Gtn-phenol hydrogels with G' ranging from 13500 to 26000 Pa, we observed a significant difference of relative gene expressions from hMSCs cultured on hydrogels of different stiffness (Figure 6-7). Gtn-HPA-Tyr-20k (G' = 20078 Pa) with intermediate stiffness between 13500 and 26000 Pa was also included in this study to determine threshold stiffness for osteogenic differentiation. A significant increase in expressions of runt-related transcription factor 2 (RUNX2) and osteocalcin (OC), two commonly studied osteogenic markers, was detected on the cells cultured on the hydrogels with G' higher than 20000 Pa in real-time PCR analysis in comparison to those cultured on the Gtn-HPA hydrogel (G'=13000 Pa). The level of upregulation of such gene expresssions was directly correlated to the hydrogel stiffness. The Gtn-HPA-Tyr-26k showed a 10 fold and 7 fold increase in the OC and RUNX2 gene expressions respectively, while Gtn-HPA-Tyr-20k showed a 3 fold increase in both genes. It suggests that the hydrogel with stiffness higher than 20000 Pa was more likely to stimulate the osteogenic differentiation, although some upregulation of myogenic transcription factor 1

(MYOD1), a well-studied myogenic differentiation factor, was also found in cells cultured on Gtn-HPA-20k. For the neural transcription factor, Gtn-HPA-Tyr-26k showed a significant down-regulation of enolase2 (ENO2).

The above observation has again validated the role of substrate stiffness in directing hMSC differentiation in the absence of other biochemical factors. The new Gtn-phenol (Gtn-HPA-Tyr) hydrogel system has allowed us to make observations on osteogenic differentiation of hMSCs. Such differentiation was not achieved with the predecessor Gtn-HPA hydrogel system of the same conjugate concentration. This was most likely due to the lack of the required stiffness for such differentiation. Our newly improved Gtn-HPA-Tyr hydrogel could serve as an appropriate platform to achieve the full benefits of stem cell differentiation for tissue regeneration, in the light of current research that directs stem cell differentiation solely by substrate stiffness.

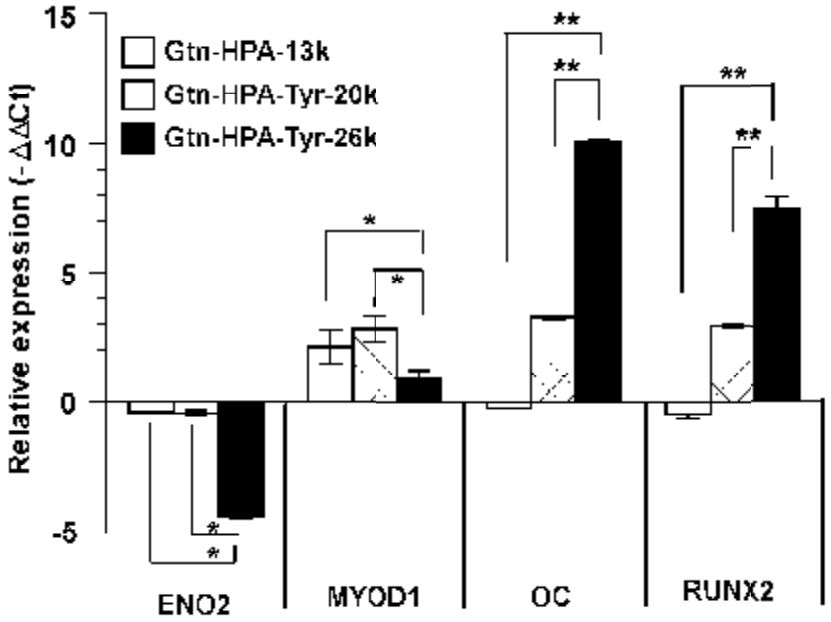

Figure 6-7. Gene expression of selected genes in hMSCs after 3 weeks of culture on Gtn-phenol hydrogels of varied stiffness. Undifferentiated hMSCs were used as reference sample and all results were normalized with respect to the expression of β-actin levels (n=3, mean ± standard deviation). *P<0.01.

6.3.5. Enzymatic degradation of Gtn-HPA-Tyr hydrogel

Enzymatic degradability of Gtn-HPA-Tyr hydrogels was examined in the presence of type-I collagenase. Type-1 collagenase, a member of the matrix metalloproteases (MMP) family, which was found to degrade the extracellular matrix, leading to cell migration and growth in the body [145]. Accordingly, they can digest proteolysis-sensitive hydrogels [15].

Figure 6-8 shows enzymatic degradation of Gtn-HPA-Tyr hydrogels with different stiffness. It is known that the enzymatic degradability of biopolymers is lowered by conjugation to the polymers [179]. Also, the enzymatic degradability of hydrogel could be diminished by increase of hydrogel stiffness. Such low hydrogel degradability is not ideal as a scaffold for tissue engineering application. Therefore, it is crucial to assess the degradability of hydrogel especially if the stiffness of hydrogel was altered. All of Gtn-HPA-Tyr hydrogels could be completely degraded by type-I collagenase although the phenol content and stiffness was higher compared to Gtn-HPA hydrogel system. It was also found that the hydrogel with higher stiffness degraded slower compared to the ones with lower stiffness. This result suggests that the enzymatic degradability of Gtn-HPA hydrogels can be well-controlled by hydrogel stiffness, and the Gtn-HPA-Tyr hydrogels would be useful for various biomedical applications.

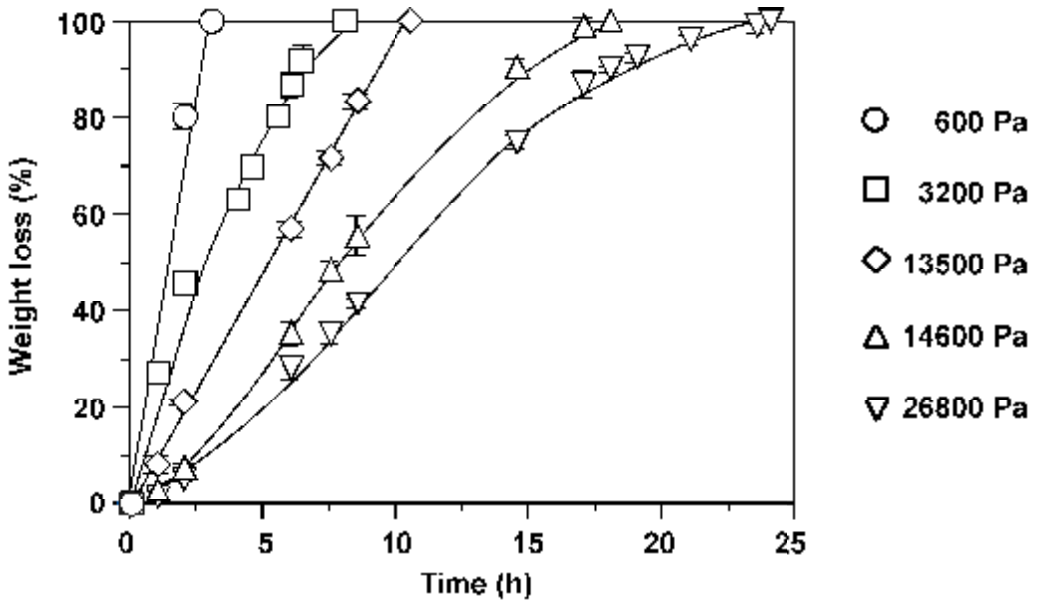

Figure 6-8. Enzymatic degradation of Gtn-HPA-Tyr hydrogels with different stiffness; 600 (™), 3200 (£), 13500 (¯), 14600 (r) and 26800 (s). The experiment was carried out in the presence of 6.7 units/ml of type I collagenase at 37°C. Results are shown as the average values ± standard deviation (n=3).

6.3.6. Cytotoxicity of fragmented Gtn-Phenol conjugates

Cytotoxicity is always a concern when a material comes into contact with the human body. This material should not liberate any agent that may be toxic or have an adverse effect on the body. *In vitro* cytotoxicity test of cell cultures is a useful technique for detecting the presence of such agents, as it offers a rapid and sensitive screening method that can be performed in the laboratory. Assessment of the injectable and biodegradable Gtn-Phenol hydrogel system for tissue engineering application was performed with the cytotoxicity study.

Once again, the hydrogels with highest G', obtained from both Gtn-HPA and Gtn-HPA-Tyr conjugates (10 wt.%) were selected in this study to illustrate the potential cytotoxicity of the fragmented products. They were prepared by enzymatic degradation of Gtn-Phenol hydrogels in an attempt to simulate the clinically relevant conditions when degradation occurred upon implantation in the body. The cytotoxicity of the degraded product from Gtn-Phenol hydrogel was evaluated by incubating it with the cells over a period of 24 to 72 h at 37 °C. At 24 h, the viability of HFF-1 was 95 and 80 % when degraded product of 0.25 and 0.6 wt.% was utilized, respectively (Figure 6-9). At both concentrations, the cell viability was unchanged after 72 h incubation. Type I collagenase at this test concentration did not have adverse effect on cell viability. In addition, we observed that a much softer Gtn-Phenol hydrogel (G'=300 Pa) degraded within one hour under the same *in vitro* enzymatic degradation study, nevertheless, it remained under subcutaneous layer without any visible inflammatory or irritative observation around the site of implantation for more than a month in our preliminary *in vivo* study. The result suggests the degradation occurring *in vivo* was much slower than that in the condition

used in this present *in vitro* study. Moreover, the degradation of Gtn-HPA-Tyr hydrogel was highly stiffness-dependent. The collective results from these experiments assured that Gtn-Phenol hydrogels and their degraded products were noncytotoxic. These results indicate that the Gtn-HPA-Tyr hydrogels were capable of providing biologically compatible supports for potential biomedical application.

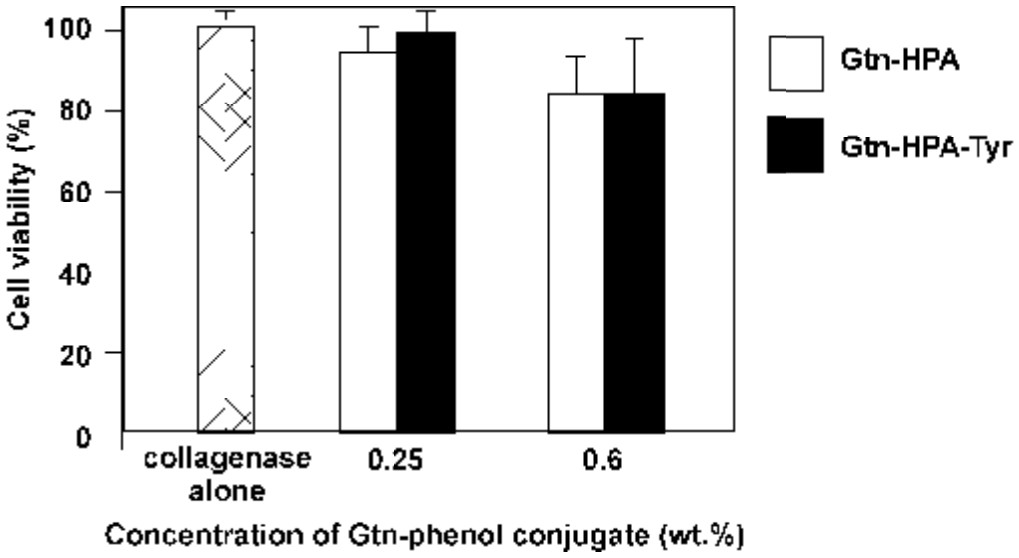

Figure 6-9. Cytotoxicity study of fragmented Gtn-Phenol hydrogels. The fragmented products were obtained by the enzymatic degradation of hydrogels in the presence of 6.7 units/ml of type I collagenase at 37°C. Results are shown as the average values ± standard deviation (n=3).

6.4. Conclusion

Gtn-HPA-Tyr conjugate was successfully synthesized by the further conjugation of Tyr to the Gtn-HPA conjugate. The phenol content of the Gtn-HPA-Tyr conjugate was enhanced when compared to that of the Gtn-HPA conjugate. We successfully formulated the Gtn-HPA-Tyr hydrogels with a broader range of stiffness by using an enzyme-mediated oxidation reaction. A significant high level of gene expressions of OC and RUNX2, which are closely associated with osteogenic differentiation of hMSCs, was observed in the cells when they were cultured on the hydrogel with stiffness higher than 20000 Pa. The level of such expressions was directly correlated to the hydrogel stiffness. This observation was only made possible in this newly improved Gtn-HPA-Tyr hydrogel system. Such differentiation was not achieved using the predecessor Gtn-HPA hydrogel system with the same conjugate concentration. Furthermore, the *in vivo* degradation of Gtn-phenol hydrogels was also stiffness-dependent and the hydrogels also did not show prominent inflammatory response *in vivo*. Thus, our new design of an injectable hydrogel system with tunable mechanical strength and rapid gelation rate would be beneficial to repair bone defects. In the light of current research on the role of substrate stiffness in many physiological processes, our hydrogel system could serve as an appropriate platform to study the effect of substrate stiffness for tissue regeneration on a broad range of various cell functions.

Chapter VII

Conclusion

7. Conclusion

The development of an injectable and biodegradable hydrogel system with tunable mechanical properties for tissue engineering application was successfully achieved. This newly designed Gtn-Phenol hydrogels were formed by the oxidative coupling reaction of phenol moiety in the presence of H_2O_2 and HRP. The stiffness of the Gtn-HPA hydrogel could be easily tuned by the H_2O_2 concentration without changing the concentration of polymer precursor solution. This decoupling of concentration of polymer and its hydrogel stiffness allowed the study of stiffness on various cell functions independently with minimum variation in other parameters associated with polymer itself. The stiffness of the hydrogel and the gelation rate were independently controlled by the H_2O_2 concentration and HRP concentration, respectively. This unique independent tuning has not been seen in other existing injectable hydrogel systems where the gelation rate is directly correlated to the stiffness.

Gtn-HPA conjugate was successfully synthesized by a general carbodiimide/active ester-mediated coupling reaction in distilled water. The synthesis of Gtn-HPA conjugate could be easily scaled up without compromising the phenol content in it. The synthesis of Gtn-HPA conjugates were proved to be simple, cost effective and easy to scale-up with high batch-to-batch reproducibility.

A wide range of stiffness of Gtn-HPA hydrogel was achieved with an efficient gelation rate. The Gtn-HPA hydrogels supported cell attachment directly without additional coating with adhesive ligands. In the case of hMSC, its cell adhesion,

morphology, migration, proliferation and differentiation on the surfaces of Gtn-HPA hydrogels were found to be stiffness-dependent. It was shown that hMSCs on stiffer hydrogels had a higher proliferation rate, larger spreading area, more organized cytoskeletons, more stable focal adhesions and faster migration rate. The stimulation of both neurogenic and myogenic differentiation of hMSCs on Gtn-HPA hydrogels exhibited a stiffness-dependence without the additional use of any biochemical signal. Neurogenesis of hMSCs was observed when the hydrogel stiffness was in the range of 600 to 2500 Pa. The cells on a softer hydrogel (600 Pa) expressed more neurogenic protein markers. The myogenesis of hMSCs was achieved instead when the hydrogel stiffness is greater than 8000 Pa. It would be a useful hydrogel scaffold system for stem-cell based cell therapy when hMSCs cultured on Gtn-HPA hydrogels with varied stiffness could be differentiated to different phenotypes and the hydrogel could be easily degraded after the differentiation of cells given its biodegradability.

Besides being an excellent platform to study the effect of stiffness on the various cell functions of hMSCs on the surface (2D), the *in situ* forming ability of Gtn-HPA hydrogels system also provided a simple and effective mean to study the cell functions in 3D environment due to the ease of encapsulation of cells and the excellent cell adhesiveness. It was found that the proliferation rate of 3D hMSC cultured in Gtn-HPA hydrogels was controlled by the hydrogel stiffness. hMSC neurogenesis in 3D was clearly demonstrated using this hydrogel system, and the degree of neurogenesis was affected by the stiffness of hydrogel without the use of any biochemical signal. With its biocompatibility and biodegradability, the Gtn-HPA hydrogel offers a promising system for regenerative applications of stem cells in tissue engineering and has the potential to

further stem cell-based *in vivo* therapies. In the future, injectable Gtn-HPA hydrogels with tunable mechanical properties for 3D cell culture and differentiation would be an important strategic tool to treat neurological disorders or brain injuries.

The study on HFF-1 validated the strong effect of stiffness on cell responses. In the 2D studies, the fibroblasts exhibited a higher proliferation rate, more organized cytoskeletons and focal adhesion when the stiffness of the hydrogel where they were grown on was increased. However, the cells cultured inside the hydrogel remained non-proliferative for 12 days before a stiffness-dependent proliferation profile was shown. An increase in the stiffness of hydrogel adversely affected the proliferation rate unlike the finding from 2D studies. The marked difference with respect to the fibroblast proliferation underlines the need of considering the effects of stiffness in the design of such materials as wound dressings in order to accelerate the wound healing process and improve the clinical outcome of it. With its *in situ* forming ability, efficient gelling mechanism, the ease of formulation, biocompatibility, biodegradability and cost effectiveness, the Gtn-HPA hydrogel offers a great potential as wound dressing material.

On the basis of the favorable properties of Gtn-HPA hydrogels system outlined above and in light of the role of stiffness of substrate on various cell functions, Gtn-HPA-Tyr system with further increase in phenol content was developed. The phenol content of Gtn-HPA-Tyr conjugate was significantly enhanced from 4.44×10^{-7} to 7.11×10^{-7} after the additional Tyr conjugation to the previous Gtn-HPA conjugate. The range of stiffness control in the case of Gtn-HPA-Tyr hydrogel was broadened to up to 26800 Pa which was not achieved from its predecessor Gtn-HPA hydrogel system. A significant high level of gene of OC and RUNX2, which are closely associated with osteogenic

differentiation of hMSCs, was observed in the cells when they were cultured on the hydrogel with stiffness higher than 20000 Pa. The level of such expressions was directly correlated to the hydrogel stiffness. This observation was only made possible in this newly improved Gtn-HPA-Tyr hydrogel system. Such differentiation was not achieved using the predecessor Gtn-HPA hydrogel system with the same conjugate concentration. The Gtn-HPA-Tyr hydrogels completely retained the favorable properties of the Gtn-HPA hydrogel including the excellent support for cell attachment and cell proliferation without the need of additional coating, biocompatibility and biodegradability. The fragmented products of Gtn-HPA-Tyr with higher amount of phenol contents remained non-toxic to the HFF-1 cells. It proved that Gtn-HPA-Tyr hydrogels offer stiffness control in a broader range and provide biologically compatible supports for potential biomedical application. In future, our Gtn-HPA-Tyr hydrogel could also serve as an appropriate platform to achieve the full benefits of stem cell differentiation for tissue regeneration in light of foregoing research on directing stem cell differentiation solely by substrate stiffness.

In our laboratory, we have initiated studies to further evaluate the stimulation of osteogenic differentiation of hMSCs using Gtn-HPA-Tyr hydrogel with much higher stiffness in the respect of protein expression and calcium deposit as a result of osteogenic differentiation. Porous hydrogels with high stiffness were also attempted to further study the differentiation of hMSCs other than neruogenesis of them in soft hydrogel in 3D setting. On the other hand, the study on the effect of stiffness on functional responses of cells is further expanded to other cell types including cardiomyocyte and chondrocyte.

Chapter VIII

References

8. References

1. Langer R, Vacanti JP. Tissue Engineering. Science 1993;260:920-926.

2. Drury JL, Mooney DJ. Hydrogels for tissue engineering: scaffold design variables and applications. Biomaterials 2003;24(24):4337-4351.

3. Ottenbrite RM, Park K, Okano T, editors. Biomedical Applications of Hydrogels handbook. New Yok: Springer, 2010.

4. Domb A, Mikos AG. Matrices and scaffolds for drug delivery in tissue engineering. Adv Drug Deliv Rev 2007;59(4-5):185-186.

5. Hoffman AS. Hydrogels for biomedical applications. Adv Drug Deliv Rev 2002;54(1):3-12.

6. Tessmar JK, Gopferich AM. Matrices and scaffolds for protein delivery in tissue engineering. Adv Drug Deliv Rev 2007;59(4-5):274-291.

7. Kidane A, Szabocsik JM, Park K. Accelerated study on lysozyme deposition on poly(HEMA) contact lenses. Biomaterials 1998;19(22):2051-2055.

8. Oxley HR, Corkhill PH, Fitton JH, Tighe BJ. Macroporous hydrogels for biomedical applications - methodology and morphology. Biomaterials 1993;14(14):1064-1072.

9. Lu SX, Anseth KS. Photopolymerization of multilaminated poly(HEMA) hydrogels for controlled release. Journal of Controlled Release 1999;57(3):291-300.

10. Engler AJ, Sen S, Sweeney HL, Discher DE. Matrix elasticity directs stem cell lineage specification. Cell 2006;126(4):677-689.

11. Stile RA, Burghardt WR, Healy KE. Synthesis and characterization of injectable poly(N-isopropylacrylamide)-based hydrogels that support tissue formation in vitro. Macromolecules 1999;32(22):7370-7379.

12. Brazel CS, Peppas NA. Pulsatile local delivery of thrombolytic and antithrombotic agents using poly(N-isopropylacrylamide-co-methacrylic acid) hydrogels. Journal of Controlled Release 1996;39(1):57-64.

13. Serres A, Baudys M, Kim SW. Temperature and pH-sensitive polymers for human calcitonin delivery. Pharm Res 1996;13(2):196-201.

14. Hubbell JA. Materials as morphogenetic guides in tissue engineering. Curr Opin Biotechnol 2003;14(5):551-558.

15. Lutolf MP, Lauer-Fields JL, Schmoekel HG, Metters AT, Weber FE, Fields GB, et al. Synthetic matrix metalloproteinase-sensitive hydrogels for the conduction of tissue regeneration: Engineering cell-invasion characteristics. Proc Natl Acad Sci U S A 2003;100(9):5413-5418.

16. Silva EA, Mooney DJ. Synthetic extracellular matrices for tissue engineering and regeneration. Current Topics in Developmental Biology , Vol 64. San Diego: Elsevier Academic Press Inc, 2004. p. 181-205.

17. West JL, Hubbell JA. Polymeric biomaterials with degradation sites for proteases involved in cell migration. Macromolecules 1999;32(1):241-244.

18. Burczak K, Gamian E, Kochman A. Long-term in vivo performance and biocompatibility of poly(vinyl alcohol) hydrogel macrocapsules for hybrid-type artificial pancreas. Biomaterials 1996;17(24):2351-2356.

19. Taguchi T, Kishida A, Akashi M. Apatite formation on/in hydrogel matrices using an alternate soaking process (III): Effect of physico-chemical factors on apatite formation on/in poly(vinyl alcohol) hydrogel matrices. J Biomater Sci-Polym Ed 1999;10(8):795-804.

20. Kawase M, Miura N, Kurikawa N, Masuda K, Higashiyama S, Yagi K, et al. Immobilization of tripeptide growth factor glycyl-L-histidyl-L-lysine on poly(vinylalcohol)-quarternized stilbazol (PVA-SbQ) and its use as a ligand for hepatocyte attachment. Biol Pharmacol Bull 1999;22(9):999-1001.

21. Lee BH, Song SC. Synthesis and characterization of biodegradable thermosensitive poly(organophosphazene) gels. Macromolecules 2004;37(12):4533-4537.

22. Lee BH, Lee YM, Sohn YS, Song SC. A thermosensitive poly(organophosphazene) gel. Macromolecules 2002;35(10):3876-3879.

23. Petka WA, Harden JL, McGrath KP, Wirtz D, Tirrell DA. Reversible hydrogels from self-assembling artificial proteins. Science 1998;281(5375):389-392.

24. Cascone MG, Barbani N, Cristallini C, Giusti P, Ciardelli G, Lazzeri L. Bioartificial polymeric materials based on polysaccharides. J Biomater Sci-Polym Ed 2001;12(3):267-281.

25. Puppi D, Chiellini F, Piras AM, Chiellini E. Polymeric materials for bone and cartilage repair. Prog Polym Sci 2010;35(4):403-440.

26. Yadav AK, Mishra P, Agrawal GP. An insight on hyaluronic acid in drug targeting and drug delivery. J Drug Target 2008;16(2):91-107.

27. Vercruysse KP, Prestwich GD. Hyaluronate derivatives in drug delivery. Crit Rev Ther Drug Carr Syst 1998;15(5):513-555.

28. Kurisawa M, Lee F, Wang LS, Chung JE. Injectable enzymatically crosslinked hydrogel system with independent tuning of mechanical strength and gelation rate for drug delivery and tissue engineering. J Mater Chem 2010;20(26):5371-5375.

29. Shu XZ, Liu YC, Palumbo FS, Lu Y, Prestwich GD. In situ crosslinkable hyaluronan hydrogels for tissue engineering. Biomaterials 2004;25(7-8):1339-1348.

30. Shu XZ, Liu YC, Luo Y, Roberts MC, Prestwich GD. Disulfide cross-linked hyaluronan hydrogels. Biomacromolecules 2002;3(6):1304-1311.

31. Choi YS, Hong SR, Lee YM, Song KW, Park MH, Nam YS. Study on gelatin-containing artificial skin: I. Preparation and characteristics of novel gelatin-alginate sponge. Biomaterials 1999;20(5):409-417.

32. Duranti F, Salti G, Bovani B, Calandra M, Rosati ML. Injectable hyaluronic acid gel for soft tissue augmentation - A clinical and histological study. Dermatol Surg 1998;24(12):1317-1325.

33. Radomsky M, Swain L, Aufdemorte T, Fox C, Poser J. Local administration of basic fibroblast growth factor in a hyaluronic acid gel accelerates fracture healing. J Bone Miner Res 1996;11:M667-M667.

34. Choi YS, Hong SR, Lee YM, Song KW, Park MH, Nam YS. Studies on gelatin-containing artificial skin: II. Preparation and characterization of cross-linked gelatin-hyaluronate sponge. J Biomed Mater Res 1999;48(5):631-639.

35. Ghosh K, Ren X, Shu XZ, Prestwich GD. Fibronectin functional domains coupled to hyaluronan stimulate adult human dermal fibroblast responses critical for wound healing. Tissue Engineering 2006;12(601-613):601.

36. Ramamurthi A, Vesely I. Smooth muscle cell adhesion on crosslinked hyaluronan gels. J Biomed Mater Res 2002;60:195-205.

37. Smidsrod O, Skjakbraek G. Alginate as immobilization matrix for cells. Trends Biotechnol 1990;8(3):71-78.

38. Lee KY, Mooney DJ. Hydrogels for tissue engineering. Chemical Reviews 2001;101(7):1869-1879.

39. Klock G, Pfeffermann A, Ryser C, Grohn P, Kuttler B, Hahn HJ, et al. Biocompatibility of mannuronic acid-rich alginates. Biomaterials 1997;18(10):707-713.

40. Gombotz WR, Wee SF. Protein release from alginate matrices. Adv Drug Deliv Rev 1998;31(3):267-285.

41. Gregory KE, Marsden ME, Anderson-MacKenzie J, Bard JBL, Bruckner P, Farjanel J, et al. Abnormal collagen assembly, though normal phenotype, in alginate bead cultures of chick embryo chondrocytes. Exp Cell Res 1999;246(1):98-107.

42. Joly A, Desjardins JF, Fremond B, Desille M, Campion JP, Malledant Y, et al. Survival, proliferation, and functions of porcine hepatocytes encapsulated in coated alginate beads: A step toward a reliable bioartificial liver. Transplantation 1997;63(6):795-803.

43. Sakai S, Kawakami K. Synthesis and characterization of both ionically and enzymatically cross-linkable alginate. Acta Biomater 2007;3(4):495-501.

44. Balakrishnan B, Mohanty M, Umashankar PR, Jayakrishnan A. Evaluation of an in situ forming hydrogel wound dressing based on oxidized alginate and gelatin. Biomaterials 2005;26(32):6335-6342.

45. Kim IY, Seo SJ, Moon HS, Yoo MK, Park IY, Kim BC, et al. Chitosan and its derivatives for tissue engineering applications. Biotechnol Adv 2008;26(1):1-21.

46. Singh DK, Ray AR. Biomedical applications of chitin, chitosan, and their derivatives. J Macromol Sci-Rev Macromol Chem Phys 2000;C40(1):69-83.

47. Bhattarai N, Ramay HR, Gunn J, Matsen FA, Zhang MQ. PEG-grafted chitosan as an injectable thermosensitive hydrogel for sustained protein release. Journal of Controlled Release 2005;103(3):609-624.

48. Ono K, Saito Y, Yura H, Ishikawa K, Kurita A, Akaike T, et al. Photocrosslinkable chitosan as a biological adhesive. J Biomed Mater Res 2000;49(2):289-295.

49. Kim TH, Nah JW, Cho MH, Park TG, Cho CS. Receptor-mediated gene delivery into antigen presenting cells using mannosylated chitosan/DNA nanoparticles. J Nanosci Nanotechnol 2006;6(9-10):2796-2803.

50. Li XB, Tushima Y, Morimoto M, Saimoto H, Okamoto Y, Minami S, et al. Biological activity of chitosan-sugar hybrids: Specific interaction with lectin. Polym Adv Technol 2000;11(4):176-179.

51. Maia J, Ferreira L, Carvalho R, Ramos MA, Gil MH. Synthesis and characterization of new injectable and degradable dextran-based hydrogels. Polymer 2005;46(23):9604-9614.

52. Jin R, Hiemstra C, Zhong ZY, Feijen J. Enzyme-mediated fast in situ formation of hydrogels from dextran-tyramine conjugates. Biomaterials 2007;28(18):2791-2800.

53. Hiemstra C, van der Aa LJ, Zhong ZY, Dijkstra PJ, Feijen J. Rapidly in situ-forming degradable hydrogels from dextran thiols through michael addition. Biomacromolecules 2007;8(5):1548-1556.

54. Van Tomme SR, Hennink WE. Biodegradable dextran hydrogels for protein delivery applications. Expert Rev Med Devices 2007;4(2):147-164.

55. Coviello T, Matricardi P, Marianecci C, Alhaique F. Polysaccharide hydrogels for modified release formulations. Journal of Controlled Release 2007;119(1):5-24.

56. Levesque SG, Shoichet MS. Synthesis of cell-adhesive dextran hydrogels and macroporous scaffolds. Biomaterials 2006;27(30):5277-5285.

57. Arnott S, Fulmer A, Scott WE, Dea ICM, Moorhouse R, Rees DA. Agarose double helix and its function in agarose-gel structure. J Mol Biol 1974;90(2):269-&.

58. Rees DA. Polysaccharide gels-molecular view. Chem Ind 1972(16):630-&.

59. Putnam AJ, Mooney DJ. Tissue engineering using synthetic extracellular matrices. Nat Med 1996;2(7):824-826.

60. Chevallay B, Herbage D. Collagen-based biomaterials as 3D scaffold for cell cultures: applications for tissue engineering and gene therapy. Med Biol Eng Comput 2000;38(2):211-218.

61. Lee CH, Singla A, Lee Y. Biomedical applications of collagen. Int J Pharm 2001;221(1-2):1-22.

62. Takahashi Y, Yamamoto M, Tabata Y. Enhanced osteoinduction by controlled release of bone morphobenetic protein-2 form biodegradable sponge composed of gelatin and b-tricalcium phosphate. Biomaterials 2005;26:4856-4865.

63. Rault I, Frei V, Herbage D, AbdulMalak N, Huc A. Evaluation of different chemical methods for cross-linking collagen gel, films and sponges. J Mater Sci-Mater Med 1996;7(4):215-221.

64. Sung HW, Hsu HL, Shih CC, Lin DS. Cross-linking characteristics of biological tissues fixed with monofunctional or multifunctional epoxy compounds. Biomaterials 1996;17(14):1405-1410.

65. Damink L, Dijkstra PJ, Vanluyn MJA, Vanwachem PB, Nieuwenhuis P, Feijen J. Cross-linking of dermal sheep collagen using hexamethylene diisocyanate. J Mater Sci-Mater Med 1995;6(7):429-434.

66. Wissink MJB, Beernink R, Pieper JS, Poot AA, Engbers GHM, Beugeling T, et al. Immobilization of heparin to EDC/NHS-crosslinked collagen. Characterization and in vitro evaluation. Biomaterials 2001;22(2):151-163.

67. Tabata Y, Ikada Y. Protein release from gelatin matrices. Adv Drug Deliv Rev 1998;31(3):287-301.

68. Kuijpers AJ, Engbers GHM, Feijen J, De Smedt SC, Meyvis TKL, Demeester J, et al. Characterization of the network structure of carbodiimide cross-linked gelatin gels. Macromolecules 1999;32(10):3325-3333.

69. Malafaya PB, Silva GA, Reis RL. Natural-origin polymers as carriers and scaffolds for biomolecules and cell delivery in tissue engineering applications. Adv Drug Deliv Rev 2007;59(4-5):207-233.

70. Park H, Temenoff JS, Tabata Y, Caplan AI, Mikos AG. Injectable biodegradable hydrogel composites for rabbit marrow mesenchymal stem cell and growth factor delivery for cartilage tissue engineering. Biomaterials 2007;28(21):3217-3227.

71. Young S, Wong M, Tabata Y, Mikos AG. Gelatin as a delivery vehicle for the controlled release of bioactive molecules. Journal of Controlled Release 2005;109(1-3):256-274.

72. Le Nihouannen D, Le Guehennec L, Rouillon T, Pilet P, Bilban M, Layrolle P, et al. Micro-architecture of calcium phosphate granules and fibrin glue composites for bone tissue engineering. Biomaterials 2006;27(13):2716-2722.

73. Fogelson AL, Keener JP. Toward an understanding of fibrin branching structure. Phys Rev E 2010;81(5):051922.

74. Wolberg AS. Thrombin generation and fibrin clot structure
Blood Review 2007;21:131-142.

75. Ye Q, Zund G, Benedikt P, Jockenhoevel S, Hoerstrup SP, Sakyama S, et al. Fibrin gel as a three dimensional matrix in cardiovascular tissue engineering. Eur J Cardio-Thorac Surg 2000;17(5):587-591.

76. Dikovsky D, Bianco-Peled H, Seliktar D. The effect of structural alterations of PEG-fibrinogen hydrogel scaffolds on 3-D cellular morphology and cellular migration. Biomaterials 2006;27(8):1496-1506.

77. Hennink WE, van Nostrum CF. Novel crosslinking methods to design hydrogels. Adv Drug Deliv Rev 2002;54(1):13-36.

78. Tsuji H. Poly(lactide) stereocomplexes: Formation, structure, properties, degradation, and applications. Macromol Biosci 2005;5(7):569-597.

79. Lim DW, Choi SH, Park TG. A new class of biodegradable hydrogels stereocomplexed by enantiomeric oligo(lactide) side chains of poly(HEMA-g-OLA)s. Macromol Rapid Commun 2000;21(8):464-471.

80. Jeong B, Bae YH, Lee DS, Kim SW. Biodegradable block copolymers as injectable drug-delivery systems. Nature 1997;388(6645):860-862.

81. Khattak SF, Bhatia SR, Roberts SC. Pluronic F127 as a cell encapsulation material: Utilization of membrane-stabilizing agents. Tissue Eng 2005;11(5-6):974-983.

82. Radu-Wu LC, Yang J, Wu K, Kopecek J. Self-Assembled Hydrogels from Poly[N-(2-hydroxypropyl)methacrylamide] Grafted with beta-Sheet Peptides. Biomacromolecules 2009;10(8):2319-2327.

83. Wang C, Stewart RJ, Kopecek J. Hybrid hydrogels assembled from synthetic polymers and coiled-coil protein domains. Nature 1999;397(6718):417-420.

84. Kretschmann O, Choi SW, Miyauchi M, Tomatsu I, Harada A, Ritter H. Switchable hydrogels obtained by supramolecular cross-linking of adamantyl-containing LCST copolymers with cyclodextrin dimers. Angew Chem-Int Edit 2006;45(26):4361-4365.

85. Langer R. Biomaterials in drug delivery and tissue engineering: One laboratory's experience. Accounts Chem Res 2000;33(2):94-101.

86. Crouzier T, Ren K, Nicolas C, Roy C, Picart C. Layer-By-Layer Films as a Biomimetic Reservoir for rhBMP-2 Delivery: Controlled Differentiation of Myoblasts to Osteoblasts. Small 2009;5(5):598-608.

87. Lee BH, West B, McLemore R, Pauken C, Vernon BL. In-situ injectable physically and chemically gelling NIPAAm-based copolymer system for embolization. Biomacromolecules 2006;7(6):2059-2064.

88. Johnson JA, Baskin JM, Bertozzi CR, Koberstein JT, Turro NJ. Copper-free click chemistry for the in situ crosslinking of photodegradable star polymers. Chem Commun 2008(26):3064-3066.

89. Lee F, Chung JE, Kurisawa M. An injectable enzymatically crosslinked hyaluronic acid-tyramine hydrogel system with independent tuning of mechanical strength and gelation rate. Soft Matter 2008;4(4):880-887.

90. Lee F, Chung JE, Kurisawa M. An injectable hyaluronic acid-tyramine hydrogel system for protein delivery. Journal of Controlled Release 2009;134(3):186-193.

91. Varghese S, Elisseeff JH. Hydrogels for musculoskeletal tissue engineering. Advances in Polymer Science 2006;203:95-144.

92. Elisseeff J, Anseth K, Sims D, McIntosh W, Langer R. Transdermal photopolymerization for minimally invasive implantation. Proc Natl Acad Sci U S A 1999;96:3104-3107.

93. Juodkazis S, Mukai N, Wakaki R, Yamaguchi A, Matsuo S, Misawa H. Reversible phase transitions in polymer gels induced by radiation forces. Nature 2000;408:178-181.

94. Kokufuta E, Zhang YQ, Tanaka T. Saccharide-sensitive phase transition of a lectin-loaded gel. Nature 1991;351:302-304.

95. Miyata T, Asami N, Uragami T. A reversibly antigen-responsive hydrogel. Nature 1999;399:766-769.

96. Varghese S, Lele AK, Mashelkar RA. Designing new thermoreversible gels by molecular tailoring of hydrophilic-hydrophobic interaction. Journal of chemical physics 2000;105:5368-5373.

97. Collier JH, Hu BH, Ruberti JW, Zhang J, Shum P, Thompson DH, et al. Thermally and photochemically triggered self-assembly of peptide hydrogels. Journal of the American Chemical Society 2001;123:9463-9464.

98. Kisiday J, Jin M, Kurz B, Huan H, Semino C, Zhang S, et al. Emerging biological materials through molecular self-assembly biotechnology advances. Proc Natl Acad Sci U S A 2002;20:321-339.

99. Nowak AP, Breedveld V, Pakstis L, Pine DJ, Pochan DJ, Deming TJ. Rapid Recovering hydrogel scaffolds from self-assembling diblock copolypeptide amphiphiles. Nature 2002;417:424-428.

100. Zhang S. Fabrication of novel materials through molecular self-assembly. Nature Biotechnology 2003;21:1171-1178.

101. Bulpitt P, Aeschlimann D. New strategy for chemical modificatin of hyaluronic acid: preparation of functionlized derivatives and their use in the formation of novel biocompatible hydrogels. J Biomed Mater Res 1999;47:152-169.

102. Reyes JMG, Herretes S, Pirouzmanesh A, A. WD, Elisseeff JH, Jun AS, et al. A modified chondroitin sulfate aldehyde adhesive for sealing corneal incisions. Investigative Ophthalmology & Visual Science 2005;46:1247-1250.

103. Sperinde JJ, Griffith LG. Control and prediction of gelation kinetics in enzymatically crosslinked poly(ethlene glycol) hydrogels. Macromolecules 2000;33:5467-5480.

104. Kobayashi S, Uyama H, Kimura S. Enzymatic polymerization. Chemical Reviews 2001;101:3793-3818.

105. Kurisawa M, Chung JE, Yang YY, Gao SJ, Uyama H. Injectable biodegradable hydrogels composed of hyaluronic acid-tyramine conjugates for drug delivery and tissue engineering. Chemical communication 2005;34:4312-4314.

106. Brandl F, Sommer F, Goepferich A. Rational design of hydrogels for tissue engineering: Impact of physical factors on cell behavior. Biomaterials 2007;28(2):134-146.

107. Brandl F, Sommer F, Goepferich A. Rational design of hydrogels for tissue engineering: impact of physical factors on cell behavior. Biomaterials 2007;28(2):134-146.

108. Lin YC, Tambe DT, Park CY, Wasserman MR, Trepat X, Krishnan R, et al. Mechanosensing of substrate thickness. Phys Rev E 2010;82(4):6.

109. Brannvall K, Bergman K, Wallenquist U, Svahn S, Bowden T, Hilborn J, et al. Enhanced neuronal differentiation in a three-dimensional collagen-hyaluronan matrix. Journal of Neuroscience Research 2007;85(10):2138-2146.

110. Tomasek JJ, Hay ED, Fujiwara K. Colalgen modulates cell shape and cytoskeleton of embryonic corneal and fibroma fibroblasts: distribution of actin, alpha-actinin, and myosin. Developmental Biology 1982;92:107-122.

111. Schneider A, Francius G, Obeid R, Schwinte P, Hemmerle J, Frisch B, et al. Polyelectrolyte multilayers with a tunable Young's modulus: Influence of film stiffness on cell adhesion. Langmuir 2006;22(3):1193-1200.

112. Yeung T, Georges PC, Flanagan LA, Marg B, Ortiz M, Funaki M, et al. Effects of substrate stiffness on cell morphology, cytoskeletal structure, and adhesion. Cell Motil Cytoskeleton 2005;60(1):24-34.

113. Cortese B, Gigli G, Riehle M. Mechanical Gradient Cues for Guided Cell Motility and Control of Cell Behavior on Uniform Substrates. Adv Funct Mater 2009;19(18):2961-2968.

114. Lo CM, Wang HB, Dembo M, Wang YL. Cell movement is guided by the rigidity of the substrate. Biophys J 2000;79(1):144-152.

115. Bhana B, Iyer RK, Chen WLK, Zhao RG, Sider KL, Likhitpanichkul M, et al. Influence of Substrate Stiffness on the Phenotype of Heart Cells. Biotechnol Bioeng 2010;105(6):1148-1160.

116. Rowlands AS, George PA, Cooper-White JJ. Directing osteogenic and myogenic differentiation of MSCs: interplay of stiffness and adhesive ligand presentation. Am J Physiol Cell Physiol 2008;295(4):C1037-1044.

117. Hadjipanayi E, Mudera V, Brown RA. Close dependence of fibroblast proliferation on collagen scaffold matrix stiffness. J Tissue Eng Regen Med 2009;3(2):77-84.

118. Wang HB, Dembo M, Wang YL. Substrate flexibility regulates growth and apoptosis of normal but not transformed cells. Am J Physiol-Cell Physiol 2000;279(5):C1345-C1350.

119. Kong HJ, Liu JD, Riddle K, Matsumoto T, Leach K, Mooney DJ. Non-viral gene delivery regulated by stiffness of cell adhesion substrates. Nat Mater 2005;4(6):460-464.

120. Nishiyama T, Akutsu N, Horii I, Nakayama Y, Ozawa T, Hayashi T. Response to growth-factors of human dermal fibroblasts in a quiescent state owing to cell-matrix contact inhibition. Matrix 1991;11(2):71-75.

121. Grinnell F. Fibroblasts, myofibroblasts, and wound contraction. J Cell Biol 1994;124(4):401-404.

122. Bianco P, Riminucci M, Gronthos S, Robey PG. Bone marrow stromal stem cells: Nature, biology, and potential applications. Stem Cells 2001;19(3):180-192.

123. Barberi T, Bradbury M, Dincer Z, Panagiotakos G, Socci ND, Studer L. Derivation of engraftable skeletal myoblasts from human embryonic stem cells. Nature Medicine 2007;13(5):642-648.

124. Winer JP, Janmey PA, McCormick ME, Funaki M. Bone Marrow-Derived Human Mesenchymal Stem Cells Become Quiescent on Soft Substrates but Remain Responsive to Chemical or Mechanical Stimuli. Tissue Eng Part A 2009;15(1):147-154.

125. Discher DE, Janmey P, Wang YL. Tissue cells feel and respond to the stiffness of their substrate. Science 2005;310(5751):1139-1143.

126. Yim EKF, Darling EM, Kulangara K, Guilak F, Leong KW. Nanotopography-induced changes in focal adhesions, cytoskeletal organization, and mechanical properties of human mesenchymal stem cells. Biomaterials 2010;31(6):1299-1306.

127. Bianco P, Robey PG. Stem cells in tissue engineering. Nature 2001;414(6859):118-121.

128. Chai C, Leong KW. Biomaterials approach to expand and direct differentiation of stem cells. Molecular Therapy 2007;15(3):467-480.

129. Hwang NS, Varghese S, Elisseeff J. Controlled differentiation of stem cells. Adv Drug Deliv Rev 2008;60(2):199-214.

130. Wong JY, Velasco A, Rajagopalan P, Pham Q. Directed Movement of Vascular Smooth Muscle Cells on Gradient-Compliant Hydrogels. Langmuir 2003;19(5):1908-1913.

131. Grinnell F, Rocha LB, Iucu C, Rhee S, Jiang HM. Nested collagen matrices: A new model to study migration of human fibroblast populations in three dimensions. Experimental Cell Research 2006;312(1):86-94.

132. Alsberg E, Anderson KW, Albeiruti A, Rowley JA, Mooney DJ. Engineering growing tissues. Proc Natl Acad Sci U S A 2002;99(19):12025-12030.

133. Freed LE, Engelmayr GC, Borenstein JT, Moutos FT, Guilak F. Advanced Material Strategies for Tissue Engineering Scaffolds. Adv Mater 2009;21(32-33):3410-3418.

134. Minh KN, Lee DS. Injectable Biodegradable Hydrogels. Macromol Biosci 2010;10(6):563-579.

135. Snyder SL, Sobocinski PZ. An improved 2,4,-trinitrobenzenesulfonic acid method for th edetermination of amines. Analytical Biochemistry 1975;64(1):284-288.

136. Luo Y, Kirker KR, Prestwich GD. Cross-linked hyaluronic acid hydrogel films: new biomaterials for drug delivery. Journal of Controlled Release 2000;69:169-184.

137. Oudgenoeg G, Hilhorst R, Piersma SR, Boeriu CG, Gruppen H, Hessing M, et al. Peroxidase-mediated cross-linking of a tyrosine-containing peptide with ferulic acid. Journal of Agricultural and Food Chemistry 2001;49(5):2503-2510.

138. Schmidt A, Schumacher JT, Reichelt J, Hecht HJ, Bilitewski U. Mechanistic and molecular investigations on stabilization of horseradish peroxidase C. Analytical Chemistry 2002;74(13):3037-3045.

139. Zhong Y, Bellamkonda RV. Biomaterials for the central nervous system. Journal of the royal society interface 2008;5(26):957-975.

140. Krabbe C, Zimmer J, Meyer M. Neural transdifferentiation of mesenchymal stem cells - a critical review. Apmis 2005;113(11-12):831-844.

141. Yim EKF, Pang SW, Leong KW. Synthetic nanostructures inducing differentiation of human mesenchymal stem cells into neuronal lineage. Experimental Cell Research 2007;313(9):1820-1829.

142. Thonhoff JR, Lou DI, Jordan PM, Zhao X, Wu P. Compatibility of human fetal neural stem cells with hydrogel biomaterials in vitro. Brain Research 2008;1187:42-51.

143. Willerth SM, Arendas KJ, Gottlieb DI, Sakiyama-Elbert SE. Optimization of fibrin scaffolds for differentiation of murine embryonic stem cells into neural lineage cells. Biomaterials 2006;27(36):5990-6003.

144. Wu SF, Suzuki Y, Kitada M, Kitaura M, Kataoka K, Takahashi J, et al. Migration, integration, and differentiation of hippocampus-derived neurosphere cells after transplantation into injured rat spinal cord. Neuroscience Letters 2001;312(3):173-176.

145. Basbaum CB, Werb Z. Focalized proteolysis: Spatial and temporal regulation of extracellular matrix degradation at the cell surface. Current Opinion in Cell Biology 1996;8(5):731-738.

146. Lee SB, Jeon HW, Lee YW, Lee YM, Song KW, Park MH, et al. Bio-artificial skin composed of gelatin and (1 -> 3), (1 -> 6)-beta-glucan. Biomaterials 2003;24(14):2503-2511.

147. Schmidt A, Schumacher JT, Reichelt J, Hecht HJ, Bilitewski U. Mechanistic and molecular investigations on stabilization of horseradish peroxidase C. Anal Chem 2002;74(13):3037-3045.

148. Lee F, Chung JE, Kurisawa M. An injectable hyaluronic acid-tyramine hydrogel system for protein delivery. J Control Release 2009;134(3):186-193.

149. Kurisawa M, Lee F, Wang LS, Chung JE. Injectable enzymatically crosslinked hydrogel system with independent tuning of mechanical strength and gelation rate for drug delivery and tissue engineering. J Mater Chem 2010;20:5371-5375.

150. Basbaum CB, Werb Z. Focalized proteolysis: Spatial and temporal regulation of extracellular matrix degradation at the cell surface. Curr Opin Cell Biol 1996;8(5):731-738.

151. Lutolf MP, Lauer-Fields JL, Schmoekel HG, Metters AT, Weber FE, Fields GB, et al. Synthetic matrix metalloproteinase-sensitive hydrogels for the conduction of tissue regeneration: Engineering cell-invasion characteristics. Proc Natl Acad Sci U S A 2003;100(9):5413-5418.

152. Ni Y, Chiang MYM. Cell morphology and migration linked to substrate rigidity. Soft Matter 2007;3(10):1285-1292.

153. Nemir S, West JL. Synthetic Materials in the Study of Cell Response to Substrate Rigidity. Ann Biomed Eng 2010;38(1):2-20.

154. Comisar WA, Kazmers NH, Mooney DJ, Linderman JJ. Engineering RGD nanopatterned hydrogels to control preosteoblast behavior: A combined computational and experimental approach. Biomaterials 2007;28(30):4409-4417.

155. Hsiong SX, Carampin P, Kong HJ, Lee KY, Mooney DJ. Differentiation stage alters matrix control of stem cells. J Biomed Mater Res Part A 2008;85A(1):145-156.

156. Marklein RA, Burdick JA. Spatially controlled hydrogel mechanics to modulate stem cell interactions. Soft Matter 2010;6(1):136-143.

157. Wang LS, Chung JE, Chan PPY, Kurisawa M. Injectable biodegradable hydrogels with tunable mechanical properties for the stimulation of neurogenesic differentiation of human mesenchymal stem cells in 3D culture. Biomaterials 2010;31(6):1148-1157.

158. Livak KJ, Schmittgen TD. Analysis of relative gene expression data using real-time quantitative PCR and the 2(T)(-Delta Delta C) method. Methods 2001;25(4):402-408.

159. Hu DD, Hoyer JR, Smith JW. Ca2+ suppresses cell adhesion to osteopontin by attenuating binding affinity for integrin alpha v beta 3. J Biol Chem 1995;270(17):9917-9925.

160. Sheppard D. Functions of pulmonary epithelial integrins:
from development to disease. Physiol Rev 2003;83:673-686.

161. Ballard VL, Sharma A, Duignan I, Holm JM, Chin A, Choi R, et al. Vascular tenascin-C regulates cardiac endothelial phenotype and neovascularization. FASEB J 2006;20(6):717-719.

162. Ivaska J, Heino J. Adhesion receptors and cell invasion: mechanisms of integrin-guided degradation of extracellular matrix. Cell Mol Life Sci 2000;57(1):16-24.

163. Shapiro SD. Matrix metalloproteinase degradation of extracellular matrix: biological consequences. Curr Opin Cell Biol 1998;10(5):602-608.

164. Anumolu SS, Menjoge AR, Deshmukh M, Gerecke D, Stein S, Laskin J, et al. Doxycycline hydrogels with reversible disulfide crosslinks for dermal wound healing of mustard injuries. Biomaterials 2011;32(4):1204-1217.

165. Zhong SP, Zhang YZ, Lim CT. Tissue scaffolds for skin wound healing and dermal reconstruction. Wiley Interdiscip Rev Nanomed Nanobiotechnol 2010;2(5):510-525.

166. Gates JL, Holloway GA. A comparison of wound environments. Ostomy Wound Manage 1992;38(8):34-37.

167. Janmey PA, Winer JP, Murray ME, Wen Q. The Hard Life of Soft Cells. Cell Motil Cytoskeleton 2009;66(8):597-605.

168. Jiang FX, Yurke B, Schloss RS, Firestein BL, Langrana NA. The relationship between fibroblast growth and the dynamic stiffnesses of a DNA crosslinked hydrogel. Biomaterials 2009;31(6):1199-1212.

169. Seib FP, Prewitz M, Werner C, Bornhauser M. Matrix elasticity regulates the secretory profile of human bone marrow-derived multipotent mesenchymal stromal cells (MSCs). Biochem Biophys Res Commun 2009;389(4):663-667.

170. Grinnell F. Fibroblast biology in three-dimensional collagen matrices. Trends Cell Biol 2003;13(5):264-269.

171. Georges PC, Janmey PA. Cell type-specific response to growth on soft materials. J Appl Physiol 2005;98(4):1547-1553.

172. Rhee S, Grinnell F. Fibroblast mechanics in 3D collagen matrices. Adv Drug Deliv Rev 2007;59(13):1299-1305.

173. Zhong SP, Zhang YZ, Lim CT. Tissue scaffolds for skin wound healing and dermal reconstruction. Wiley Interdiscip Rev Nanomed Nanobiotechnol 2010;2(5):510-525.

174. Hafemann B, Ensslen S, Erdmann C, Niedballa R, Zuhlke A, Ghofrani K, et al. Use of a collagen/elastin-membrane for the tissue engineering of dermis. Burns 1999;25(5):373-384.

175. Carsin H, Ainaud P, Le Bever H, Rives J, Lakhel A, Stephanazzi J, et al. Cultured epithelial autografts in extensive burn coverage of severely traumatized patients: a five year single-center experience with 30 patients. Burns 2000;26(4):379-387.

176. Discher DE, Janmey P, Wang YL. Tissue cells feel and respond to the stiffness of their substrate. Science 2005;310(5751):1139-1143.

177. Jia X, Colombo G, Padera R, Langer R, Kohane DS. Prolongation of sciatic nerve blockade by in situ cross-linked hyaluronic acid. Biomaterials 2004;25:4797-4804.

178. Fraga AN, Williams RJJ. Thermal-properteis of gelatin films. Polymer 1985;26(1):113-118.

179. Verheul RJ, Amidi M, van Steenbergen MJ, van Riet E, Jiskoot W, Hennink WE. Influence of the degree of acetylation on the enzymatic degradation and in vitro biological properties of trimethylated chitosans. Biomaterials 2009;30:3129-3125.

Chapter IX

Appendices

9. Appendices

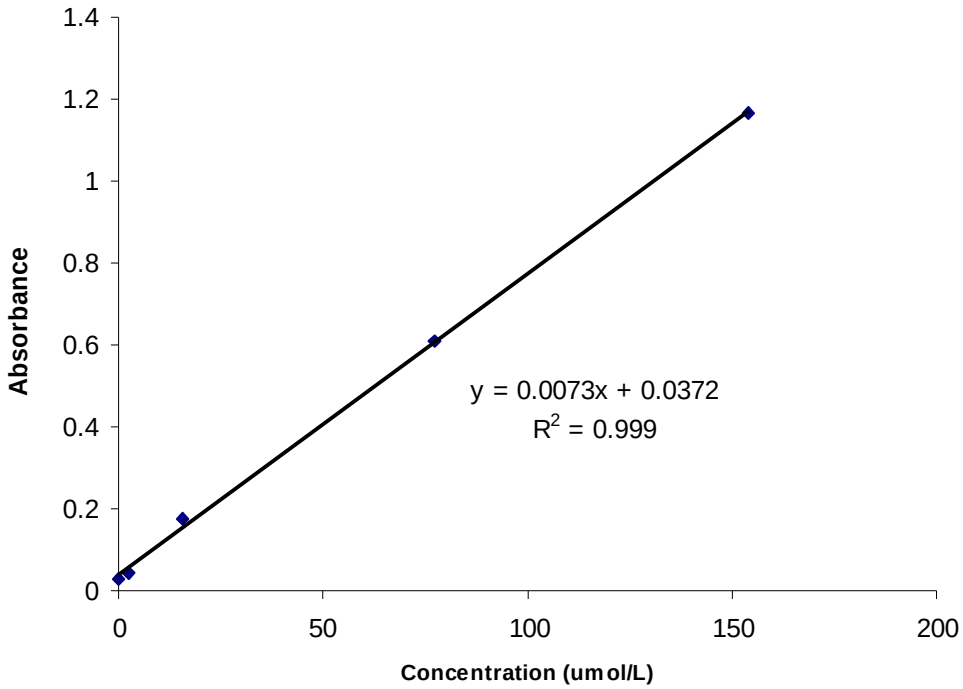

Appendix 9-1. Standard curve of absorbance of glycine with TNBS reagent at 420nm.

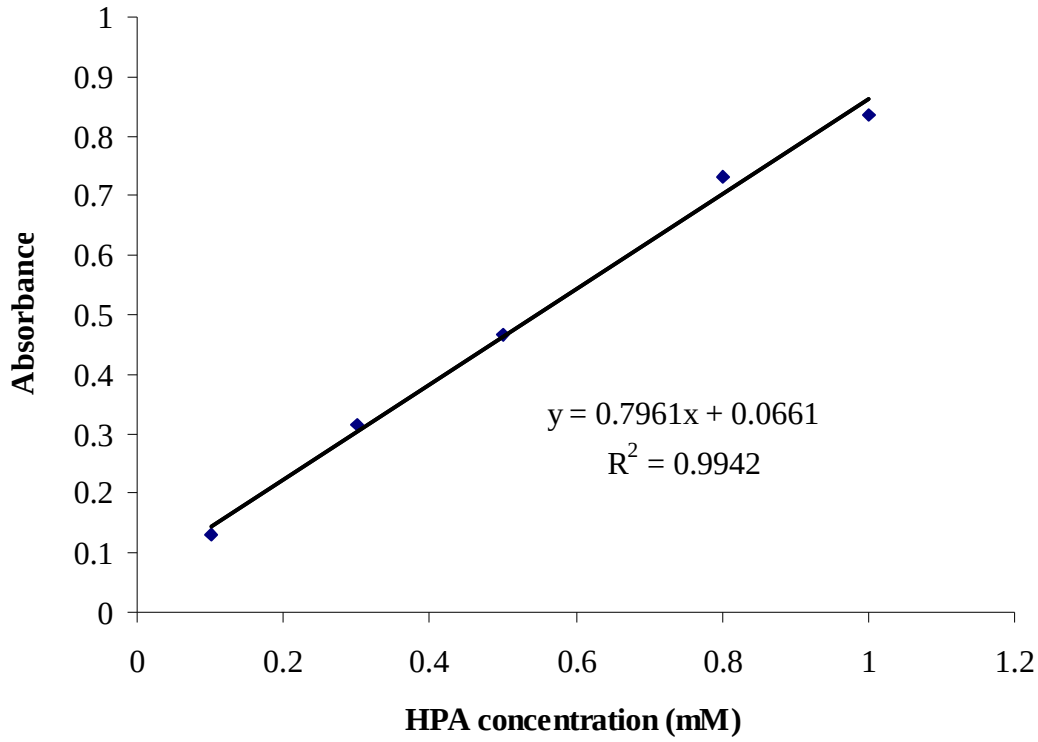

Appendix 9-2. Standard curve of absorbance of HPA at 276 nm.

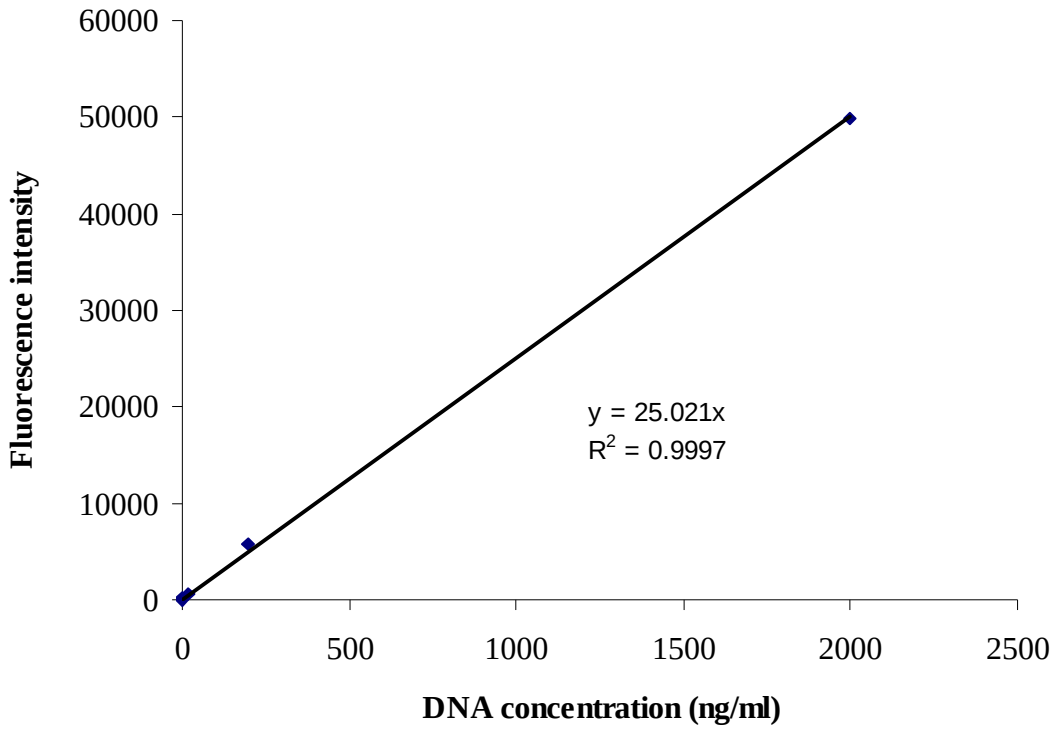

Appendix 9-3. Standard curve of fluorescence intensity of dsDNA with excitation and emission at 480 and 520 nm respectively using picogreen®.

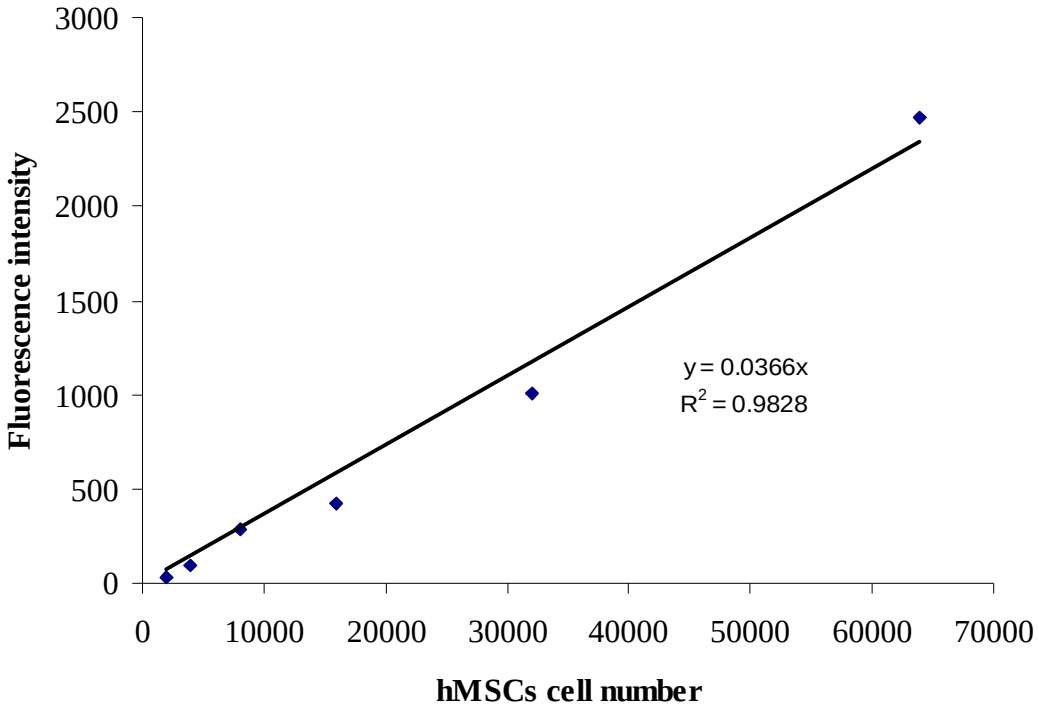

Appendix 9-4. Standard curve of fluorescence intensity of extracted DNA from hMSCs with excitation and emission at 480 and 520 nm respectively using Picogreen®.

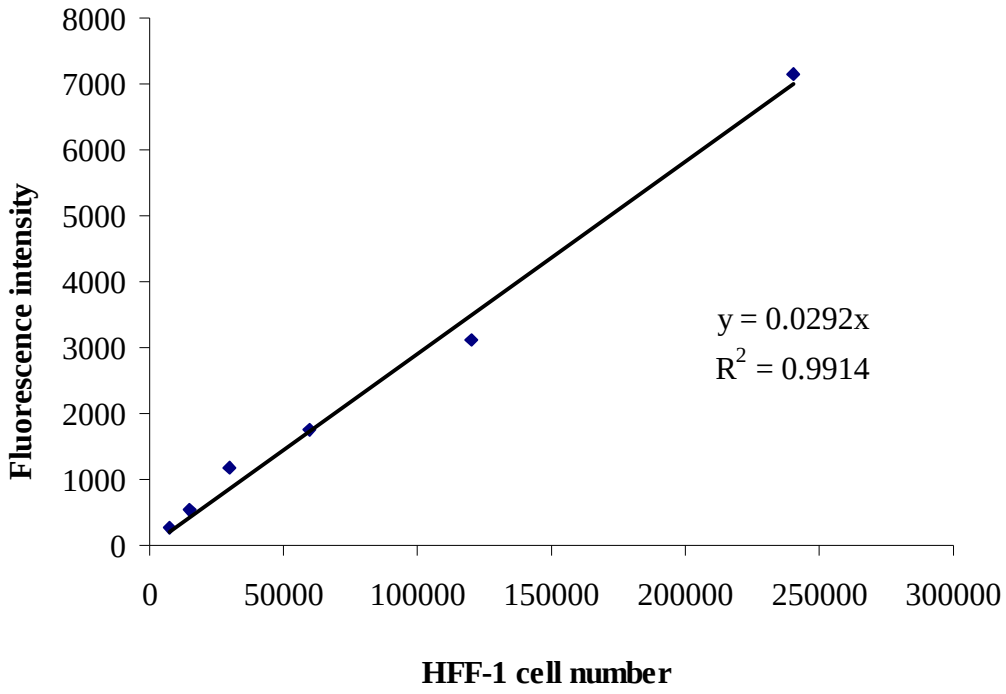

Appendix 9-5. Standard curve of fluorescence intensity of extracted DNA from HFF-1 with excitation and emission at 480 and 520 nm respectively using Picogreen®.

Chapter X

Publications and patents

10. Publications and patents

1. **L. S. Wang**, J. E. Chung, M. Kurisawa, Controlling Fibroblast Proliferation with Dimensionality-Specific Responses by Stiffness of Injectable Gtn-HPA Hydrogels (in press)
2. **L. S. Wang**, J. Boulaire, P. P.Y. Chan, J. E. Chung, M. Kurisawa, The role of stiffness of gelatin-hydroxyphenylpropionic acid hydrogels formed by enzyme-mediated crosslinking on the differentiation of human mesenchymal stem cell, Biomaterials **31** (2010) 8608-8616.
3. M. Kurisawa, F. Lee, **L. S. Wang**, J. E. Chung, Injectable enzymatically crosslinked hydrogel system with independent tuning of mechanical strength and gelation rate for drug delivery and tissue engineering, *Journal of Materials Chemistry*, **20** (2010), 5371–5375.
4. **L. S. Wang**, J. E. Chung, P. Chan, M. Kurisawa, Injectable biodegradable hydrogels with tunable mechanical properties for the stimulation of neurogenesic differentiation of human mesenchymal stem cells in 3D culture, *Biomaterials*, **31** (2010) 1148–1157.
5. M. Hu, M. Kurisawa, R. S. Deng, C.-M. Teo, A. Schumacher, Y.-X. Thong, **L. S. Wang**, K. M. Schumacher, J. Y. Ying, Cell immobilization in gelatin–hydroxyphenylpropionic acid hydrogel fibers, *Biomaterials*, **30** (2009) 3523–3531.

6. **L. S. Wang**, J. E. Chung, M. Kurisawa, Design of injectable enzymatically crosslinked gelatin-phenol hydrogels with broader stiffness range. *Journal of Materials Chemistry* **20** (2010), 5371–5375.

7. **L. S. Wang**, D. Chan, J. E. Chung and M. Kurisawa, "Enzymatically Crosslinked Gelatin-Phenol Hydrogels with Broader Stiffness Range for Osteogenic Differentiation of Human Mesenchymal Stem Cells," *Acta Biomaterialia* (in revision.

8. **L. S. Wang**, Chan Du, A. C. A. Wan, S. J. Gao and M. Kurisawa, "Design of Injectable Enzymatically Crosslinked Hydrogels with Tunable Mechanical Properties for Cartilage Tissue Engineering," *Biomaterials,* Submitted.

9. **L. S. Wang,** Controlling 3D neurogenesis human mesenchymal stem cells by the stiffness of biodegradable hydrogel, 8th International Symposium on Frontiers in Biomedical Polymers, oral presentation, May 20-23, 2009, Mishima, Japan.

10. **L. S. Wang,** Controlling 3D Neurogenesis of Human Mesenchymal Stem Cells by Stiffness of Gelatin-Hydroxyphenylpropionic Acid Hydrogel, 1st Nano Today conference, Oral presentation, August 2-5, 2009, Singapore.

11. **L. S. Wang,** The role of stiffness of gelatin hydrogels formed by enzyme-mediated crosslinking on cell differentiation, International Conference on Biomaterials Science 2011, oral presentation, March 15th -18th, Tsukuba, Japan, 2011.

12. M. Kurisawa, **L. S. Wang**, J. E. Chung, Gelatin-Phenol hyrogels as tissue engineering scaffold, Provisional US Patent application filed May 2008.

13. M. Kurisawa, **L. S. Wang**, J. E. Chung, Development of hydrogels with phase-separated structure for tissue engineering, Provisional Singapore patent application filed April 2010.